7-17-1963

Non-isothermal flow of air in a vertical pipe at low velocities.

Ujjal S. Gulati
University of Windsor

INFORMATION TO USERS

This manuscript has been reproduced from the microfilm master. UMI films the text directly from the original or copy submitted. Thus, some thesis and dissertation copies are in typewriter face, while others may be from any type of computer printer.

The quality of this reproduction is dependent upon the quality of the copy submitted. Broken or indistinct print, colored or poor quality illustrations and photographs, print bleedthrough, substandard margins, and improper alignment can adversely affect reproduction.

In the unlikely event that the author did not send UMI a complete manuscript and there are missing pages, these will be noted. Also, if unauthorized copyright material had to be removed, a note will indicate the deletion.

Oversize materials (e.g., maps, drawings, charts) are reproduced by sectioning the original, beginning at the upper left-hand corner and continuing from left to right in equal sections with small overlaps.

NON-ISOTHERMAL   FLOW   OF   AIR

IN   A   VERTICAL   PIPE

AT   LOW   VELOCITIES

A Thesis
Submitted to the Faculty of Graduate Studies through
the Department of Mechanical Engineering in Partial
Fulfillment of the Requirements for the Degree
of Master of Applied Science
at
Assumption University of Windsor

by

UJJAL S. GULATI

B.E. (Mechanical), M. S. University of Baroda, India, 1960

Windsor, Ontario, Canada
1963

UMI Number:EC52509

UMI®

AB03262

APPROVED BY:

M. H. Colbourne

_Ch. J._

W. B. [signature]

AB03262

ABSTRACT

The non-isothermal flow of air in round vertical pipes at low velocities was considered in the present work. The results were generalized to apply to other gases, however, the results were only confirmed when air was used.

The relation for radial velocity distribution in a vertical pipe was derived analytically. Heat transfer and temperature dependent properties were both taken into account in the derivations. The analytical velocity distribution equation could be solved only if we had the temperature distribution. The radial temperature profiles at various cross-sections along the vertical axis of the pipe were measured experimentally.

It was observed in this work that the eddies caused by natural convection were present at Reynolds numbers below 2000. Because of these eddies it was necessary to introduce the eddy diffusivity (ϵM) term into the momentum equation. The magnitude of ϵM was lower than that for isothermal turbulent flow. The velocity profiles for non-isothermal flow were more elongated in the central region as compared to the isothermal laminar velocity profile.

It was also found that the local Nusselt number (N_{Nux}) was higher than the one calculated analytically by Kays (23) by assuming laminar flow below N_{Re} = 2000. Finally an attempt was made to compare the non-isothermal friction factor with the isothermal friction factor. The non-isothermal friction factor (f_n) was lower than the isothermal friction factor (f_i).

ACKNOWLEDGEMENTS

The author wishes to express his sincere thanks to the following:

Professor W. G. Colborne, without whose advice, guidance and encouragement this work would not have been possible.

Dr. G. T. Csanady, Professor G. B. Babiy and Professor H. J. Tucker for their assistance throughout the course of this work.

Mr. R. G. Myers and Mr. Otto Brudy of the machine shop for their kind co-operation and help.

Miss Heidi Weikert for having typed this thesis.

iv

TABLE OF CONTENTS

(a) Analytical approach for calculating the
variation of velocity along the radius
(b) Analytical approach for calculating the
variation of temperature along the radius

(a) Description of the equipment installed
(b) Construction of electric furnace
(c) Air supply and its control
(d) Air flow measuring station
(e) Miscellaneous instruments
(f) Calibration of measuring station
(g) Leakage test

(a) Evaluation of $f(r)$
(b) Evaluation of $\dfrac{du}{dr}$
(c) Evaluation of velocity at any r
(d) Solution for turbulent flow
(e) Evaluation of mean velocity

(a) Calculation of $f(r)$
(b) Calculation of $\dfrac{du}{dr}$
(c) Calculation of velocity at any r

Chapter

NOMENCLATURE

Dimensions are given in terms of mass (M), length (L), time (T), temperature (θ) and heat (H).

A = cross-sectional area. L^2

A_o = surface area. $2\pi r_o dx$. L^2

C_p = specific heat at constant pressure. $H/M\theta$

d_o = inside diameter of pipe. L

g = acceleration due to gravity. L/T^2

g_c = conversion constant.

H = height. L

h = heat transfer coefficient. $H/L^2 T\theta$

h_f = fluid friction loss in pipe. L

k = thermal conductivity. $H/LT\theta$

P = pressure. M/LT^2

q_o = rate of heat flow through pipe wall. H/T

q_o' = rate of heat flow through pipe wall per unit area. H/TL^2

q_r = rate of radial heat flow at radius r. H/T

r = radius, distance from tube centre. L

r_o = inside tube radius. L

T = absolute temperature at any radius. θ

T_m = mean absolute temperature. θ

t = temperature in fahrenheit at any radius. θ

u = velocity in x-direction at any radius. L/T

u_m = mean velocity. L/T

x $\quad$ = distance from the entrance. L

dx $\quad$ = length of small section of tube. L

ρ $\quad$ = mass density at any radius. M/L^3

ρ_m $\quad$ = mean density. M/L^3

μ $\quad$ = absolute viscosity. M/LT

ν $\quad$ = kinematic viscosity. L^2/T

ϵ_H $\quad$ = eddy diffusivity for heat. L^2/T

ϵ_M $\quad$ = eddy diffusivity for momentum. L^2/T

α $\quad$ = thermal diffusivity. L^2/T

τ $\quad$ = shear stress. M/LT^2

β $\quad$ = coefficient of thermal expansion $1/\theta$

N_{Re} $\quad$ = Reynolds number $\dfrac{ud}{\nu}$

N_{Gr} $\quad$ = Grashof number $\dfrac{gd^3 \beta \Delta t}{\nu^2}$

N_{Nu} $\quad$ = Nusselt number $\dfrac{hd}{k}$

f $\quad$ = friction factor $\dfrac{2gd_0}{\rho_m u_m^2} \dfrac{-d\,P_f}{dx}$

LIST OF ILLUSTRATIONS

ix

CHAPTER I

SURVEY OF THE LITERATURE

The analysis of non-isothermal flow of gases in circular
pipes has been considered in references 2, 3, 10, 11, 12. Most
of these analyses were based on certain assumptions such as:

   (i) Uniform wall temperature or

  (ii) Uniform heat flux or

 (iii) Uniform internal heat generation or

 (iv) Constant fluid properties, i.e. fluid properties
     do not vary with temperature.

Most of the work done on non-isothermal laminar flow of
fluids in round pipes has been analytical. R. G. Diessler (2) in
his paper predicts analytically the radial distribution of velocity
and temperature for fully developed laminar flow of gases with fluid
properties being variable along the radius. This analysis is
applicable to flow in horizontal pipes. The analytical relations
for temperature and velocity profiles obtained in this paper are
valid at large distances from the entrance. The following assump-
tions were made:

  (a) The velocity u at any given distance from the wall is
     independent of distance along the tube.

  (b) The difference in temperature between the wall and a
     given radius is independent of the distance along the
     tube.

  (c) The viscosity, the thermal conductivity and the density
     vary with temperature.

It was observed from the velocity profiles that the heat
addition sharpened the peak in the centre region of the tube whereas
heat extraction caused a flattening at the centre of the tube. The

1

changes in sharpness of the temperature profile at the tube centre with heat addition and heat extraction were in the same direction as those for velocity profiles.

T. M. Hallman (10) attempted to predict the flow and heat transfer characteristics for a fluid flowing in a vertical tube under the conditions of combined forced and free convection. His solutions are valid only if the temperature and velocity profiles are fully developed. He considered the fluid properties as constant and a uniform heat flux at the wall of the pipe. The following two equations were solved to find the temperature and velocity profiles:

$$\frac{1}{r}\frac{d}{dr}\left(r\frac{du}{dr}\right) + \frac{\rho\beta g\theta}{\mu} = \frac{1}{\mu}\left(\frac{dP}{dx} + \rho_w g\right) \tag{1-1}$$

$$\frac{1}{r}\frac{d}{dr}\left(r\frac{d\theta}{dr}\right) - \frac{\rho g C_p A\mu}{k} = -\frac{Q}{k} \tag{1-2}$$

Where θ = the difference between the temperature at some radial position and the wall temperature at the same section

         Q = heat source term BTU/sec.(cu.ft.)

         ρ_w = mass density of fluid at wall   lb sec^2/ft^4

The result of large free convection effects in combined forced and free convection flow is to decrease radial temperature differences and increase Nusselt numbers over those for pure forced convection heat transfer. An increased free convection effect also changes the axial pressure gradient from that for pure forced convection.

R. L. Pigford (3) in his paper considered mathematically the heat transfer to a fluid flowing in laminar motion through a vertical tube. He considered the variation of density and viscosity with the temperature. He allowed the viscosity to vary in the radial direction only. He assumed that the velocity profile is partly established when the fluid enters the vertical pipe. It was also assumed that the wall temperature tw varies linearly with distance along the tube and the temperature distribution is given by:

$$\phi\left(\frac{r}{R}\right) = \frac{t - tw}{t_1 - tw} = \frac{1}{3!}\int_0^{\left(\frac{\sigma}{9}\right)^{1/3}\left(1 - \frac{r}{R}\right)} e^{-s^3}\,ds \tag{1-3}$$

Where   r = radial co-ordinate in tube, ft.

R = radius of tube, ft.

s = dummy dimensionless variable used in definite integral

6 = dimensionless quantity related to Graetz number

t_1 = temperature of entering fluid

It was found that the effect of a natural convection driving force, was smaller, the larger the flow rate. It was also noted that the normal parabolic velocity profile was distorted even though natural convection may be absent.

Hanratty (12) presented experiments and calculations to illustrate the effect of heat transfer on water flow in a vertical tube at low Reynolds numbers. He pointed out that the density variation plays a more important role than viscosity and a change in density causes a change in the force of gravity on a volume of fluid. A stream of dye was injected in the centre and the effect of heat transfer upon the field was reflected by distortion of the dye stream path. It was found that cooling the fluid in upflow gave rise to an unstable flow field. The fluid near the wall was retarded and the velocity gradient at the wall could become zero. It was observed that at a Reynolds number of 50 and a temperature difference of $10^{\circ}F$ between the heat transfer medium and the incoming water produced complete turbulence throughout the flow field. The distortion of the flow field was explained by considering the effect of natural convection upon the flow.

Brown (24) points out from his study of combined free and forced convection at low flow rates in a vertical tube that for water with density increasing from bottom to top the flow was generally turbulent even for Reynolds numbers as low as 50. He reached this conclusion because of the fluctuation of the temperature of the water at a particular cross-section. The amplitude of the fluctuation of the temperature was $\frac{1}{3}(T - Tw)$. The wall temperature Tw was also fluctuating. He also observed that the Nusselt number was higher at these low Reynolds numbers than the Nusselt number calculated from the laminar flow theory.

Yamagata (7) considered empirically the effects of free convection due to changes in density on the mean coefficient of friction and the mean dimensionless coefficient of heat transfer (Nusselt number) which were given by:

$$f_m = \frac{64}{Rew} \phi_f \psi_f \qquad (1\text{-}4)$$

$$\frac{hmD}{k} = f_m \, (\phi_h) \, \psi_h \qquad (1\text{-}5)$$

Where $\psi_f = 1 + C \, (Gr.Pr)^m$

$\psi_h = 1 + K \, (Gr.Pr)^n$

$$\phi_f = \cfrac{1}{1 - (1 - \frac{\mu_w}{\mu_1}) \, F \, (\frac{\sigma}{\gamma}_f)}$$

$$\phi_h = \cfrac{1}{1 - (1 - \frac{\mu_w}{\mu_1}) \, F \, (\frac{\sigma}{\gamma}_h)}$$

γ_f , γ_h , C, m, K and n are the factors which depend on the properties of the fluid and their magnitude could be found from the experimental data.

CHAPTER II

INTRODUCTION TO PRESENT PROJECT
AND
ANALYTICAL DERIVATIONS

Most of the papers mentioned in Chapter I and others on the same subject of non-isothermal flow of fluids in circular pipes made assumptions of the type described in the first paragraph of Chapter I. In practical problems of non-isothermal flow of fluids in pipes (e.g. heat exchangers, chimneys, etc.) it is noticed that the wall temperature does not remain constant in the axial direction. The wall temperature may or may not follow the linear law as assumed by Pigford (3). The case of uniform heat flux is also quite rare in practical problems. Lastly, for most of the fluids used in actual practice, the properties such as density, viscosity and thermal conductivity vary considerably with temperature and the assumption that the fluid properties do not vary with temperature could introduce considerable error.

It was felt necessary to treat the case of non-isothermal flow of gases at low velocities in vertical pipes where none of the assumptions made by the previous authors 2, 3, 10, 11, 12 are used, i.e. a more practical case. The property variations in the radial direction as well as in the axial direction were considered. The variation of temperature along the radius as well as along the direction of flow was measured experimentally. Knowing the temperature profile at a particular cross-section, the velocity profile was calculated by making use of the momentum equation. An attempt was made to compare the non-isothermal friction factor with the isothermal friction factor in the vertical pipes, as well as to compare the local Nusselt number (N_{NU_x}) for the present case with the ones calculated for the cases where either the wall temperature was constant or there was a constant heat flux.

5

We now outline the analytical investigation for laminar and turbulent flow of gases in vertical pipes with heat transfer and fluid properties being variable along the radius.

(a) Analytical approach for calculating the variation of velocity along the radius --

For steady isothermal turbulent flow in a circular tube at a large distance from the entrance where the mean radial velocity is zero, the Reynolds momentum equation (when cylindrical coordinates are used) reduces to

$$\frac{g_c}{\rho} \frac{\partial P}{\partial x} = -\frac{1}{r} \frac{\partial}{\partial r} (r \; \overline{u'v'}) + \frac{1}{\rho r} \frac{\partial}{\partial r} (\mu r \frac{\partial u}{\partial r}) \qquad (2\text{-}1)$$

where u' is the turbulent fluctuation in the x-direction and v' is the fluctuation in the radial direction. The first term in the above equation (2-1) represents the pressure forces, the second term the forces due to turbulent fluctuations in the mean flow and the last term the forces due to viscosity of the fluid.

The equation (2-1) is perfectly satisfactory for application to problems of forced convection wherein the body force due to gravity would be expected to be small in comparison to the inertia forces of the motion. At low velocities the effect of free convection will not be negligible. In free convection, it is the body force which sustains the fluid motion and hence it certainly must be included in the equation (2-1).

The body force is generally referred to as the buoyancy force. The variation of density with temperature as represented by the coefficient of thermal expansion β is an important factor in natural convection and is given by

$$\frac{1}{\rho} = \frac{1}{\rho_a} (1 + \beta \Delta\theta)$$

or $\frac{\rho_a}{\rho} = 1 + \beta \Delta\theta$

where $\Delta\theta = T - T_a$

ρ_a is the density at ambient air temperature Ta and ρ is the density of the fluid element at temperature T.

For a perfect gas if the pressure variation is small

$$\frac{\rho_a}{\rho} = \frac{PaT}{PTa} \simeq \frac{T}{Ta}$$

$$\frac{\rho_a}{\rho} = 1 + \beta\Delta\theta = \frac{T}{Ta}$$

$$\text{or } \beta\Delta\theta = \frac{T}{Ta} - 1$$

$$= \frac{\Delta\theta}{Ta}$$

$$\beta = \frac{1}{Ta}$$

Buoyancy force per unit mass $= \dfrac{(\rho_a - \rho)}{\rho} \dfrac{g}{g_c}$

$$= \frac{(T - Ta)}{Ta} \frac{g}{g_c}$$

$$= \beta \frac{g}{g_c} \Delta\theta$$

Now we can write the equation (2-1) as

$$\frac{1}{\rho} \frac{P}{\partial x} = - \frac{1}{r} \frac{\partial}{\partial r} (\frac{r}{g_c} \overline{u' v'}) + \frac{1}{\rho r} \frac{\partial}{\partial r} (\mu \frac{r}{g_c} \frac{\partial u}{\partial r}) + \beta \frac{g}{g_c} \Delta\theta$$

Using Prandtl concept of mixing length and the eddy diffusivities the above equation can be written as

$$\frac{1}{\rho} \frac{\partial P}{\partial x} = \frac{1}{r} \frac{\partial}{\partial r} (\frac{r}{g_c} \epsilon_M \frac{\partial u}{\partial r}) + \frac{1}{\rho r} \frac{\partial}{\partial r} (\mu \frac{r}{g_c} \frac{\partial u}{\partial r}) + \beta \frac{g}{g_c} \Delta\theta \qquad (2-2)$$

(i) In the laminar flow ϵ_M is assumed to be zero, since turbulent forces are postulated absent. So the equation (2-2) reduces to

$$\frac{1}{\rho} \frac{\partial P}{\partial x} = \frac{1}{\rho r} \frac{\partial}{\partial r} (\mu \frac{r}{g_c} \frac{\partial u}{\partial r}) + \beta \frac{g}{g_c} \Delta\theta \qquad (2-3)$$

or $\frac{1}{\rho} \frac{\partial P}{\partial x} - \beta \frac{g}{g_c} \Delta\theta = \frac{1}{\rho r} \frac{\partial}{\partial r} (\mu \frac{r}{g_c} \frac{\partial u}{\partial r})$

or $\frac{\partial}{\partial r} (\mu \frac{r}{g_c} \frac{\partial u}{\partial r}) = (\frac{1}{\rho} \frac{\partial P}{\partial x} - \beta \frac{g}{g_c} \Delta\theta) \, r \rho$ (2-3a)

The right hand side of the equation (2-3a) can be written as a function of r because ρ, $\Delta\theta$ and μ are functions of temperature and hence of radius r.

$$f(r) = (\frac{1}{\rho} \frac{\partial P}{\partial x} - \beta \frac{g}{g_c} \Delta\theta) \, r \rho$$

writing the equation (2-3a) again, we obtain

$$\frac{\partial}{\partial r} (\mu \frac{r}{g_c} \frac{\partial u}{\partial r}) = f(r)$$ (2-4)

Integrating both sides of equation (2-4) with the boundary condition

at $r = 0$; $\frac{\partial u}{\partial r} = 0$

we obtain

$$\mu \frac{r}{g_c} \frac{\partial u}{\partial r} = \int_0^r f(r) \, dr$$ (2-5)

The right hand side of the above equation (2-5) was integrated numerically for each r and then the value of $\frac{\partial u}{\partial r}$ for each r was known from equation (2-5). Knowing $\frac{\partial u}{\partial r}$, the value of u at any radius r was readily found.

(ii) In turbulent flow, the eddy diffusivity ϵ_M has a value very much higher than the kinematic viscosity v. ϵ_M is sometimes called apparent kinematic viscosity and it represents the contribution due to the momentum exchanged by macroscopic turbulent eddies.

Writing equation (2-2) again

$$\frac{1}{\rho} \frac{\partial P}{\partial x} = \frac{1}{r} \frac{\partial}{\partial r} (\frac{r}{g_c} \epsilon_M \frac{\partial u}{\partial r}) + \frac{1}{\rho} \frac{\partial}{\partial r} (\mu \frac{r}{g_c} \frac{\partial u}{\partial r}) + \beta \frac{g}{g_c} \Delta\theta$$ (2-2)

or $\frac{1}{\rho} \frac{\partial P}{\partial x} = \frac{1}{r} \frac{\partial}{\partial r} [r (\epsilon_M + v) \frac{\partial u}{\partial u}] + \beta \frac{g}{g_c} \Delta\theta$

From the previous work (15, p 439) on turbulent flow (N_{Re} 10^4) we know that the eddy diffusivity (ϵ_M) is a function of the position in the cross-section of the pipe. The temperature and velocity profiles were measured experimentally and then the values of the eddy diffusivities were calculated. So it was suspected that the eddy diffusivity (ϵ_M) might vary across the cross section in the present case also. But because of the difficulty of measuring the velocity profile it was not possible to evaluate ϵ_M at various radii and therefore it was assumed as a constant across the cross section. The kinematic viscosity ν was also assumed constant was evaluated at the mean temperature.

$$\frac{\partial}{\partial r} \left(r \frac{\partial u}{\partial r} \right) = \left(\frac{1}{\rho} \frac{\partial P}{\partial x} - \beta \frac{g}{g_c} \Delta\theta \right) \frac{r}{(\epsilon_M + \nu)} \qquad (2\text{-}6)$$

The right hand side of the equation (2-6) is a function of r and so we can write this equation in a simpler form as

$$\frac{\partial}{\partial r} \left(r \frac{\partial u}{\partial r} \right) = F(r) \qquad (2\text{-}7)$$

where $F(r) = \left(\frac{1}{\rho} \frac{\partial P}{\partial x} - \beta \frac{g}{g_c} \Delta\theta \right) \frac{r}{(\epsilon_M + \nu)} \qquad (2\text{-}7a)$

Integrating both sides of equation (2-7) with the boundary condition at $r = 0$; $\frac{\partial u}{\partial r} = 0$

we get $\quad r\frac{\partial u}{\partial r} = \int_0^r F(r) \, dr \qquad (2\text{-}8)$

The right hand side of equation (2-8) was integrated numerically for each r and then the value of $\frac{\partial u}{\partial r}$ for each r was known. Knowing $\frac{\partial u}{\partial r}$, the value of u at any radius r could be found.

(b) <u>Analytical approach for calculating the variation of temperature</u>
    <u>along the radius</u> --

This is an analytical approach for calculating the variation of temperature along the radius. For obtaining this temperature distribution, we write a heat balance for an annulus of fluid with

inside radius r and outside radius (r + dr) and length dx.

$$q_r = 2\pi r\; q'\; dx$$

$$q_{r + dr} = 2\pi\; (r + dr)(q' + dq')\; dx$$

we now write the energy balance as follows --
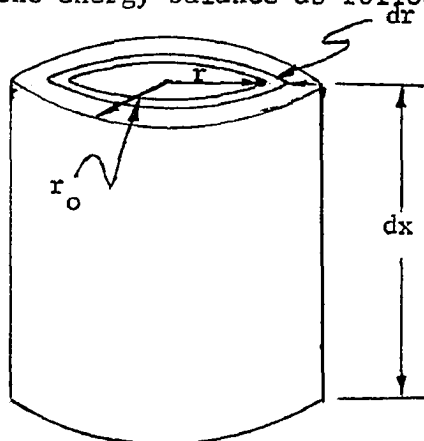
Input = Output + Accumulation

$$2\pi r\; q'\; dx = 2\pi\; (r + dr)\; (q' + dq')\; dx + 2\pi r dr\; \rho g\; u\; C_p\; \left(\frac{\partial t}{\partial x}\right)_r dx$$

or $\quad -2\pi dx\; (r\; dq' + q' dr) = 2\pi\; r\; dr\; \rho g\; u\; C_p\; \left(\frac{\partial t}{\partial x}\right)_r dx \quad \ldots \quad (2\text{-}9)$

(The differentials of the higher order than the first have been neglected).

Writing equation (2-9) in a simpler form

$$\frac{\partial(rq')}{\partial r} = -r \rho g\; u\; C_p\; \left(\frac{\partial t}{\partial x}\right)_r \tag{2-10}$$

Now writing the heat balance for the whole cross-section of the tube --

$$2\pi ro\; q'_o = \pi ro^2\; \rho_b\; g\; U_b\; C_p\; \left(\frac{\partial t}{\partial x}\right)_b$$

or $\quad 2\; q'_o = ro\; \rho_b\; g\; U_b\; C_p\; \left(\frac{\partial t}{\partial x}\right)_b$

$$\tag{2-11}$$

Dividing equation (2-10) by equation (2-11) we obtain

$$\frac{\partial(rq')}{\partial r} = -\frac{2r}{ro}\; \frac{\rho}{\rho_b}\; q_o\; \frac{U}{U_b}\; \frac{(\partial t)_r}{(\partial t)_b} \tag{2-12}$$

The static pressure is assumed to be constant across the tube. From the perfect gas law

$$\frac{\rho}{\rho_b} = \frac{T_b}{T}$$

$$\frac{\partial(rq')}{\partial r} = -\frac{2r}{ro}\frac{T_b}{T}q'_o\frac{U}{U_b}\frac{(\partial t/\partial x)r}{(\partial t/\partial x)b}$$

Integrating the above equation we obtain

$$\int d(rq') = -2\int\frac{r}{ro}\frac{T_b}{T}q'_o\frac{U}{U_b}\frac{(\partial t/\partial x)r}{(\partial t/\partial x)b} \tag{2-13}$$

or $q' = -\frac{1}{r} + \frac{1}{(\frac{\partial t}{\partial x})_b}\frac{2}{r}\int\frac{r}{ro}\frac{T_b}{T}q'_o\frac{U}{U_b}(\frac{\partial t}{\partial x})_r\ dr$ $\qquad$ (2-14)

We know that the law for heat conduction is

$$q' = -k\frac{dt}{dr} \tag{2-15}$$

Equating equation (2-14) and equation (2-15)

$$-k\frac{dt}{dr} = -\frac{1}{r} + \frac{1}{(\partial t/\partial x)b}\frac{2}{r}\int\frac{r}{ro}\frac{T_b}{T}q'_o\frac{U}{U_b}(\frac{\partial t}{\partial x})_r$$

If we integrate the above equation we obtain

$$1 - t = -\int\frac{1}{k}[-\frac{1}{r} + \frac{1}{(\partial t/\partial x)b}\frac{2}{r}\int\frac{r}{ro}\frac{T_b}{T}\frac{U}{U_b}q'_o(\frac{\partial t}{\partial x})_r\ dr]\ dr \tag{2-16}$$

In the above equation (2-13), t is the temperature at any radius r.

Our main purpose was the solution of the velocity profile equation. Since the temperature profile equation could only be solved by

(i) knowing the velocity profile or

(ii) assuming a particular heat flux

the decision was made to measure the temperature experimentally. This experimentally determined profile could then be used to solve the velocity profile equation and a further advantage would be that

no assumption would have to be made regarding the heat flux.

The experimental test set up was therefore designed to measure accurately the temperature profiles at the various sections.

CHAPTER III

EQUIPMENT, INSTRUMENTATION AND CALIBRATION

(a) <u>Description of the equipment</u>:

The equipment used for the present work was designed and installed with the able guidance of Prof. W. G. Colborne. Shown in figure 1 is a schematic diagram of the major components of the test installation. Air was delivered from the fan into a 5" dia. pipe. The air was delivered from this pipe into a 1.6" ID brass measuring tube through a gradual reduction as shown in figure 1. The air after leaving the brass tube entered another pipe of 4.5" ID through a short diverging piece and then entered the electric furnace. The heated air from the furnace entered the vertical aluminum test pipe having an OD = 4.5", ID = 4.3125" and length = 36 ft. An inlet pressure was measured by providing a piezometer ring about 18" away from the start of the vertical aluminum pipe as shown.

(b) <u>Construction of electric furnace</u>:

The electric furnace is shown in figure 3. The air from the 4.5" ID pipe entered the bottom of the furnace through a sheet metal transition shown in figure 3a. A wire mesh screen was provided just below the heaters to distribute the air uniformly across the heaters. There were five Nichrome wire electric heaters. Four of the heaters were 3000 Watts each and the uppermost heater was 2000 Watts. The 2000 Watt heater was connected through a variac for the purpose of providing fine control. The furnace was covered with 2-inch magnesia blocks to reduce the heat loss to the ambient air and to improve the temperature distribution entering the test pipe.

13

SCHEMATIC LAYOUT OF THE EQUIPMENT
USED IN THE PRESENT INVESTIGATION

FIGURE 1

14

TEST PIPE SHOWING
LOCATIONS OF TESTING
SECTIONS
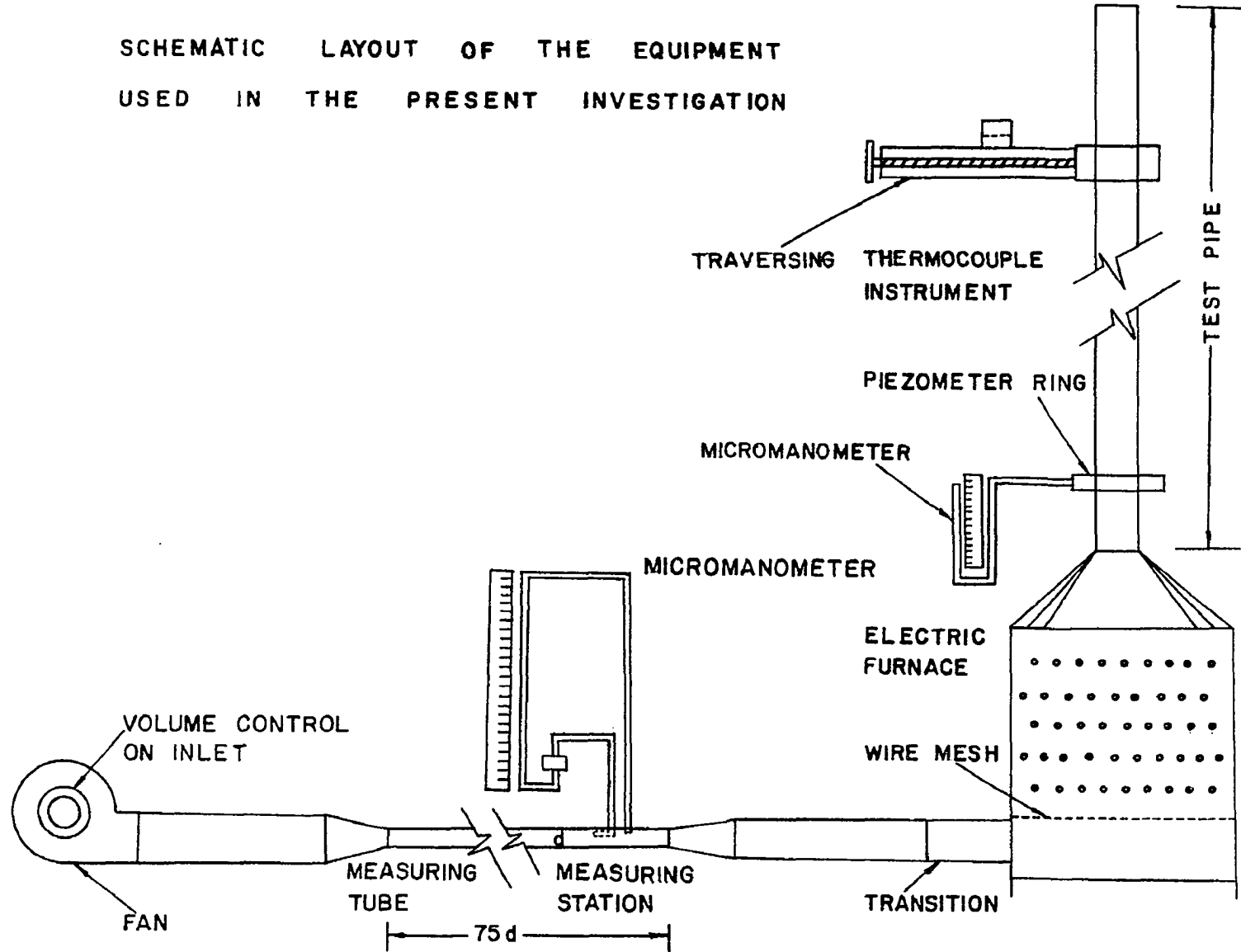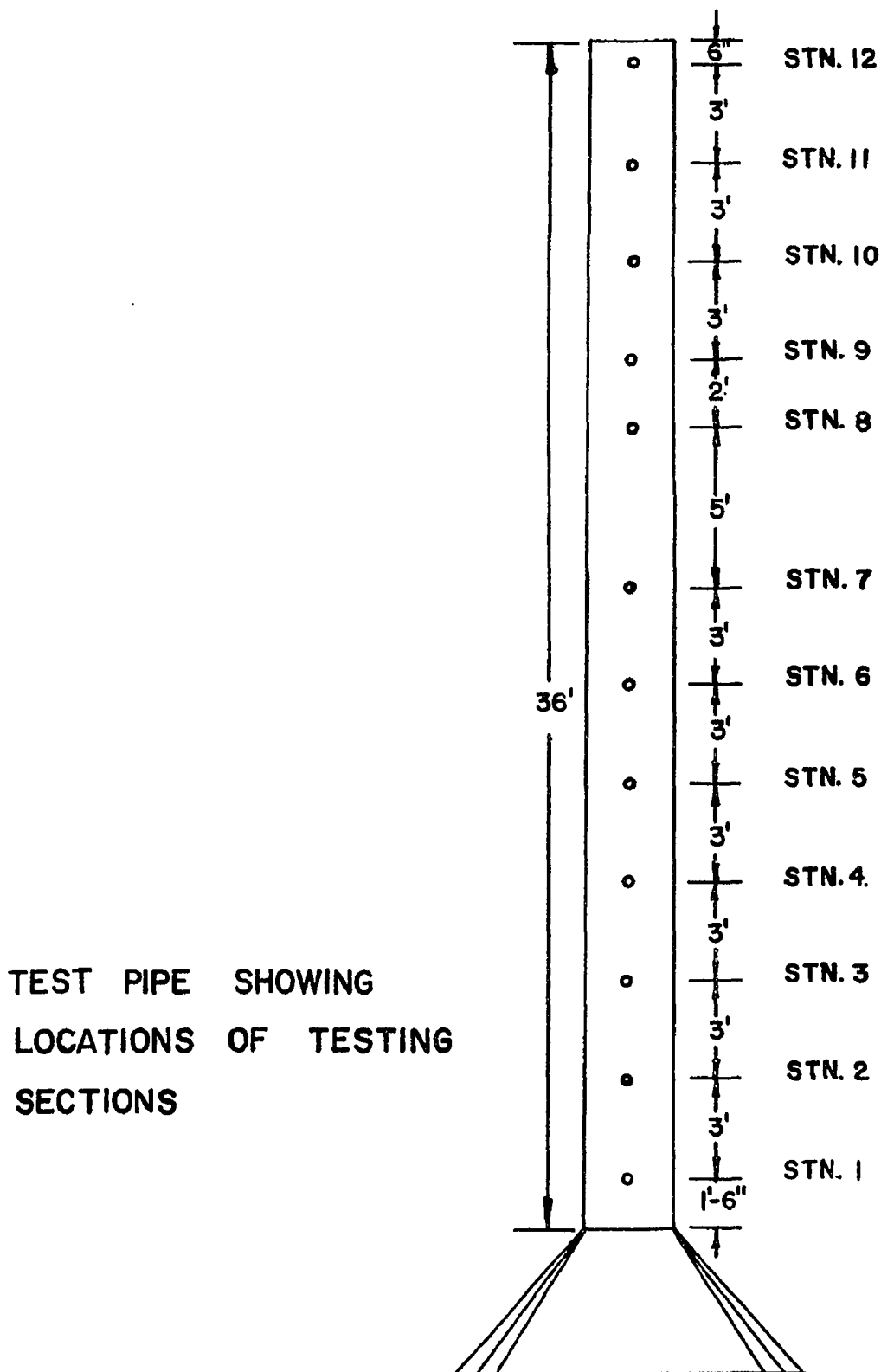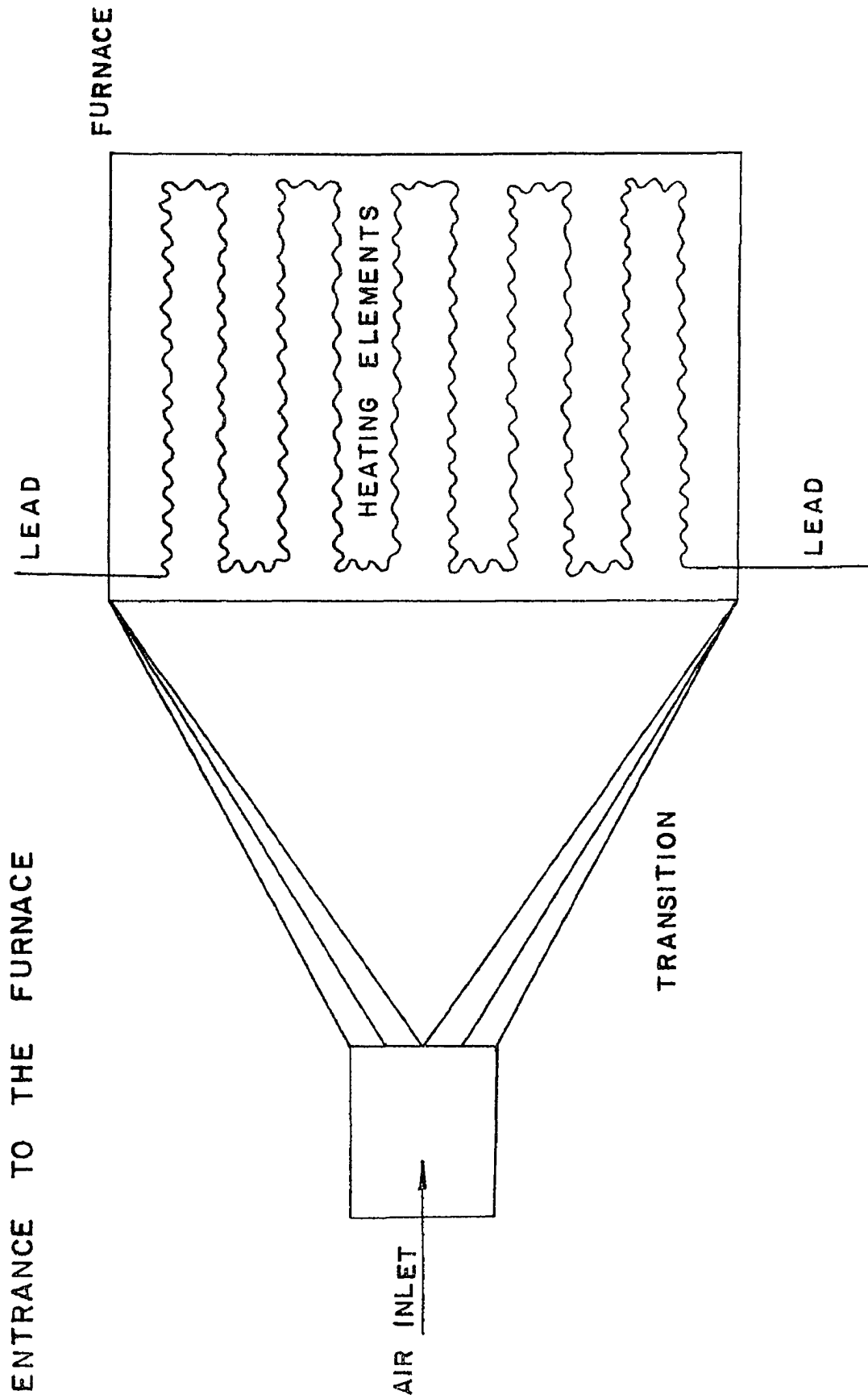
FIGURE 2

FIGURE 3a

(c) <u>Air supply and its control</u>:

The air was supplied by a centrifugal fan driven by a 3-phase 1/2 H.P. motor. The air delivery of the fan was controlled by varying the size of the inlet opening to the fan. This was effected by providing a circular metal plate which moved toward or away from the fan inlet along a threaded rod as the plate was rotated. This control arrangement is shown in figure 4. This meant that the air path from the fan to the measuring station was symmetrical and unobstructed except for the gradual reduction, which it was felt would not disrupt the regularity of the air flow to any great extent.

(d) <u>Air flow measuring station</u>:

The airflow through the entire set-up was measured by a 20 point velocity traverse across the measuring tube some 10 ft. (75 diameters approximately) from the conical reduction. The layout of the measuring station is shown in detail, with pertinent dimensions in figure 5. The three static pressure taps consisted of three 5/16" O.D. brass tubes equally spaced around the circumference of the measuring tube, each of which was centered over a 0.05-inch hole drilled through the wall of the tube. The inside of the measuring tube was smoothed with emery cloth to ensure that the taps would give a true indication of static pressure.

The total pressure tube was a hypodermic needle bent to a right angle approximately 3/4-inch from one end. To the other end was attached a short length of brass tubing and to this in turn was attached a needle pointer to serve as a position indicator. An 8-inch diameter aluminum plate about 1/8-inch thick with a locking arrangement was fixed at 3/4-inch downstream from the static pressure taps. A guide for traversing the hypodermic needle could be positioned at the proper point in the traverse by lining up the needle pointer with the position marked on the guide. An indicator needle parallel to the bent portion of the hypodermic needle was provided on the brass tube attached to the total pressure needle to assure the correct angle of the hypodermic needle relative to the

NOT TO SCALE

HYPODERMIC NEEDLE

MEASURING TUBE

5/16"O.D. BRASS STATIC
PRESSURE TAPS

HYPODERMIC NEEDLE

GUIDE FOR TRAVERSING
HYPODERMIC NEEDLE

1.6"

120°

8"DIA. ALUMINUM
PLATE 1/8" THICK

MEASURING STATION DETAILS
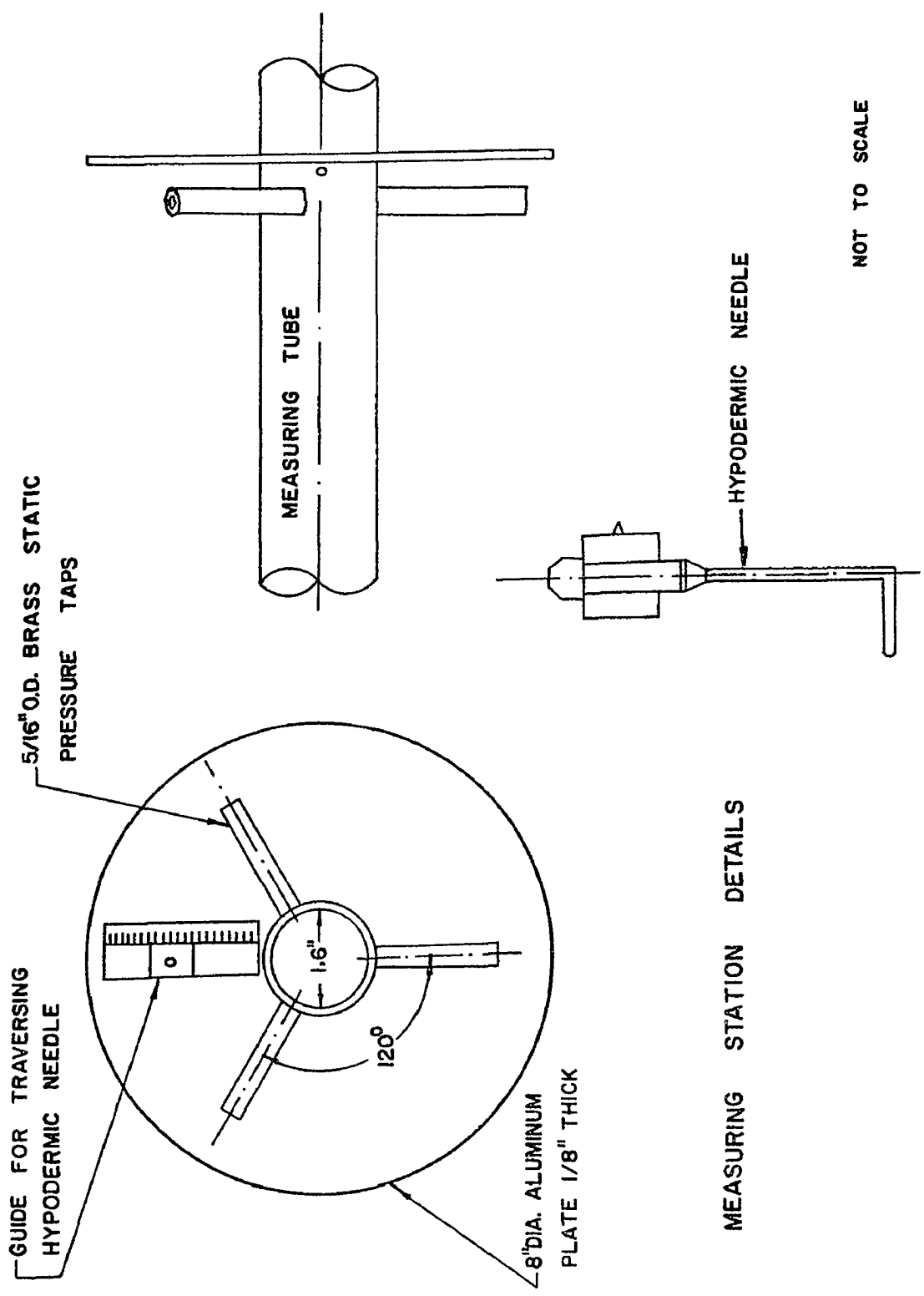
FIGURE 5

direction of the flow.

The pressure lines were led to either side of the micromanometer which read directly in inches of water and was graduated in thousandths of an inch. Figure 6 is a photograph of the measuring station showing the micromanometer connected to the static and total pressure taps.

(e) Miscellaneous instruments:

The barometric pressure was read from a standard laboratory mercury barometer which measured the pressure with an accuracy of 0.01-inch. The ambient air temperature was read from three thermocouples provided at three different heights between the furnace and the top of the vertical aluminum pipe. The surface temperature of the furnace was measured from time to time with the surface pyrometer to ensure that the furnace did not overheat. All the thermocouples used for measuring air and surface temperature were of Iron-Constantan 30-gauge wire.

(f) Calibration of measuring station:

From the experimental work done by a number of scientists, we know that the flow pattern for the range of velocities being used in our present investigation is well established in a length of 50 to 80 diameters of pipe, the indication being the shape of the velocity profile. At the entrance under ideal conditions the velocity profile will be perfectly flat through the cross-section (the velocity will be zero at the wall). As the flow progresses further and further down the pipe, the transition layer becomes progressively thicker until a final parabolic flow pattern is established.

The first step was to make a number of velocity traverses for different airflows by controlling the size of the fan inlet. Then we plotted the mean of the square roots of the velocity pressures against the various centre line velocity pressures and obtained a curve as shown in figure 7. Throughout the course of our experimental work, we had the hypodermic needle at the centre of the pipe. For any particular value of the centre line velocity
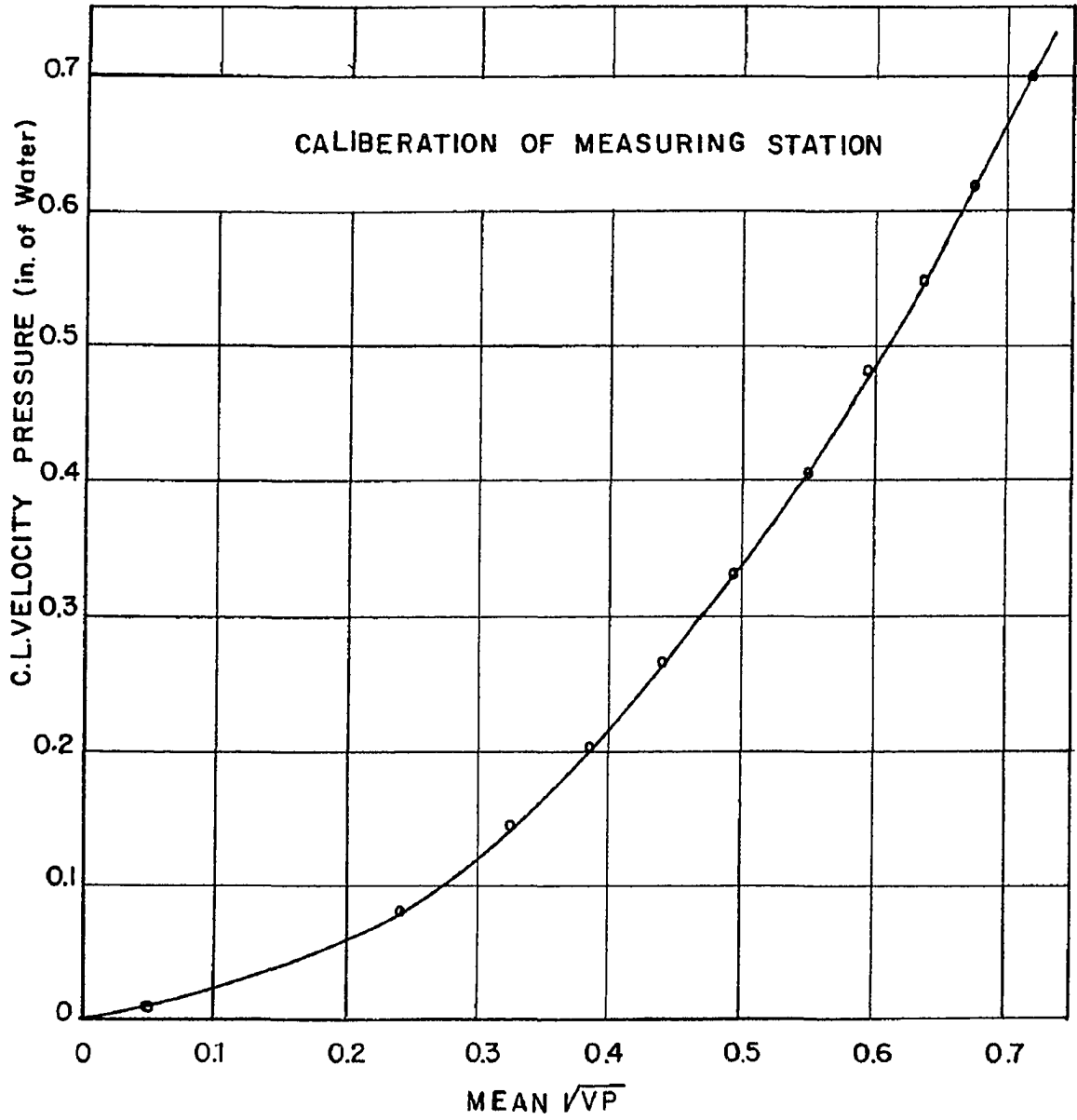
FIGURE 7

pressure, we could find from figure 7 the corresponding mean square root of the velocity pressure and hence calculate the quantity of air flowing.

(g) Leakage test:

It was felt necessary that before starting the actual experimental work, it must be checked whether there were any leaks between the measuring station and the furnace because of a number of joints between the fan and the furnace. To do this, the weight flows at various stations along the aluminum test pipe were compared with the weight flow at the measuring station. These values were found to be in good agreement with each other.

CHAPTER IV

SOLUTION OF VELOCITY PROFILE EQUATION

For laminar flow:

(a) <u>Evaluation of f(r)</u>:

From Chapter II we have the equation

$$\frac{\partial}{\partial r} \left(\mu \frac{r}{g_c} \frac{\partial u}{\partial r} \right) = \left(\frac{1}{\rho} \frac{\partial P}{\partial x} - \beta \frac{g}{g_c} \Delta\theta \right) r\rho \qquad (2\text{-}3a)$$

On the right hand side of the above equation, the density ρ and the difference between the temperature at any r and ambient air, $\Delta\theta$ are functions of the radius r. To integrate this equation (2-3a), the temperature profile for the cross-section under consideration was required to find the properties on the right hand side of the above equation. The $\frac{\Delta P}{\Delta x}$ was measured over a length of 6 ft. or 3 ft. each side of the chosen test section with the assumption that $\frac{\partial P}{\partial x}$ is equal to $\frac{\Delta P}{\Delta x}$ in this height of 6 ft. From the above explanation, it is obvious that the right hand side of equation (2-3a) is a function of r. Hence writing this equation in a simpler form, we have

$$\frac{\partial}{\partial r} \left(\frac{\mu r}{g_c} \frac{\partial u}{\partial r} \right) = f(r) \qquad (4\text{-}1)$$

Integrating this equation, we get

$$\frac{\mu r}{g_c} \frac{\partial u}{\partial r} = \int_0^{R} f(r) \, dr \qquad (4\text{-}2)$$

where

$$f(r) = \left(\frac{1}{\rho} \frac{\partial P}{\partial x} - \beta \frac{g}{g_c} \Delta\theta \right) r\rho$$

22

(b) <u>Evaluation of $\frac{\partial u}{\partial r}$:</u>

From equation (4-2)

$$\frac{\partial u}{\partial r} = \frac{g_c}{\mu r} \int_0^r f(r)\ dr$$

$$= \frac{g_c}{\mu r}\ [\int_0^{r_1} f_1(r)\ dr + \int_{r_1}^{r_2} f_2(r)\ dr + \ldots\ldots] \qquad (4\text{-}3)$$

From equation (4-3), $\frac{\partial u}{\partial r}$ for $r = r_1$ is

$$(\frac{\partial u}{\partial r})_{r\ =\ r_1} = \frac{g_c}{\mu_1 r_1} \int_0^{r_1} f_1(r)\ dr$$

And $\frac{\partial u}{\partial r}$ for $r = r_2$ is

$$(\frac{\partial u}{\partial r})_{r\ =\ r_2} = \frac{g_c}{\mu_2 r_2}\ [\int_0^{r_1} f_1(r)\ dr + \int_{r_1}^{r_2} f_2(r)\ dr]$$

and so on. Then $f(r)$ was plotted against r for different radii from $r = 0$ to $r = r_o$. To find the slope $\frac{\partial u}{\partial r}$ at any r, the area under the curve (Plot of $f(r)$ versus r) between $r = 0$ and $r = r_{reqd}$ was measured.

$\frac{\partial u}{\partial r}$ was found at various radii between $r = 0$ and $r = r_o$ in the manner said above. Then $\frac{\partial u}{\partial r}$ was plotted against r.

(c) <u>Evaluation of velocity at any r:</u>

We know the boundary conditions

at $r = 0$; $u = u_{max}$

at $r = r_o$; $u = 0$

At $r = r_1$, find the slope $\frac{\partial u}{\partial r}$ between $r = 0$ and $r = r_1$ from the plot of $\frac{\partial u}{\partial r}$ versus r. Knowing the numerical value of $\frac{\partial u}{\partial r}$, the velocity u_1 at $r = r_1$ is given by

$$\frac{\partial u}{\partial r} = \frac{u_{max} - u_1}{o - r_1} = \beta_1 \qquad (4\text{-}4)$$

where β_1 is the numerical value of $\frac{\partial u}{\partial r}$ from the plot of $\frac{\partial u}{\partial u}$ versus r. The velocity u_1 in terms of u_{max} is found from equation (4-4). Similarly to find u_2 at $r = r_2$, find the slope $\frac{\partial u}{\partial r}$ between $r = r_1$ and $r = r_2$ and we can write

$$\frac{\partial u}{\partial r} = \frac{u_1 - u_2}{r_1 - r_2} = \beta_2 \qquad (4-5)$$

where β_2 is the numerical value of $\frac{\partial u}{\partial r}$ from the plot of $\frac{\partial u}{\partial r}$ versus r. In equation (4-5), the only unknown is u_2 which is easily found. In this way, we can find u_1, u_2, u_3 .... etc. in terms of u_{max}. Then plot the velocity against radius r, starting from $r = 0$ where $u = u_{max}$ and extrapolating this curve to the wall of the pipe which will give the numerical value of u_{max}. Knowing the numerical value of u_{max}, the actual velocity at each r can be found. After calculating the velocity at each r, it is easy to check the weight flow.

(d) Solution for turbulent flow:

The solution of the momentum equation for turbulent flow is done in exactly the same way as for laminar flow. For turbulent flow the function of r is given by equation (2-7a)

$$F(r) = (\frac{1}{\rho}\frac{\partial P}{\partial x} - \beta\frac{g}{g_c}\Delta\theta)\frac{r}{(\epsilon_M + \nu)} \qquad (2-7a)$$

To evaluate ϵ_M, we make use of the energy equation which involves the term ϵ_H, the eddy diffusivity for heat which represents the turbulent exchange of thermal energy. From Prandtl's analogy, we know that for Prandtl number of unity the eddy diffusivity ϵ_H, bears a relation to the true thermal diffusivity α, which is analogous to the relationship which the apparent kinematic viscosity ϵ_M, bears to the laminar kinematic viscosity ν. In our case $N_{pr} = 0.7$ which is very close to unity and we assumed that Prandtl's analogy would apply.

The energy equation can be written as

$$\frac{q}{A} = -\rho C_p (\epsilon_H + \alpha)\frac{dt}{dr} \qquad (4-6)$$

In the equation (4-6) we know everything except the value of ϵ_H. Calculating ϵ_H from this equation we can find the ratio $\epsilon_{H/\alpha}$ and then use the same value of the ratio for $\epsilon_{M/\nu}$. Knowing the relation between ϵ_M and ν we can evaluate the function $F(r)$. Once having calculated the value of $F(r)$ at various radii, the rest of the solution is done in exactly the same way as in section (a) and (b) of this chapter.

(e) Evaluation of mean velocity:

To calculate the mean velocity at a particular cross-section, we proceeded as follows --
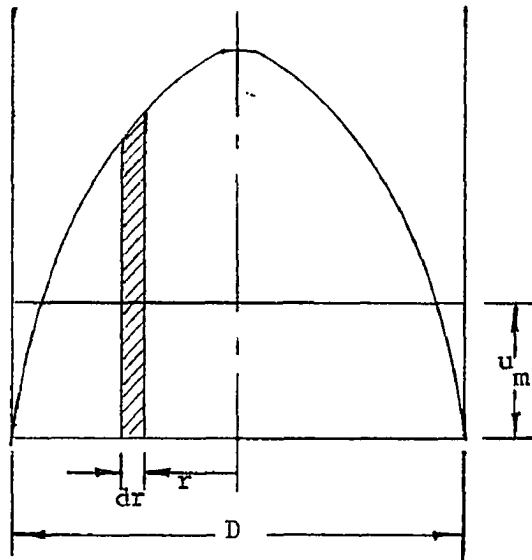
where D is the inside diameter of pipe.

Treating this as a three dimensional problem, we can write

$$\frac{\pi}{4} D^2 u_m = \int_0^r 2\pi r u dr \tag{4-7}$$

The equation (4-7) can be written in a simpler form as

$$u_m = \frac{8}{D^2} \int_0^r u r dr$$

$$\text{or} \quad u_m = \frac{8}{D^2} [\int_0^{r_1} u r dr + \int_{r_1}^{r_2} u r dr + \int_{r_2}^{r_3} u r dr + \ldots] \tag{4-8}$$

Then we plotted r versus ur. The area under the curve was equal to the bracketted term in equation (4-8).

MOMENTUM EQUATION CALCULATIONS

(LAMINAR FLOW)

From the previous work 2, 3, 7 on non-isothermal flow, it was assumed that the laminar flow exists up to a Reynolds number of 2000.

As mentioned in Chapter IV, we shall first proceed to find the value of the function $f(r)$.

(a) Calculation of $f(r)$.

Station number 7, which is 18 ft. away from the piezometer ring will be taken as an example for the sample calculations. In this test the weight flow was 12.23 lbs/hr, inlet C. L. temperature was $355^{\circ}F$ and ambient air temperature $83^{\circ}F$. The temperatures at various radii are shown in table 1.

At $r = 0.25"$

$$f(r) = (- \frac{1}{543} \times 32.2 \times 36.1 + \frac{32.2}{0.06692} \times \frac{0.005 \times 62.4}{12 \times 7}) \frac{0.25 \times 0.06692}{12}$$

$$= - 0.0005 \text{ lb/ft sec}^2$$

At $r = 0.75"$

$$f(r) = (- \frac{1}{543} \times 32.2 \times 35.5 + \frac{32.2}{0.06699} \times \frac{0.005 \times 62.4}{12 \times 7}) \frac{0.75 \times 0.06699}{12}$$

$$= - 0.00136 \text{ lb/ft sec}^2$$

In the above manner, we calculated the numerical values of $f(r)$ for different radii.

(b) Calculation of $\frac{\partial u}{\partial r}$ --

We have from the relation (4-3) that

$$\frac{\partial u}{\partial r} = \frac{g_c}{\mu r} \left[\int_0^{r_1} f_1(r)\, dr + \int_{r_1}^{r_2} f_2(r)\, dr + \ldots\ldots \right] \quad (4\text{-}3)$$

Now to find the numerical value of $\frac{\partial u}{\partial r}$ at each r, we plotted $f(r)$ versus r as shown in figure 8 and then found the area under the curve for any required r between $r = 0$ and $r = r_{reqd}$. The values of $\frac{\partial u}{\partial r}$ for various radii at the station under consideration are shown in table 1. We then plotted $\frac{\partial u}{\partial r}$ versus r as shown in figure 9.

(c) Calculation of velocity at any r --

From the plot of $\frac{\partial u}{\partial r}$ versus r (figure 9), we can find the slope $\frac{\partial u}{\partial r}$ at any r. At $r = 0.25"$, we find from figure 9 that $\frac{\partial u}{\partial r}$ between $r = 0$ and $r = 0.25"$ is $- 11$. Then

$$\frac{\partial u}{\partial r} = \frac{u_{max} - u_{0.25}}{0 - \frac{0.25}{12}} = -11$$

or $u_{0.25} = u_{max} - 0.23$

Similarly at $r = 0.5"$, $\frac{\partial u}{\partial r}$ between $r = 0.25"$ and $r = 0.5"$ is $- 27.3$

$$\frac{\partial u}{\partial r} = \frac{u_{0.25} - u_{0.5}}{(0.25 - 0.5)\frac{1}{12}} = -27.3$$

substituting the value of $u_{0.25}$ in terms of u_{max}, we obtain

$u_{0.5} = u_{max} - 0.799$

In the same way u at any r is found in terms of u_{max} and this is shown in table 1.

We then plotted u versus r where u was in terms of u_{max} as shown in figure 10. From this figure 10, the numerical value of $u_{max} = 11.1$ ft/sec. Knowing the numerical value of u_{max}, we found the ratio u/u_{max} for various radii as shown in table 1.

Then checking the weight flow as follows --

$$(\rho_1 A_1 u_1 + \rho_2 A_2 u_2 + \ldots\ldots\ldots\ldots) = W \text{ lbs/hr} \qquad (5\text{-}1)$$

$$u_{max}(0.002942) \times 3600 = W \text{ lbs/hr}$$

or W = 11.1 x 0.002942 x 3600
   =119.88 lbs/hr

The measured weight flow is 12.23 lbs/hr. The calculated weight flow differs from the measured value. It was suspected that there might be an error in the experimental measurement of ΔP between the two stations. The micromanometer can be read to 0.001 inches and the error in reading this instrument can be $\pm$ 0.001". The above set of calculations was for dP = 0.005" of H_2O in a length of 7 ft. We repeated the calculations for dP = 0.0048" of H_2O in which case the value of u_{max} came out to be 13.8 ft/sec and when dP = 0.0052" of H_2O, the u_{max} was 8 ft/sec. This shows that an error of $\pm$ 0.0002" can cause such a drastic change in the magnitude of u_{max}. So we plotted u_{max} against dP as shown in figure 11 and extrapolated this line from three points. Then another set of calculations were performed for dP = 0.0055" and dP = 0.0056", since from figure 11 it appears that u_{max} in the range of these two dPs might give us a weight flow very close to the actual value. When dP = 0.0055", the u_{max} came out to be 3.6 ft/sec but there was a reversal near the wall. The weight flow in this case was 23 lbs/hr which is still twice as large as actual weight flow. With dP = 0.0056", the u_{max} came out to be 2.225 ft/sec and corresponding weight flow was 12.6 lbs/hr. This weight flow was reasonable and was only 3% greater than the actual weight flow. But we had the velocity profile as shown in figure 12 with a reversal near the wall.

The reversal near the wall indicates that eddies formed near the wall and so the momentum equation for laminar flow can no longer be applicable. To check these eddies, we put a piece of plastic tube about 8" long at 20 ft. from the entrance and

introduced smoke into the tube at various radii. We noticed that the smoke did not go up in a streamline but in a wavy shape which indicated the formation of eddies. The flow of smoke also indicated that there was no flow in the downward direction.

Due to the presence of eddies it was evident that the flow was not laminar and the introduction of eddy diffusivity to allow for momentum exchange is necessary in the momentum equation. The sample calculation for the Momentum Equation containing apparent kinematic viscosity ϵ_M is shown in Appendix "A".
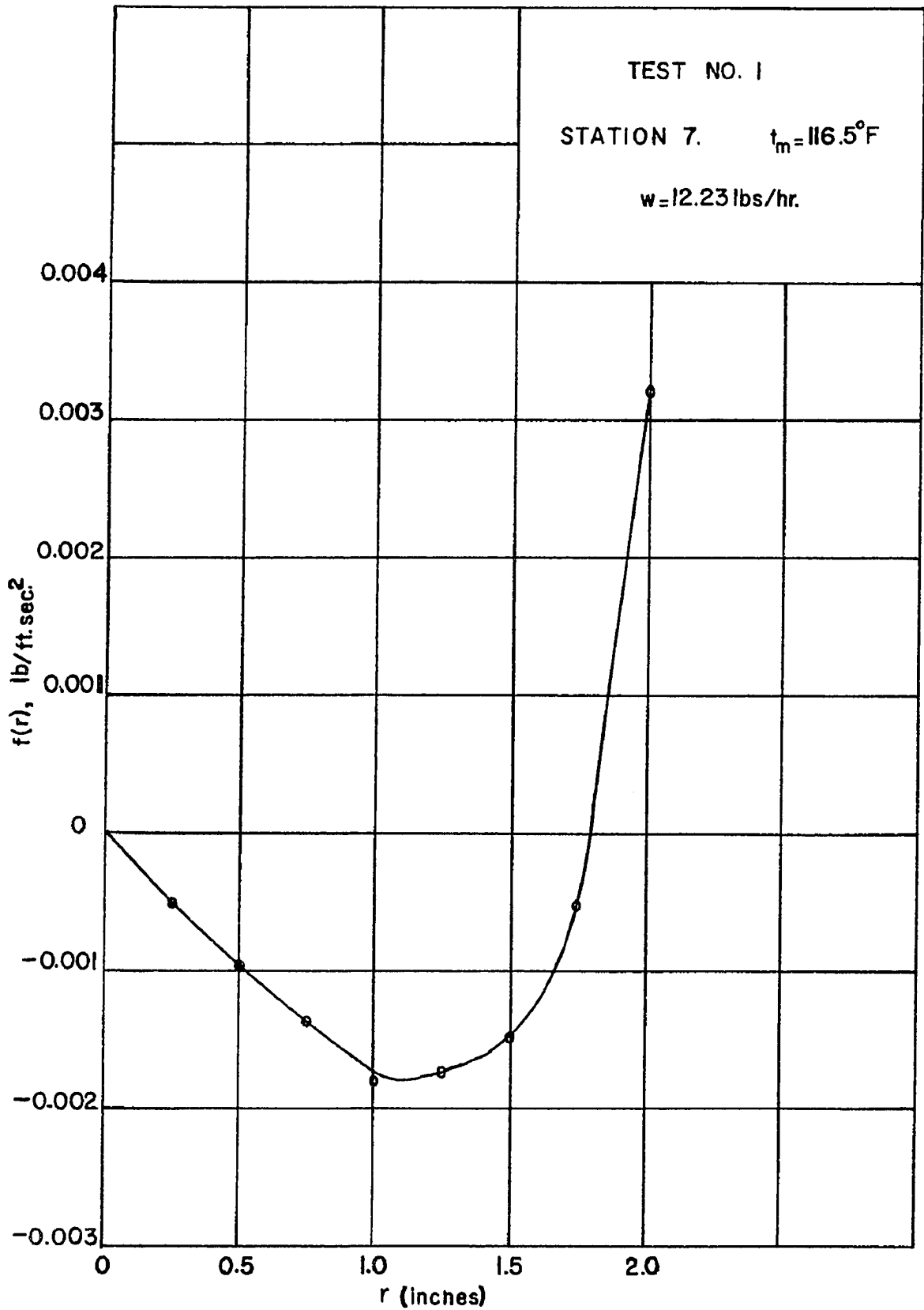
FIGURE 8   PLOT OF f(r) VERSUS r
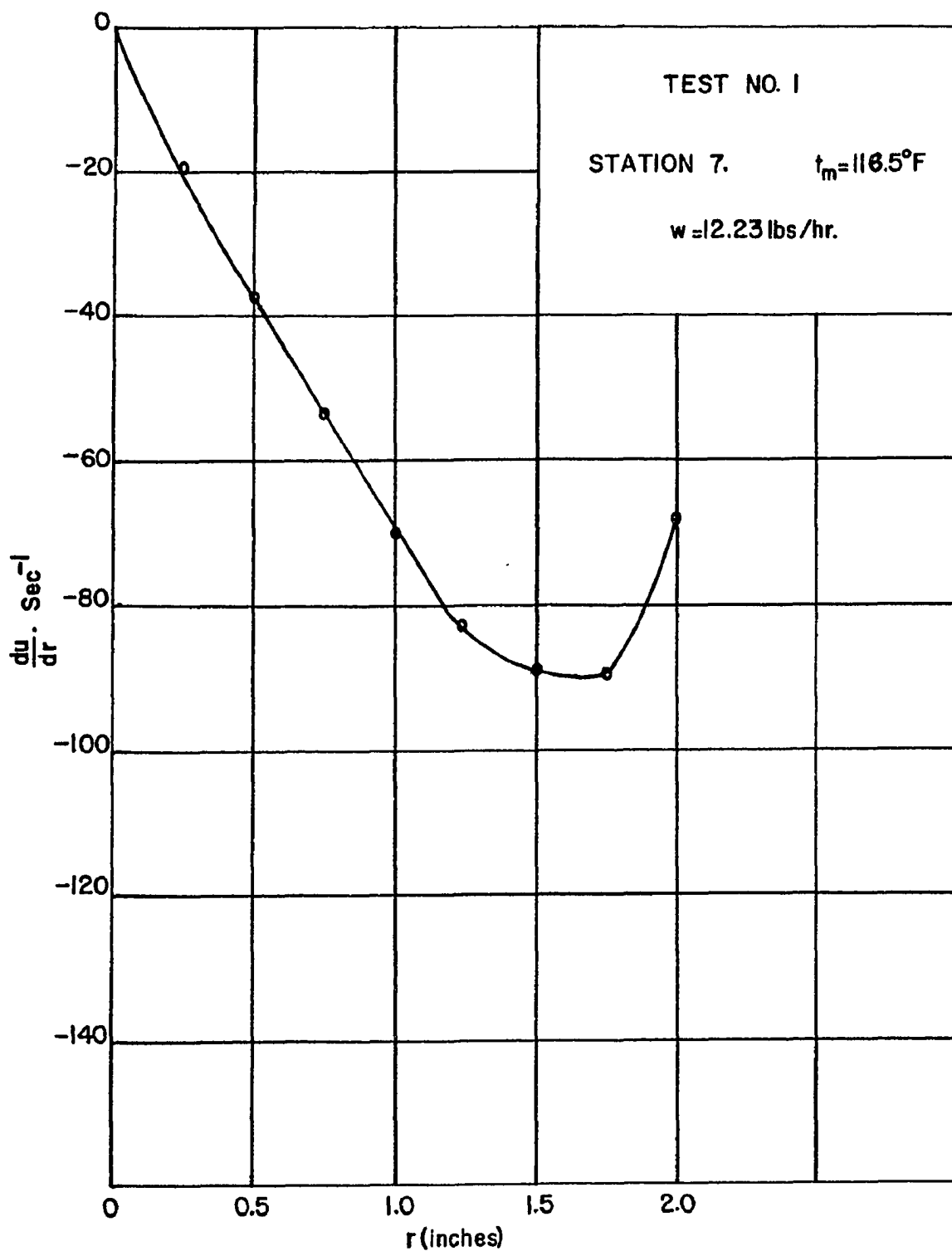
FIGURE 9   PLOT OF $\frac{du}{dr}$ VERSUS r
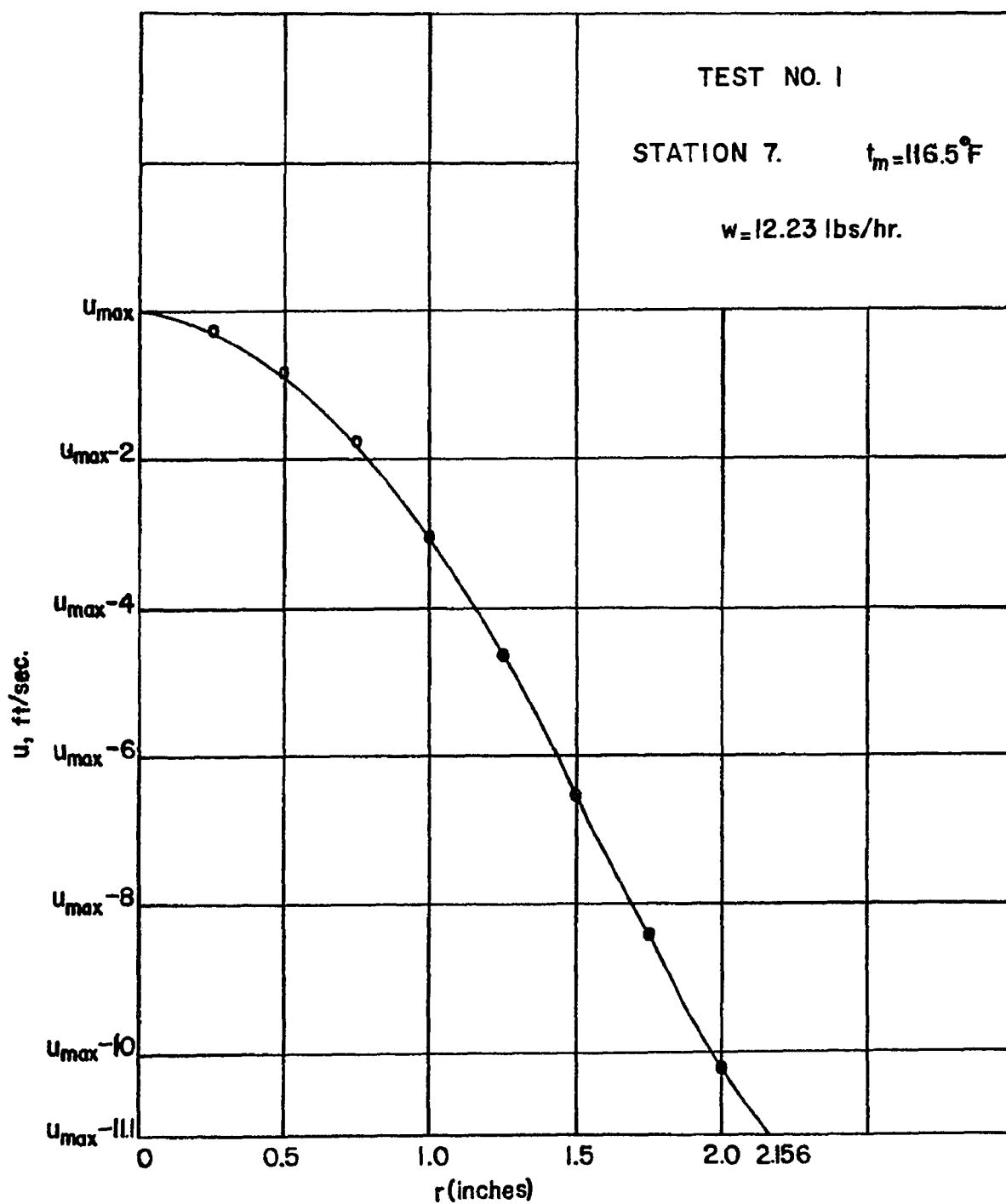
FIGURE 10   PLOT OF u VERSUS r

Test No. 1, Station No. 7, 18 ft. away from Piezometer ring   TABLE 1

Actual Weight flow = 12.23 lbs/hr

Inlet C. L. temp. = $355^{o}F$

Mean temp.   = $116.5^{o}F$

Pressure difference
between Stn. 6 and Stn. 8 = $0.005"$ H_2O

Ambient air temp. = $83^{o}F$

r (in inches)	Temperature of	Buoyant term $\beta g \Delta \theta$ ft/sec^2	Pressure term $\frac{g}{\rho}\frac{\partial P}{\partial x}$ ft/sec^2	f(r) lb/ft sec^2	$\frac{\partial u}{\partial r}$	u in terms of u_{max}	u/u_{max}
0	119.1	2.1407	1.781	0	0	u_{max}	1.0
0.25	119.1	2.1407	1.781	-0.0005	-19.54	u_{max} - 0.230	0.98
0.50	118.8	2.1229	1.780	-0.00095	-37.14	u_{max} - 0.799	0.93
0.75	118.5	2.1051	1.7796	-0.00136	-53.2	u_{max} - 1.736	0.848
1.00	118.5	2.1051	1.7796	-0.00181	-70.4	u_{max} - 3.040	0.733
1.25	117.1	2.0221	1.7753	-0.00172	-82.77	u_{max} - 4.68	0.589
1.50	115.9	1.9509	1.7717	-0.00150	-89.53	u_{max} - 6.50	0.429
1.75	113.7	1.8205	1.7648	-0.00054	-89.94	u_{max} - 8.38	0.265
2.00	110.765	1.4647	1.7465	+0.00320	-67.9	u_{max} -10.20	0.105

33
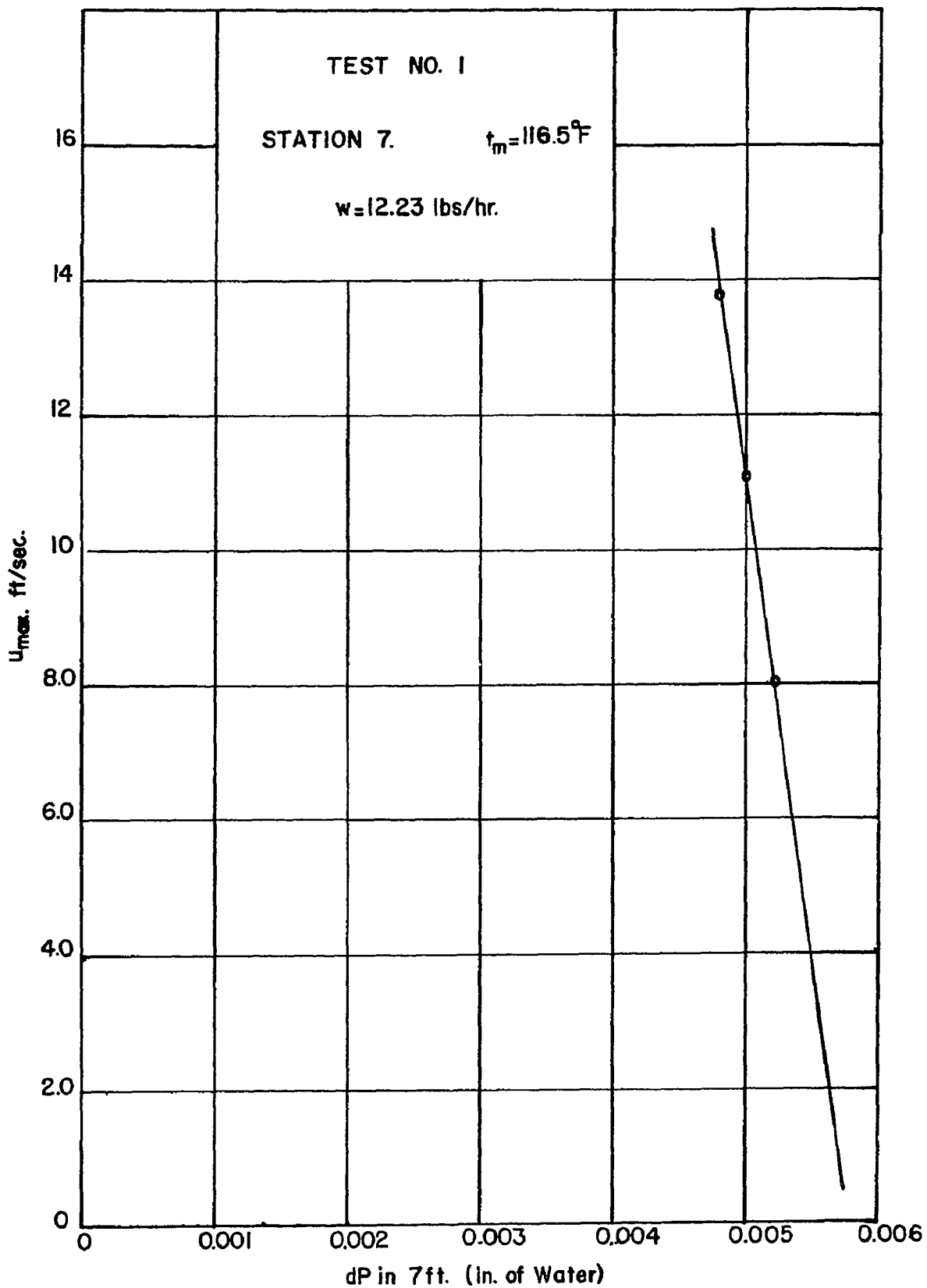
FIGURE 11   PLOT OF u_{max} VERSUS dP
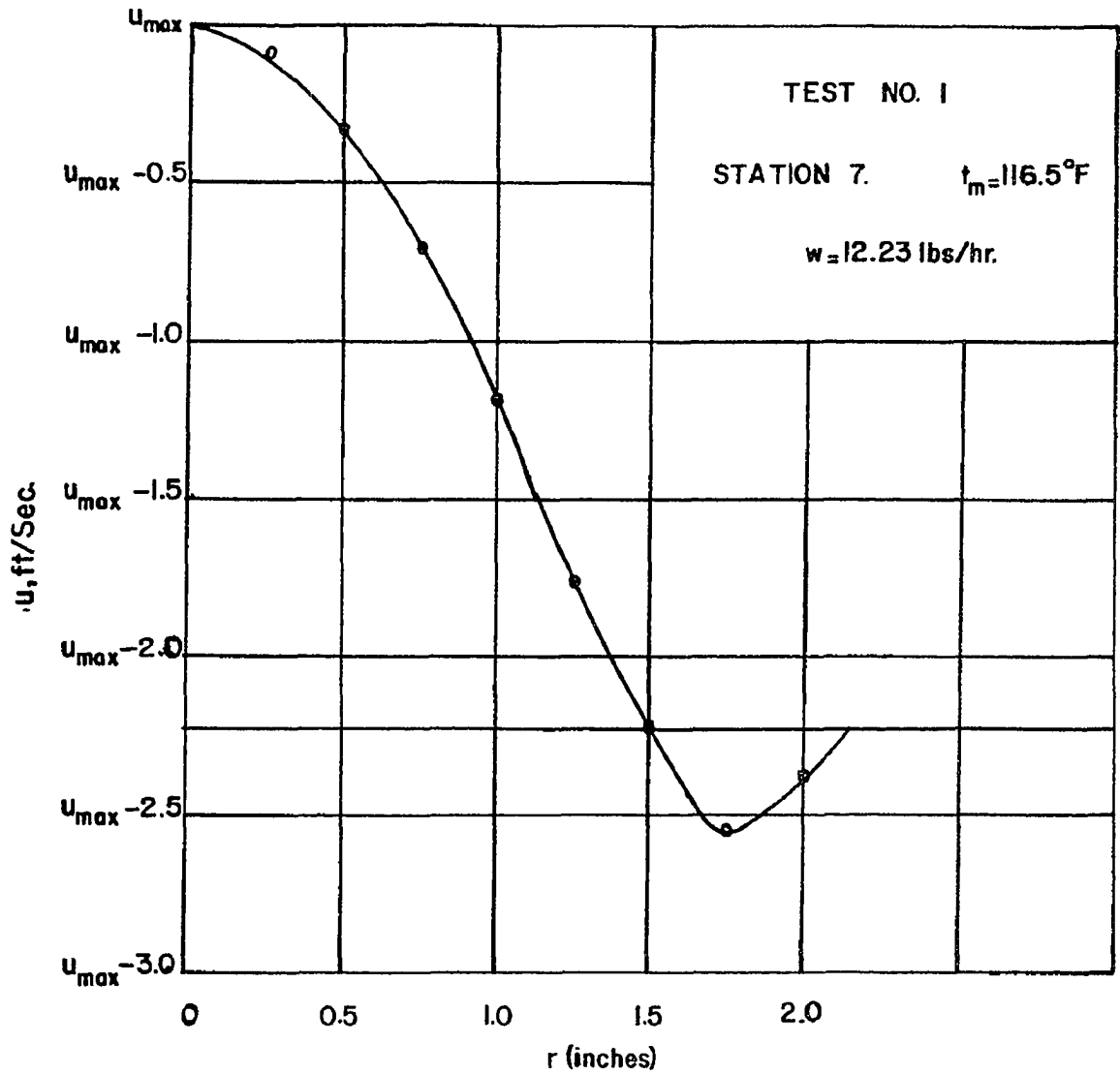
FIGURE 12   PLOT OF u VERSUS r

CHAPTER VI

EXPERIMENTAL RESULTS

The purpose of the present investigation was to study the non-isothermal flow of air in a vertical pipe and to observe the variation of temperature along the radius at various cross-sections, as well as, along the vertical axis at low velocities of flow. These temperature profiles at various cross-sections were used to solve the momentum equation to get the velocity profiles. The following weight flows and inlet centre line temperatures at the piezometer ring were selected to cover a range of Reynolds numbers between 750 and 1700.

Test No.	1	2	3	4	5
W lbs/hr	12.23	17.15	17.20	19.17	22.22
t_i °F	355	460	542	568	300

It was also decided to run a few tests for the higher velocities of flow (i.e. higher Reynolds numbers) for the sake of comparison of temperature variations. The following weight flows and inlet centre line temperatures were selected:

Test No.	6	7	8	9	10	11
W lbs/hr	75.66	76.22	75.28	180.93	176.9	179.1
t_i °F	574	460	355	484.3	360	300

36

First, the opening at the fan inlet was adjusted for the required weight flow. This was observed from the measuring station. The required inlet temperature at the level of the piezometer ring was then adjusted by adjusting the furnace heating elements and the variac. It took four to five hours for the inlet temperature to reach a steady state condition.

For each run, the following readings were taken --

(i) Velocity pressure at the centre line of the measuring station.

(ii) Centre line inlet temperature at the piezometer ring.

(iii) Pressure at the piezometer ring.

(iv) The temperature at each station at various r's, from the 2nd station to the 10th station.

(v) Ambient air temperature at various heights along the axis of the vertical pipe.

(vi) Temperature of the air coming out of the fan.

(vii) Surface temperature at each station.

(viii) Barometric pressure.

(ix) The pressure difference between stations.

(x) An incidental reading of the temperature of the furnace walls to ensure against overheating.

The variation of mean temperature t_m, the centre line temperature t_c and the wall temperature t_w along the vertical axis for various inlet centre line temperatures and various weight flows are shown in figures 13 to 21.

Temperature profile at a cross-section --

Figure 22 shows the temperature profiles for three different Reynolds numbers 1261, 5240 and 11263. All these profiles are for a cross-section 20 ft. (55 diameters) from the entrance. They are for the same ratio of $\frac{t_w}{t_m}$ 0.69. As can be seen from figure 22, as the Reynolds number increases, the temperature profile gets sharper. These curves are drawn from actual measured temperatures at various radii for different weight flows.

FIGURE 13   PLOT OF t_m VERSUS X (N_{Re} = 750 - 1700)
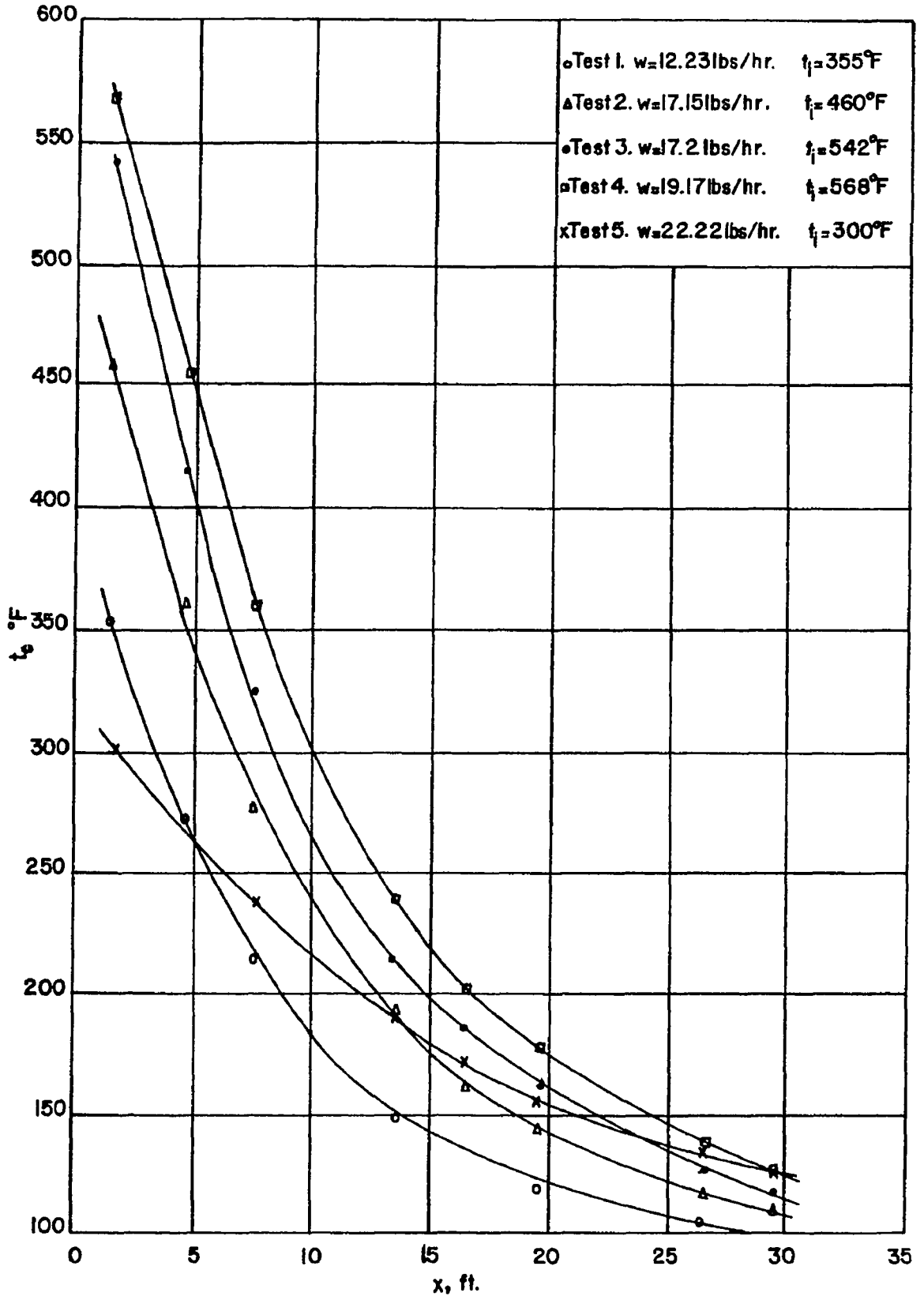
FIGURE 14   PLOT OF t_c VERSUS X (N_{Re} = 750 - 1700)

The legend in the figure reads:

oTest I. w=12.23lbs/hr. t_i=355°F
▲Test 2. w=17.15lbs/hr. t_i= 460°F
•Test 3. w=17.2 lbs/hr. t_i=542°F
□Test 4. w=19.17lbs/hr. t_i=568°F
xTest 5. w=22.22lbs/hr. t_i=300°F

FIGURE 15   PLOT OF t_w VERSUS X (N_{Re} = 750 - 1700)

FIGURE 16   PLOT OF t_m VERSUS X (N_{Re} = 3950 - 5300)

Legend within figure:

o Test 6.   w=75.66 lbs/hr. t_i=574°F

□ Test 7.   w=76.22 lbs/hr. t_i=460°F

x Test 8.   w=75.28 lbs/hr. t_i=355°F

Y-axis: t_m °F

X-axis: X, ft.

FIGURE 17   PLOT OF t_c VERSUS X (N_{Re} = 3950 - 5300)

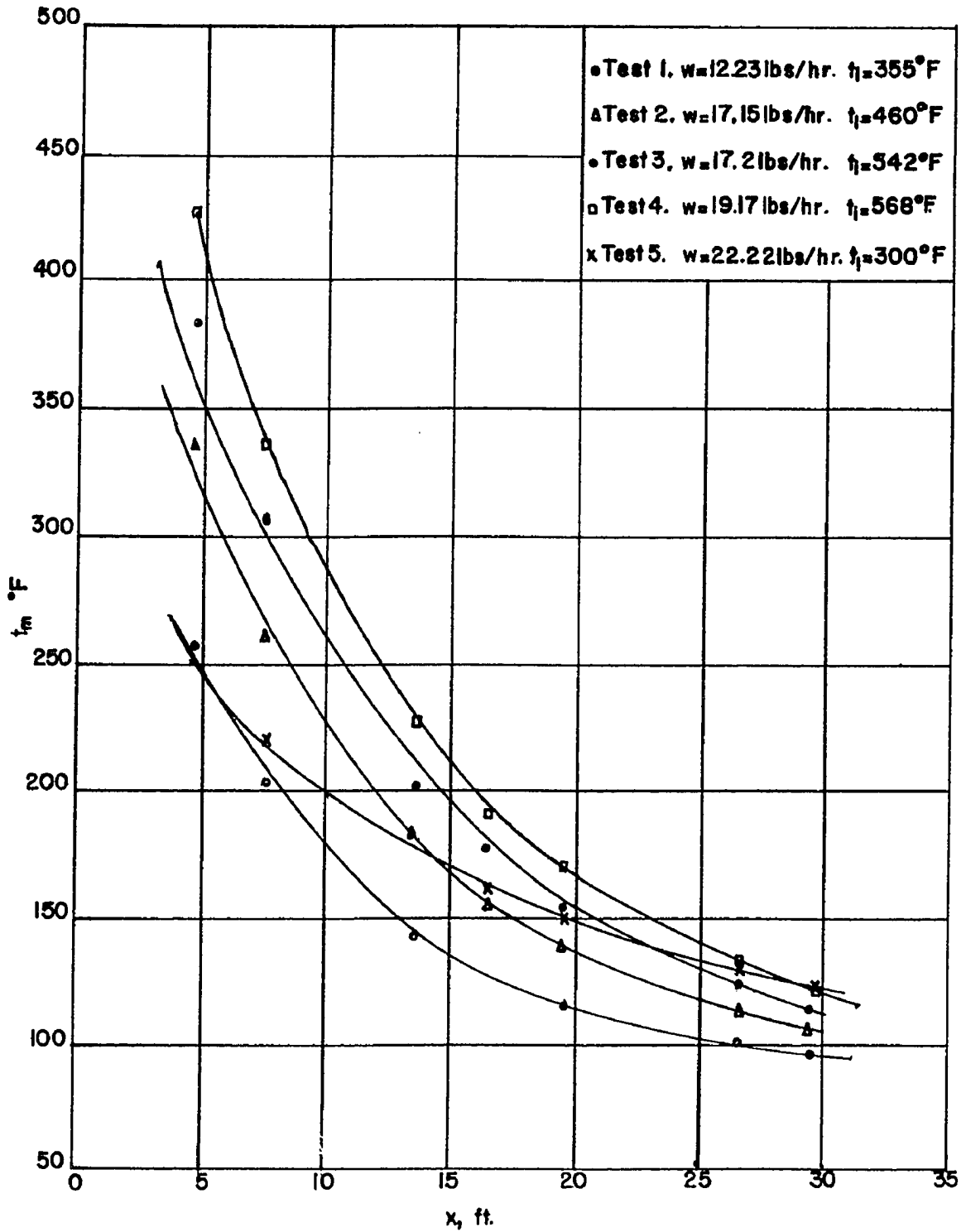FIGURE 18   PLOT OF t_w VERSUS X (N_{Re} = 3950 - 5300)
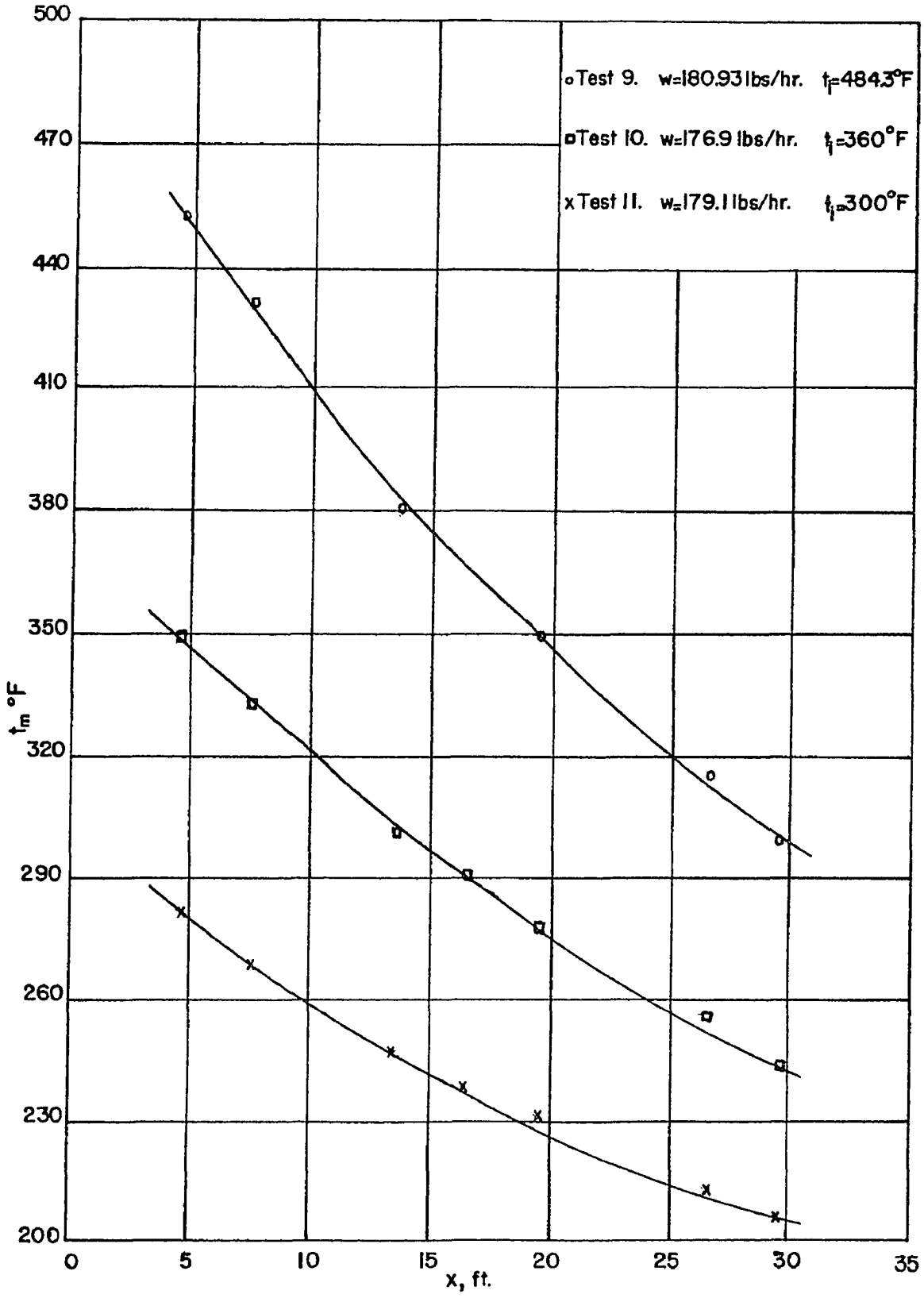
FIGURE 19   PLOT OF t_m VERSUS X $(N_{Re} = 9800 - 12200)$
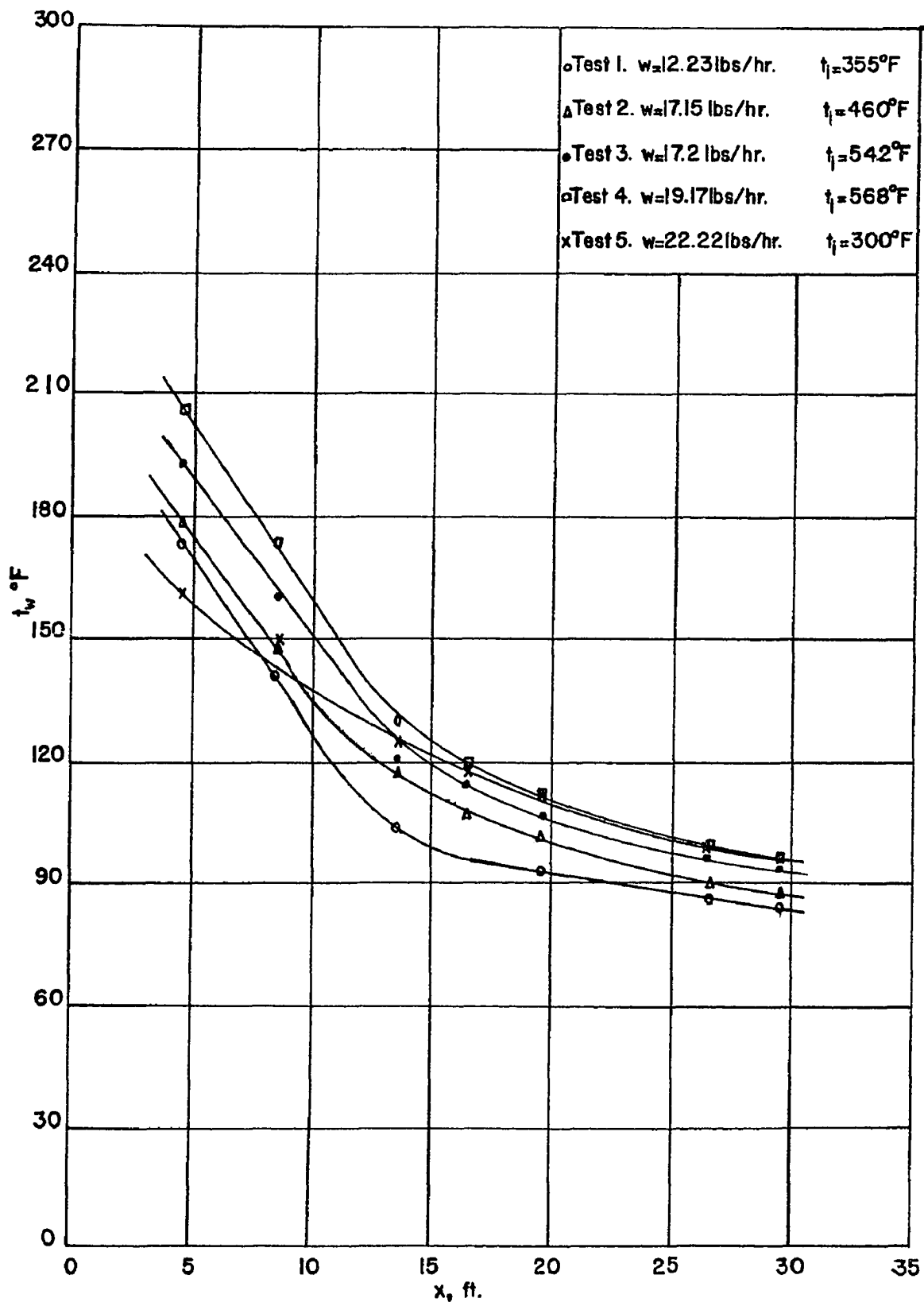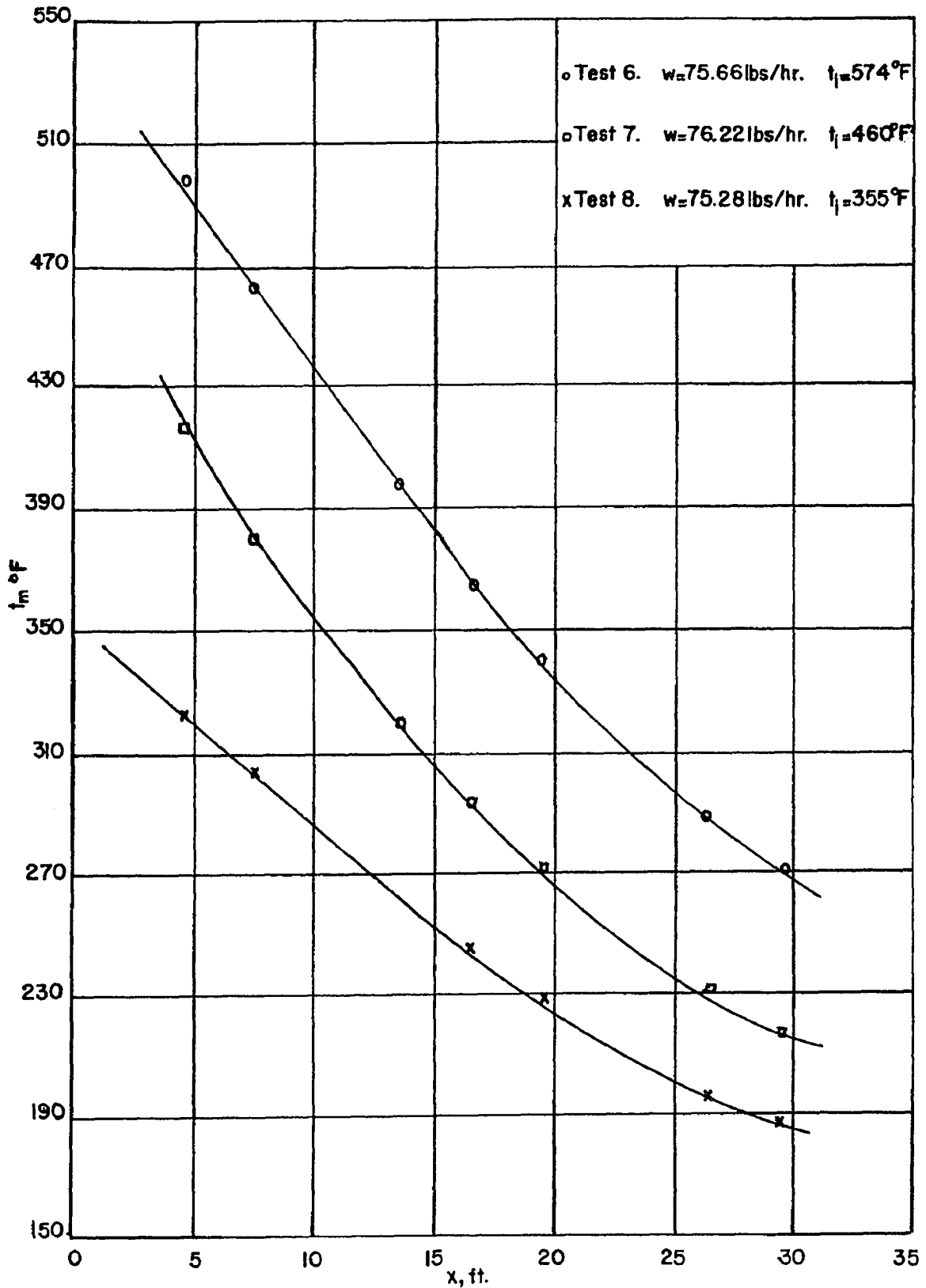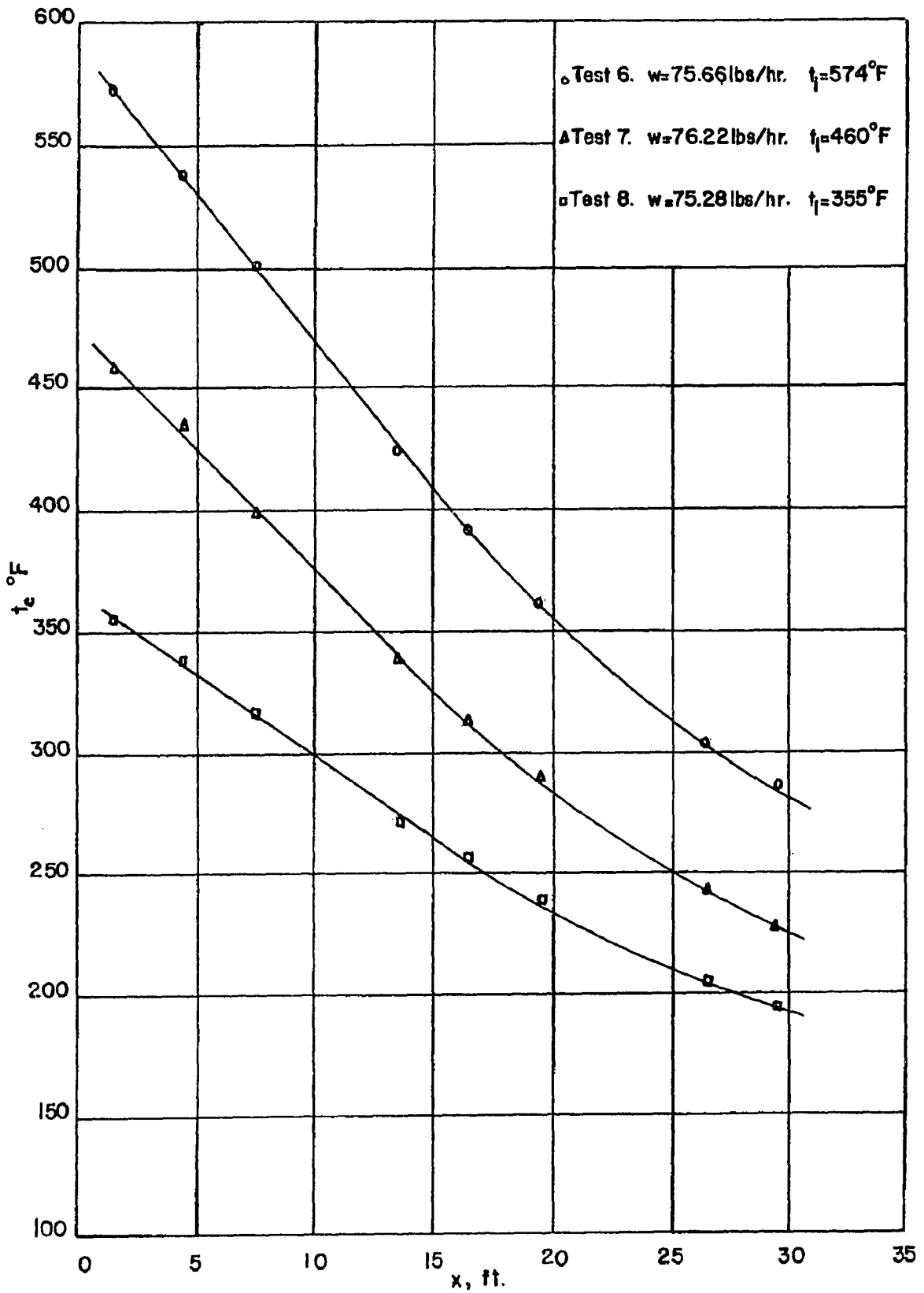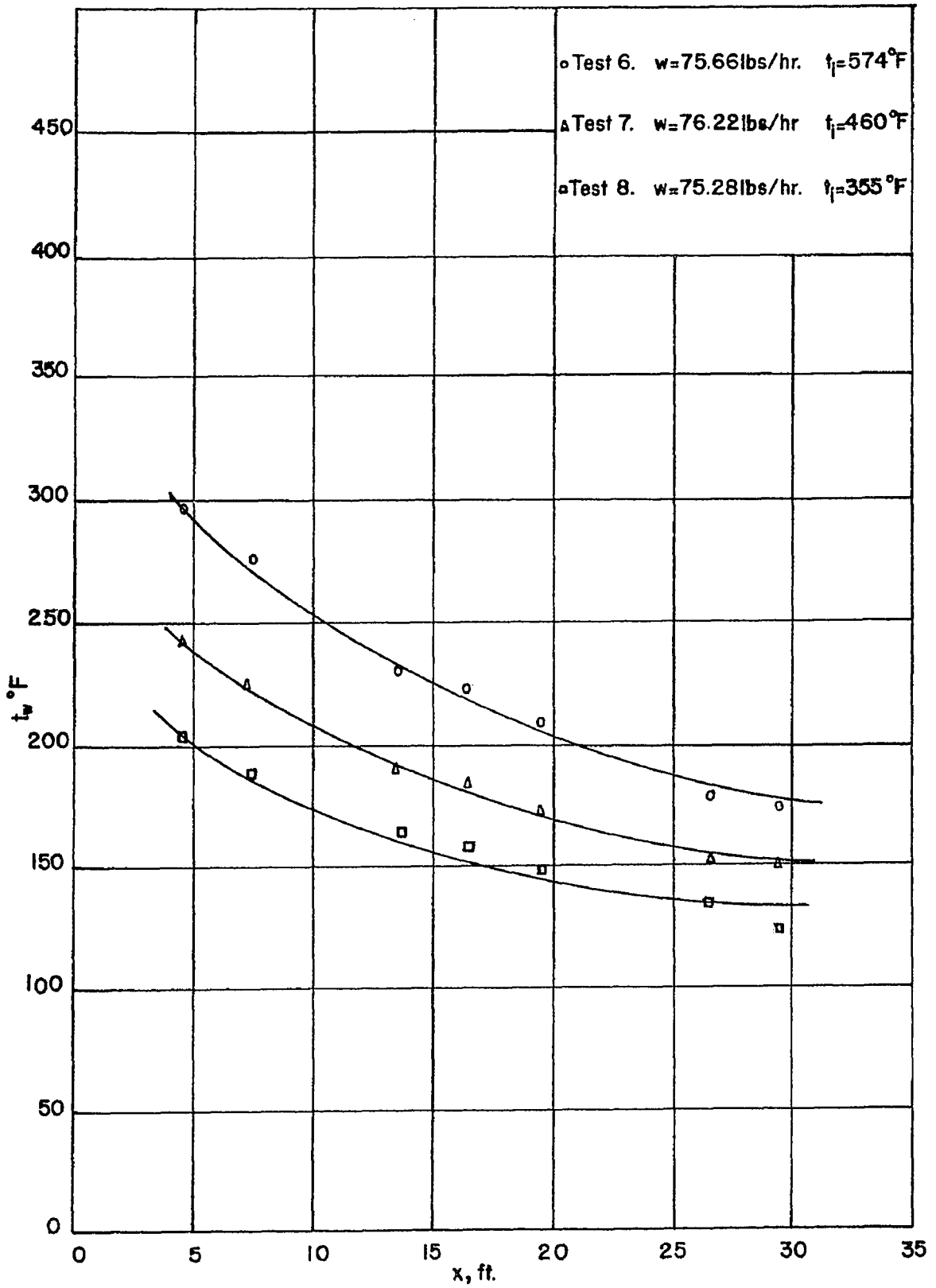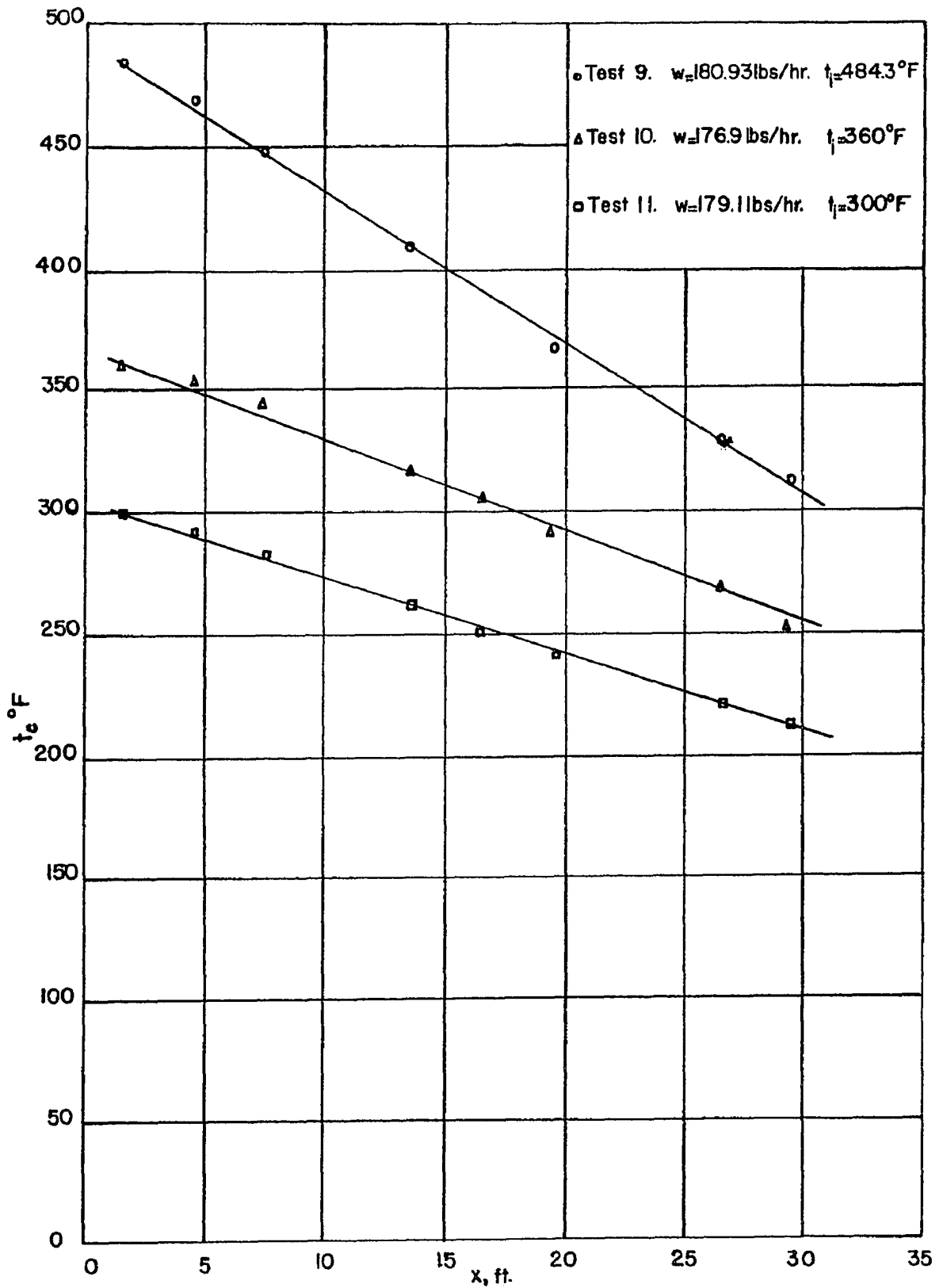
FIGURE 20   PLOT OF t_c VERSUS X (N_{Re} = 9800 - 12200)
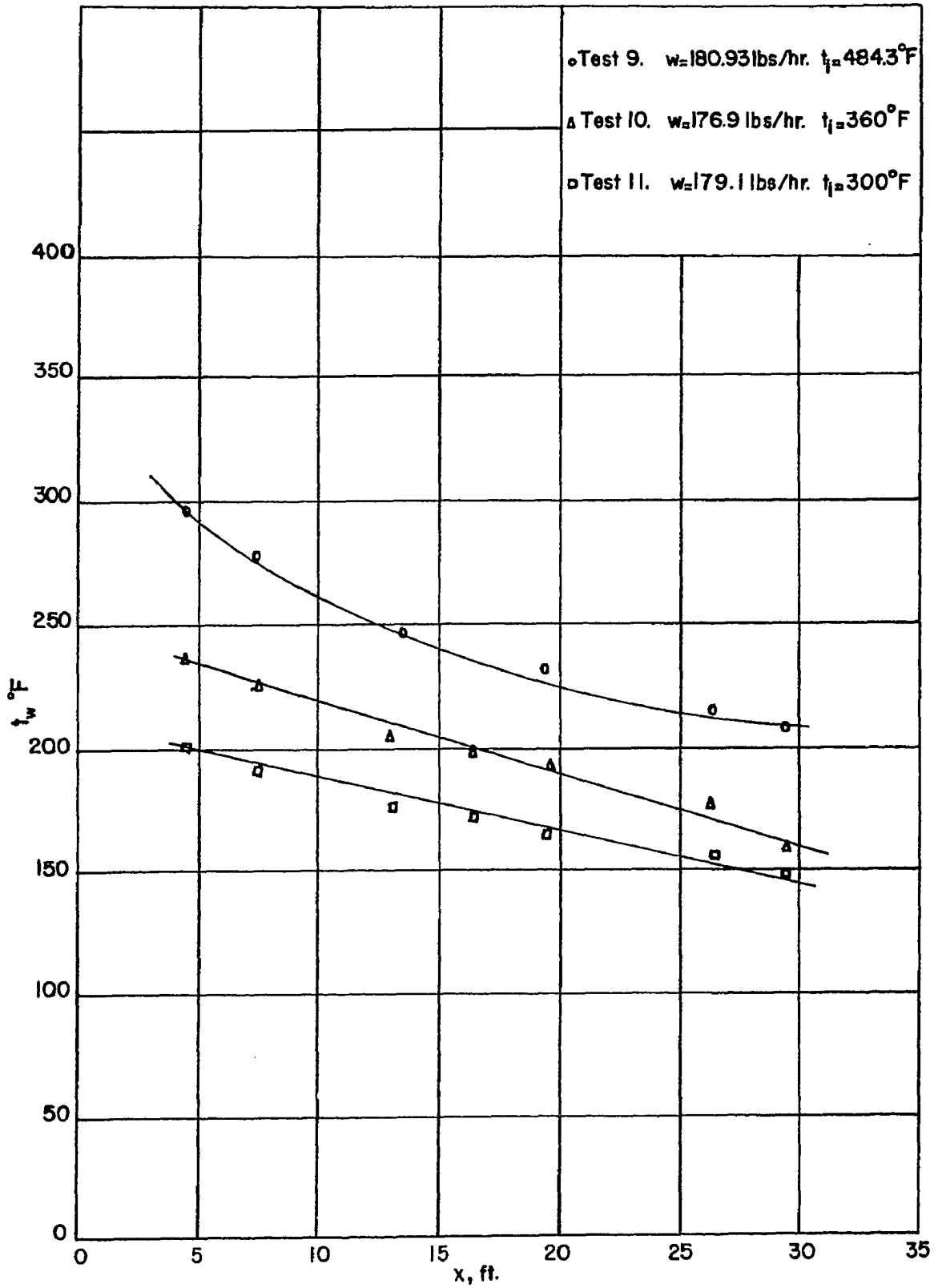
FIGURE 21   PLOT OF t_w VERSUS X (N_{Re} = 9800 - 12200)
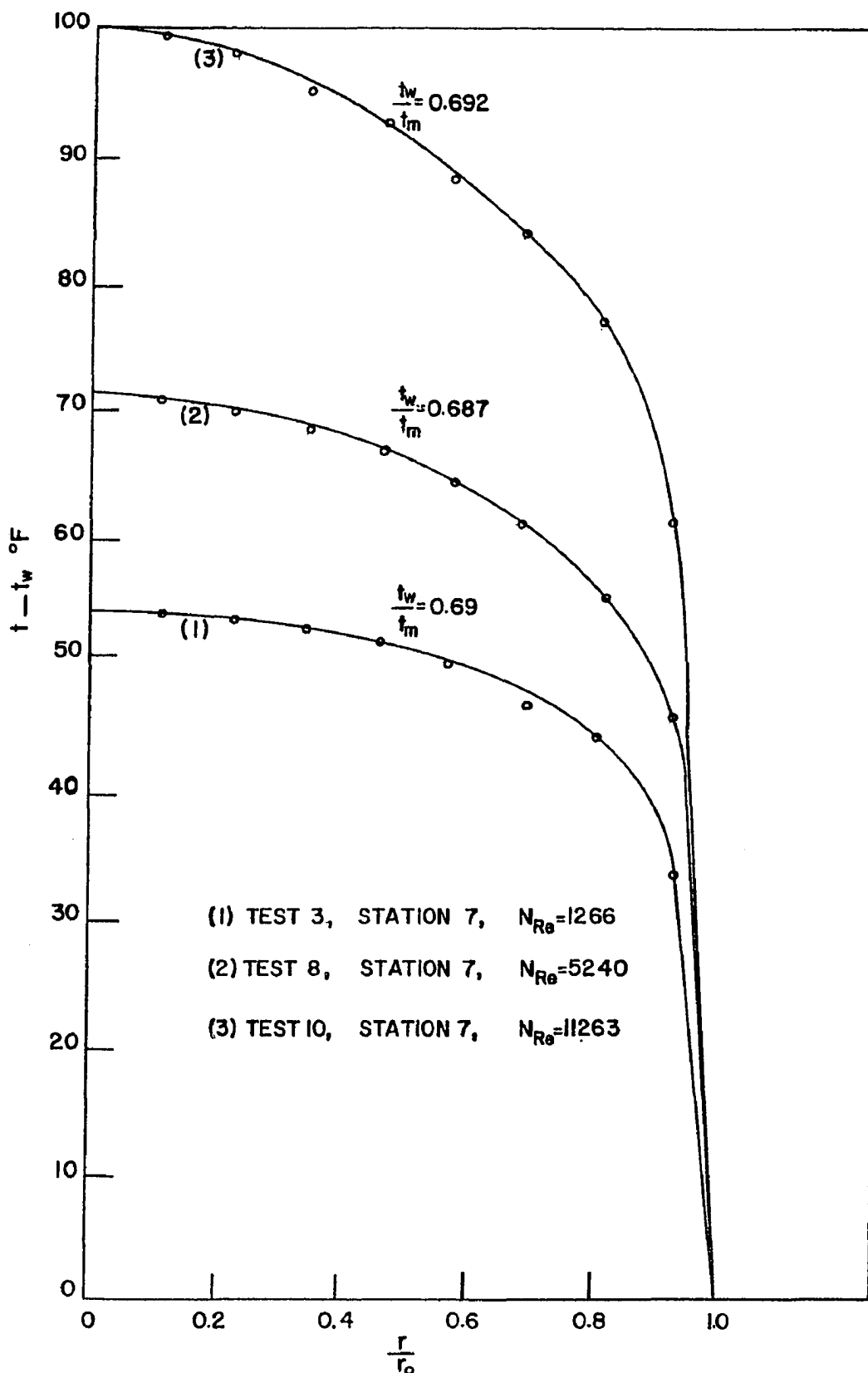
FIGURE 22   PLOT OF $(t - t_w)$ VERSUS r/r_o

CHAPTER VII

DISCUSSION OF RESULTS

(a) Type of flow:

In most of the previous work 2, 3, 7, 9 on non-isothermal
flow of gases in circular pipes, it was assumed that laminar flow
exists up to a Reynolds number of 2000. The laminar flow does
exist up to a Reynolds number of approximately 2000 for isothermal
flow, which we know from Moody's diagram. Therefore, when this
investigation was started, we also assumed that laminar flow
existed up to a Reynolds number of 2000 for non-isothermal flow
of gases in pipes. When smoke was introduced into the pipe at
x = 20 ft. (55 diameters from the entrance) at various radii, it
was noticed that the smoke did not go up in a stream line but in
a wavy shape which indicated the formation of eddies. The presence
of eddies meant that the flow was no longer laminar. The hot wire
probe 55A22 connected to DISA Constant Temperature Anemometer
55A01 was introduced into the pipe and it was observed that the
needle of the Bridge DC Voltage Meter was fluctuating which con-
firmed the presence of eddies in the flow.

Brown (24) points out from his experimental results on water
flowing in a vertical tube with density increasing from bottom to
top, the flow was generally turbulent even for Reynolds numbers as
low as about 50. The tube diameter in his work was 15 mm.
Hanratty (12) also observed in his experiments with a tube of
2.19 cm. (ID) with cooling in upflow that a Reynolds number of 50
and a temperature difference of $10^{\circ}F$ between a heat transfer
medium and the incoming water produced complete turbulence through-
out the flow field. He actually introduced a jet of dye into the
stream and observed its flooding with the flow field.

48

(b) <u>Velocity Profile</u>:

As mentioned above, the eddies caused by natural convection were noticed at low Reynolds numbers. Because of these eddies, the introduction of the eddy diffusivity term in the momentum equation was necessary. In the normal turbulent flow which exists at a Reynolds number of 6000 or higher depending upon the roughness of the pipe, the eddy diffusivity is much higher than the laminar kinematic viscosity. In the present investigation, the Reynolds numbers were low, the eddy diffusivity was 5 to 15 times higher than the laminar kinematic viscosity. The turbulence caused by natural convection at low Reynolds numbers is a turbulence of low intensity. A turbulence reading was not obtainable on the hot-wire anemometer, although a rather slow velocity fluctuation was noted. Some scientists (25) call it a non-laminar flow.

Even though there were eddies formed in the flow, it was still expected that the buoyant effect might predominate because of the large difference in temperature between the air inside the pipe and the ambient air. Due to this buoyant effect the velocity profile still might have a tendency to elongate in the central region of the pipe as compared to the isothermal parabolic velocity profile.

The velocity profiles obtained from the numerical solution of the momentum equation by making use of the experimental temperature profiles are shown in Appendix B. It may be observed from the velocity profiles that the peak is sharpened in the central region of the tube as compared to the isothermal laminar velocity profile. Since the velocity profile is elongated in the central region of the pipe, a greater quantity of air will flow in this region. This will reduce the flow and hence the velocity near the wall because of continuity. This ultimately reduces the slope of the velocity profile near the wall. This effect was noticed in practically all the velocity profiles for non-isothermal flow in the present work.

(c) <u>Temperature variation along the axis</u>:

If we carefully observe the variation of mean temperature t_m along the vertical axis in figures 13, 16 and 19, we will notice

that for small weight flows i.e. Reynolds numbers below 2000,
the curves are very steep for the first few feet (figure 13) and
then tend to flatten out. Whereas for moderate flows (figure 16)
i.e. Reynolds numbers between 3000 and 6000, the mean temperature
curves are not as steep as for low weight flows (figure 13).
Here the curves tend to flatten out at very near the outlet.
Accordingly, for higher weight flows i.e. higher Reynolds numbers
the mean temperature curves drop less rapidly and are less steep
than the previous curves. The lower the velocity of flow, the
higher the temperature drop and the higher the velocity of flow
the lower the temperature drop.

Exactly the same is true for the variation of centre line
temperature t_c and the wall temperature t_w along the vertical
axis x as it has been said for the variation of t_m. This can be
easily observed in figures 14, 17, 20 and 15, 18, 21 respectively.

(d) Heat transfer characteristics:

Figure 25 shows the plot of local Nusselt number N_{Nux} as a
function of $\frac{x}{d_o} \frac{1}{N_{Re} N_{Pr}}$. The curves 1 and 2 were calculated by
W. M. Kays (23) by using the velocity distribution given by
Langhaar for laminar flow. The curve 1 shows the N_{Nux} as a function
of $\frac{x}{d_o} \frac{1}{N_{Re} N_{Pr}}$ for constant wall temperature and the curve 2 is for
constant heat input. These curves are for air being heated in a
circular tube and are valid for Reynolds number up to 2000. Laminar
flow was supposed to exist up to this Reynolds number. The curve 3
is the representation of our experimental work and the range of
Reynolds number was between 750 and 1600. We observed turbulence
even at these small Reynolds numbers as mentioned in previous
sections. In our case, neither the wall temperature nor the rate
of heat loss was constant.

The curves 1 and 2 for heating and the curve 3 for cooling
seem to be almost parallel, with the Nusselt number being highest
in both cases. The Nusselt number decreases asymptotically in the
direction of flow for all the three curves. The curves 1 and 2
were drawn from theoretical results by Kays (23) for laminar flow

with heating from the entrance and the curve 3 is drawn for cooling from the entrance from our experimental work. The curve 3 is higher than the curves 1 and 2 even though the Reynolds numbers are in the same range. The reason being that we observed turbulent eddies at these Reynolds numbers, whereas Kays assumed that the laminar flow exists at these Reynolds numbers. According to Moody's chart, the laminar flow exists up to a Reynolds number of 2000, but it is true only for isothermal flow. Due to the formation of eddies, the Nusselt number will be expected to have a higher value. From figure 25 it is observed that the Nusselt number is higher in our case as compared to curves 1 and 2.

The Nusselt number has been defined as

$$N_{Nux} = \frac{q(x)}{(t_m - t_w) A} \frac{2 r_0}{k}$$

The Reynolds number has been evaluated at the mean temperature t_m, at the section under consideration.

(e) Non-isothermal friction factor:

The velocity profile for non-isothermal flow is elongated in the centre and flatter at the wall as compared to the isothermal laminar velocity profile. If the flow was laminar for both cases (i.e. isothermal and non-isothermal) the flatter slope at the wall would result in a lower friction factor for non-isothermal case. Since the flow in our case was not strictly laminar, there would be a laminar sub-layer and because of that the velocity gradient at the wall was difficult to predict accurately.

The friction factor for non-isothermal flow was calculated from the following two equations --

$$\frac{dP_g}{dx} + \frac{dP_B}{dx} + \frac{dP_f}{dx} = 0 \tag{7-1}$$

$$f_n = \frac{2 g d_o}{\rho_m u_m{}^2} \frac{-dP_f}{dx} \tag{7-2}$$

The first equation (7-1) is just the balance of forces, the first term represents the pressure force, the second term the buoyant force and the last term the viscous force or the pressure drop due to friction. The pressure drop dP_g was measured experimentally between two stations 6 ft. apart. dP_B was also known since we measured the temperature profile at each section. So knowing the first two terms, it was easy to evaluate the last term dP_f/dx. After evaluating dP_f/dx for various stations, its numerical value was substituted into equation (7-2) to calculate the non-isothermal friction factor f_n. The isothermal friction factor f_i was calculated based on a fluid temperature equal to t_m of the non-isothermal case and the same weight flow. The plot of f_n/f_i versus N_{Gr} is shown in figure 23.

Figure 24 was then plotted making use of the information from figure 23. This shows the usual plot of f versus Reynolds number. The curves for the various Grashof numbers in the range of 0×10^6 and 5×10^6 are shown in figure 24. Figure 24 shows the correlation of f, N_{Re} and N_{Gr}.

(f) Values of eddy diffusivity ϵ_M:

As mentioned in section (a) that the eddy action was noticed in the flow and because of that, it was necessary to evaluate eddy diffusivity ϵ_M for the calculation of the velocity profiles. The eddy diffusivity ϵ_M was added to the kinematic viscosity to account for the eddy action. The formation of eddies was due to natural convection phenomenon and therefore dependent on the temperature difference. The values found for ϵ_M should therefore be related to the temperature difference between the air inside the pipe and the ambient air. The plot of ϵ_M/ν versus $\frac{t_m - t_o}{t_o}$ is shown in figure 26. From this figure, it is evident that as $(t_m - t_o)$ increases, the eddy diffusivity ϵ_M also increases.
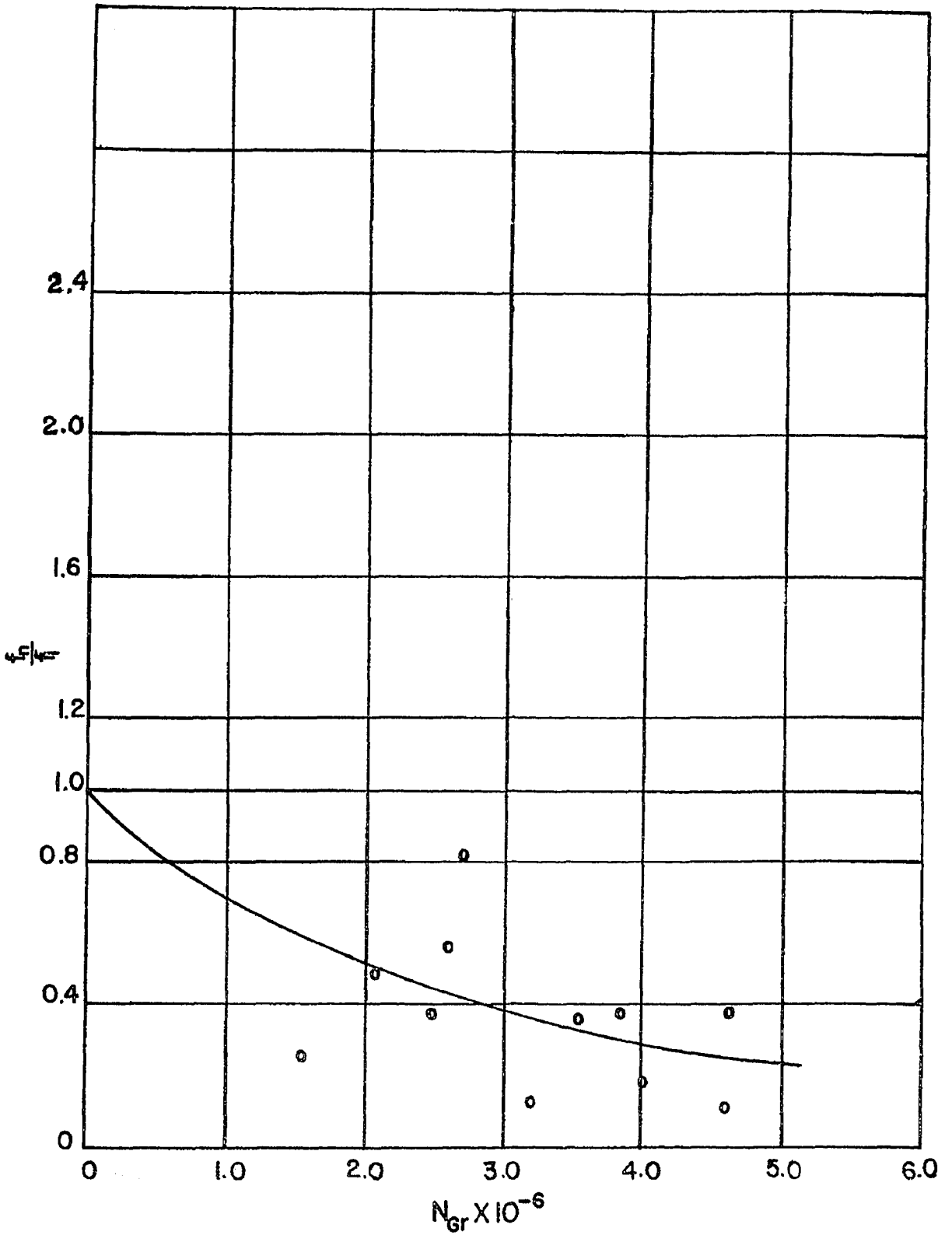
FIGURE 23   PLOT OF f_n/f_1 VERSUS GRASHOF NUMBER
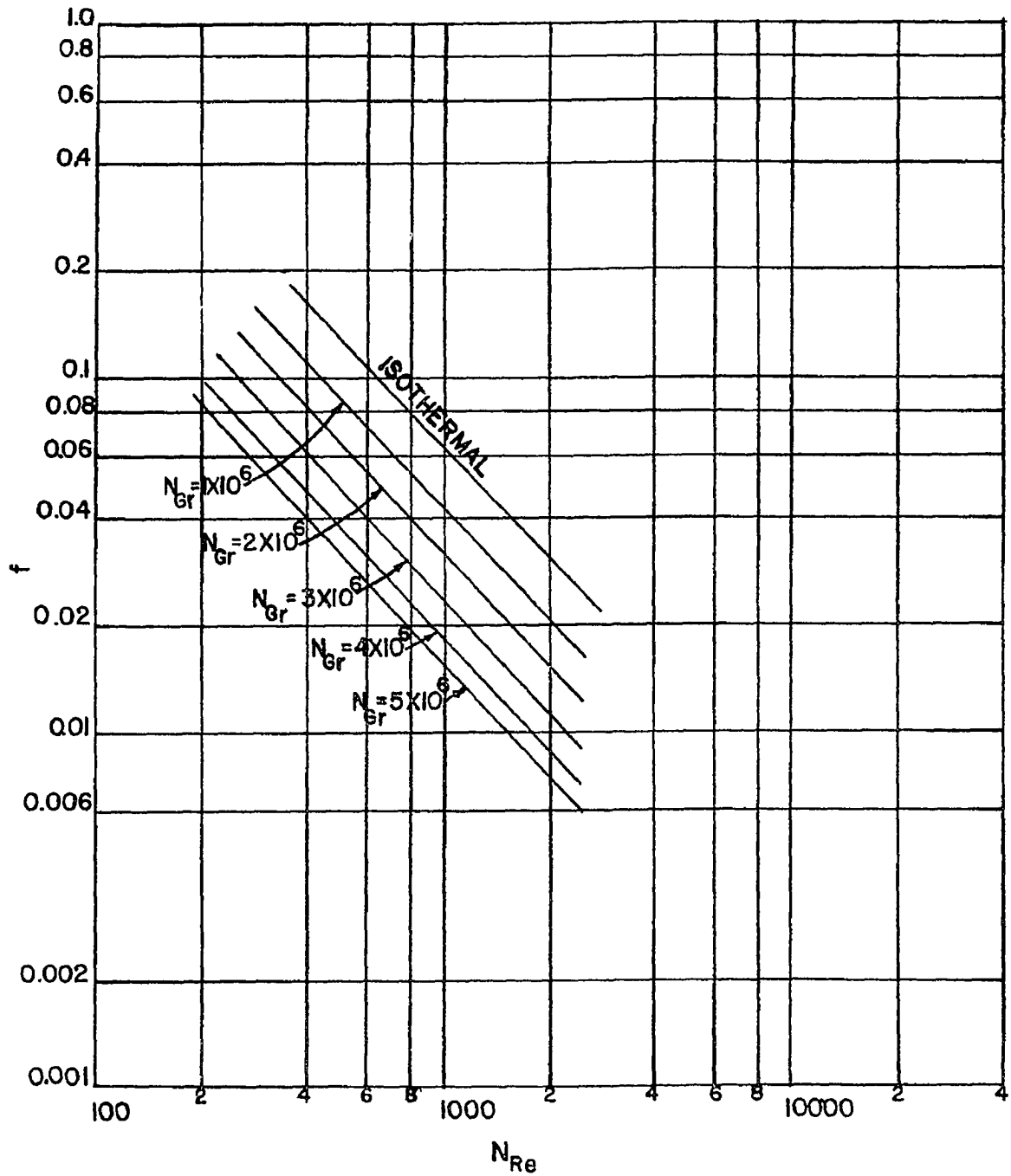
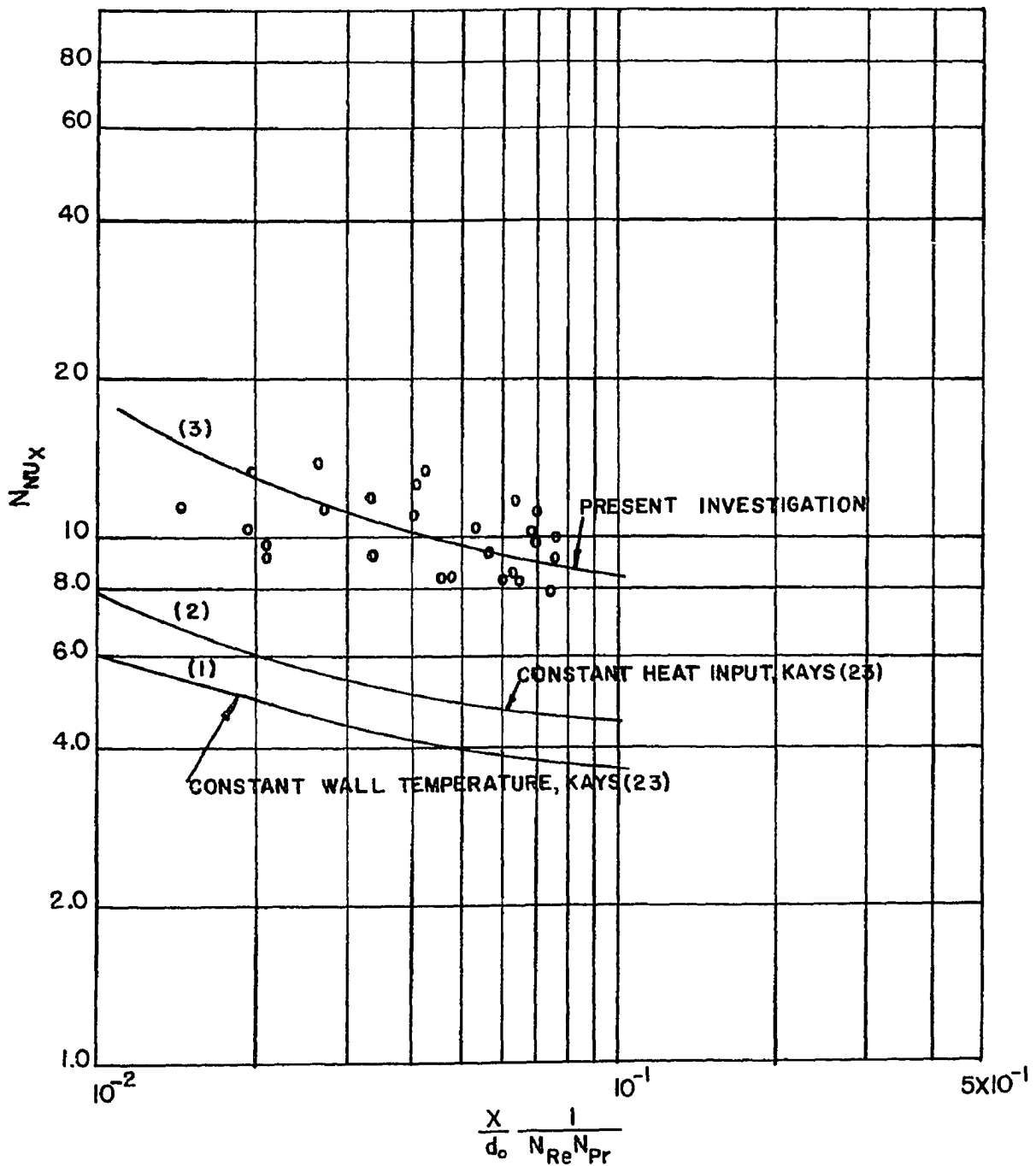FIGURE 24   PLOT OF FRICTION FACTOR VERSUS REYNOLDS NUMBER

FIGURE 25   PLOT OF LOCAL NUSSELT NUMBER VERSUS $\frac{X}{d_o}$ $\frac{1}{N_{Re} N_{Pr}}$
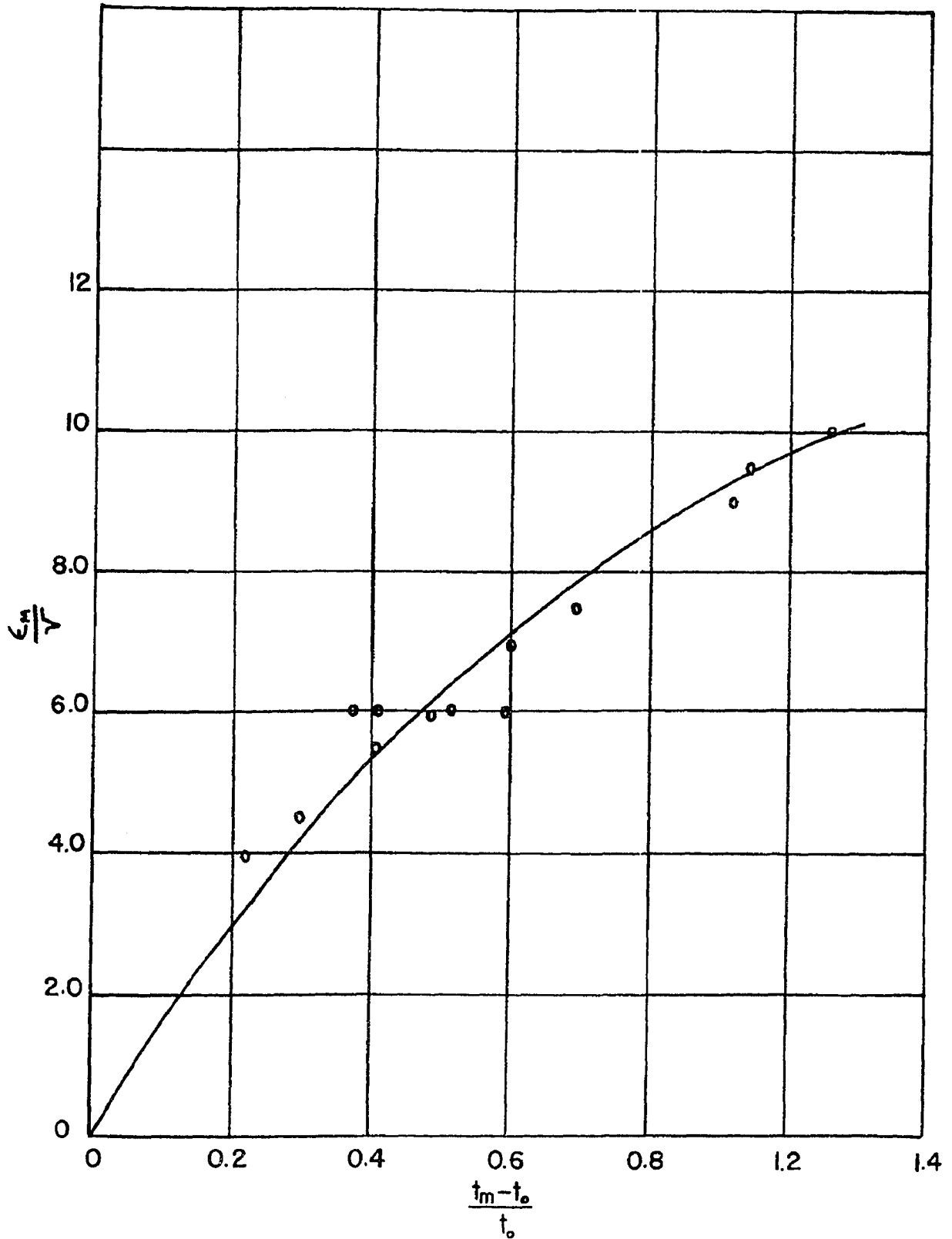
FIGURE 26   PLOT OF $\dfrac{\epsilon M}{\nu}$ VERSUS $\dfrac{t_m - t_o}{t_o}$

CHAPTER VIII

CONCLUSIONS

In the present work, the main purpose was to study the non-isothermal flow of air in a vertical pipe at low velocities and observe the effects of buoyant force on the velocity profiles. The attempt was also made to investigate the effect of temperature on the eddy diffusivity ϵ_M. We also wanted to investigate the effect of non-isothermal flow on the value of the friction factor. As a result of the present investigation, the following conclusions may be stated --

(i) The flow was observed to be non-laminar at the lowest Reynolds number of 750 used in the present work. Brown (24) and Hanratty also observed turbulence for the non-isothermal flow of water in vertical pipes at Reynolds number as low as 50.

(ii) The turbulence associated with higher velocity flow appeared as predicted from Moody's Chart above a Reynolds number of 2000. There was a well defined region in which there was intermittent turbulent and laminar flow and at still higher Reynolds numbers, there was continuous turbulence. The thermal turbulence and the mechanical turbulence were separate and distinct one from the other.

(iii) In the case of air which is above the temperature of the surroundings and flowing upward in a vertical pipe with heat loss, the velocity profile will be more elongated than the profile in the case of isothermal laminar flow.

(iv) As a result of an elongated profile, the velocity gradient at the wall of the pipe is less than for isothermal laminar flow.

(v) The eddy diffusivity term ϵ_M added to the kinematic viscosity appeared to be a satisfactory method of making allowance for the thermal turbulence. The value of $\frac{\epsilon_M}{\nu}$ was related to the dimensionless temperature difference between the fluid and the surroundings.

(vi) The calculated Nusselt number (N_{Nux}) from this experimental work (with boundary condition - heat loss varying along the axis) was higher in the same range of Reynolds numbers than the one calculated from the analytical solution with the assumption that laminar flow exists up to a Reynolds number of 2000 for non-isothermal flow and different boundary conditions [(i) constant wall temperature. (ii) constant heat input.].

(vii) The non-isothermal friction factor was a function of Reynolds number and Grashof number at Reynolds numbers less than 2000. The non-isothermal friction factor f_n appeared to be less than the isothermal friction factor f_i in all cases within the range of this experimental work.

APPENDIX A

SAMPLE CALCULATION FOR THE SOLUTION OF

MOMENTUM EQUATION FOR TURBULENT FLOW

The calculations presented here are for Station 7, Test No. 1 (the same as that used in Chapter V).

(a) First of all, we solve the energy equation to find the relation between α and ϵ_H. The energy equation is

$$\frac{q_o}{A_o} = -\rho C_p (\alpha + \epsilon_H)(\frac{dt}{dr})_{r=ro} \qquad (4\text{-}6)$$

or
$$\frac{W\Delta t}{\pi DL} = -\rho(\alpha + \epsilon_H)(\frac{dt}{dr})_{r=ro}$$

It was assumed that $\epsilon_H = \epsilon_M$ which is true for $N_{Pr} = 1$ from Prandtl's Analogy. The value of ϵ_H was calculated very close to the wall of the pipe and was assumed as constant across the cross section.

$$\frac{12.23 \times 7.5}{\pi \times \frac{4.5}{12} \times 2} = 0.06722 (\alpha + \epsilon_H) \frac{1 \times 12}{0.1}$$

$$\alpha + \epsilon_H = \frac{6 \times 12.23 \times 7.5}{8 \times 14.13}$$

$$= 5.0 \text{ ft}^2/\text{hr}$$

we know that $\alpha = 0.9697 \text{ ft}^2/\text{hr}$

$$\epsilon_H = 4.03 \text{ ft}^2/\text{hr}$$

$$\frac{\epsilon_H}{\alpha} = 4.16$$

This shows that ϵ_H is 4.16 times α.

59

(b) The function $F(r)$ is

$$F(r) = (-\beta g \Delta \theta + \frac{g}{\rho} \frac{\partial P}{\partial x}) \; (\frac{r}{\epsilon_M + \nu})$$

The ratio ϵ_H/α from the energy equation came out to be 4.16. From Prandtl's Analogy $\epsilon_H/\alpha = \epsilon_M/\nu$ and hence $\epsilon_M/\nu = 4.16$. The weight flow after substituting this value of ϵ_M/ν came out to be higher than the measured value. It was then decided to alter the value of ΔP from 0.005" of H_2O to 0.0052" of H_2O and the weight flow still came out to be higher. When the value of ΔP was still increased above 0.0052" of H_2O, we got a reversal near the wall which as mentioned in Chapter V is not true. So instead of altering ΔP, the value of ϵ_M/ν was increased still further, the weight flow could be made to agree. The value of ϵ_M/ν came out to be 5.5 and the weight flow came very close to the measured value. This appeared to be a very reasonable approach.

At $r = 0.25$"

$$F(r) = (-\frac{1}{543} \times 32.2 \times 36.1 + \frac{32.2}{0.06692} \times \frac{0.0052 \times 62.4}{12 \times 7}) \; \frac{0.25 \times 10^4}{12 \times 6 \times 1.895}$$

$$= -4.88 \; sec^{-1}$$

At $r = 0.5$"

$$F(r) = (-\frac{1}{543} \times 32.2 \times 35.8 + \frac{32.2}{0.06695} \times \frac{0.0052 \times 62.4}{12 \times 7}) \; \frac{0.5 \times 10^4}{12 \times 6 \times 1.895}$$

$$= -9.2 \; sec^{-1}$$

In the same manner, we calculated the values of $F(r)$ at various radii.

(c) Evaluation of $\frac{\partial u}{\partial r}$ --

Using the relation (2-8)

$$r \frac{\partial u}{\partial r} = \int_0^r F(r) \, dr \qquad (2-8)$$

or

$$\frac{\partial u}{\partial r} = \frac{1}{r} \int_0^r F(r) \, dr$$

$$= \frac{1}{r} \left[\int_0^{r_1} F_1(r) \, dr + \int_{r_1}^{r_2} F_2(r) \, dr + \dots \dots \right]$$

To find the value of $\frac{\partial u}{\partial r}$ at each r, we plotted $F(r)$ versus r as shown in figure 28 and found the area under the curve for any required r between $r = 0$ and $r = r_{reqd}$. The numerical values of $\frac{\partial u}{\partial r}$ are shown in Table 2. Then we plotted $\frac{\partial u}{\partial r}$ versus r as shown in figure 29.

(d) Evaluation of velocity at any r --

This part of the calculations was performed in exactly the same way as mentioned in part (c) of Chapter V. The actual values of velocity at various radii are shown in Table 2. The u_{max} came out to be 1.32 ft/sec.

(e) Evaluation of weight flow --

$$(\rho_1 A_1 U_1 + \rho_2 A_2 U_2 + \rho_3 A_3 U_3 + \dots \dots \dots) = W$$

or

$$W = u_{max}(0.000023 + 0.00017 + 0.000337 + 0.000443 + 0.000497 +$$

$$0.000483 + 0.000396 + 0.000249 + 0.0001)$$

$$= 1.32 \times 3600 \times 0.0027$$

$$= 12.83 \text{ lbs/hr}$$

The actual weight flow is 12.23 lbs/hr. The error is only +5% which is tolerable. This much error in weight flow will not make any appreciable change in the shape of the velocity profile.

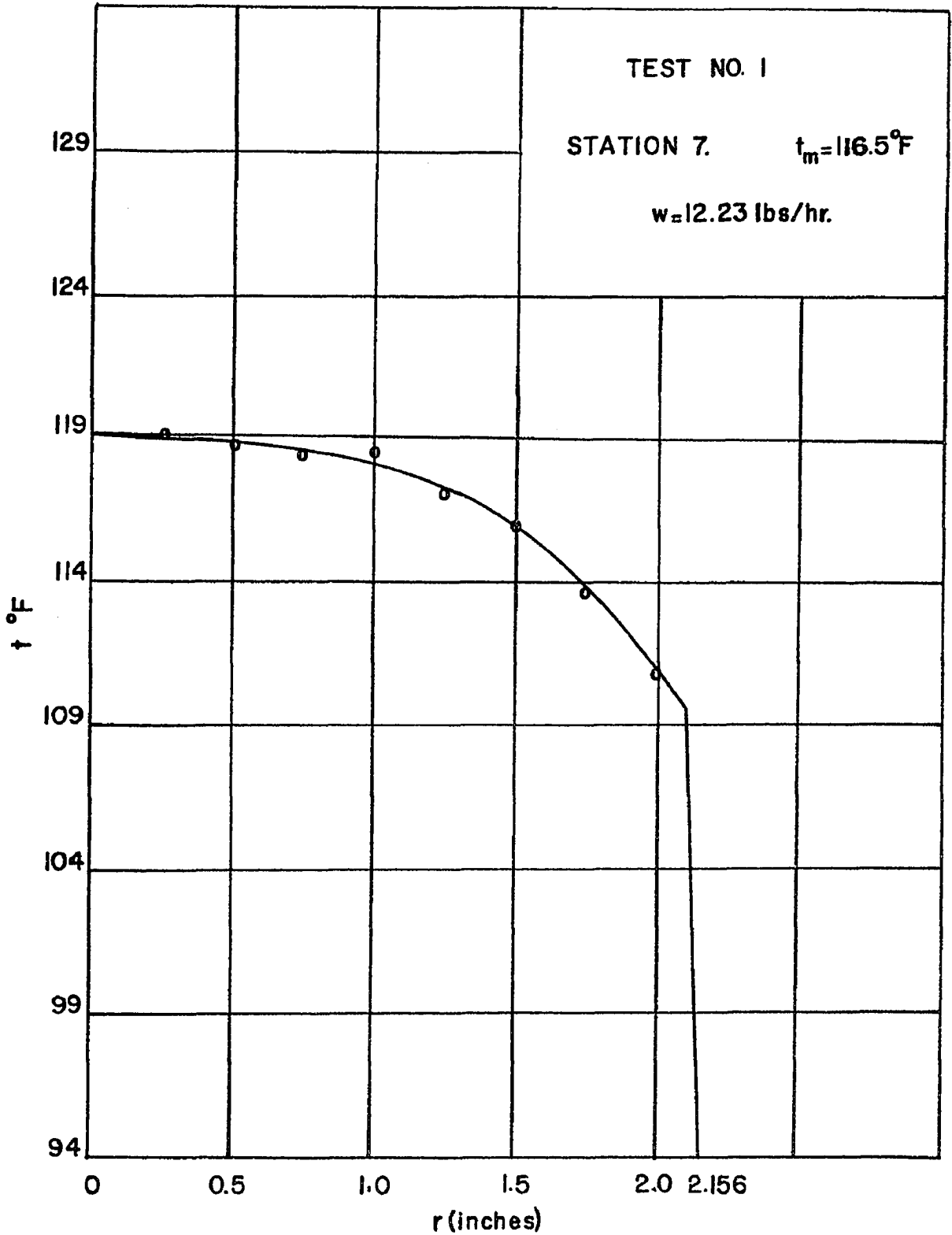FIGURE 27 PLOT OF t VERSUS r

TEST NO. I

STATION 7. t_m=116.5°F.   w=12.23 lbs/hr.
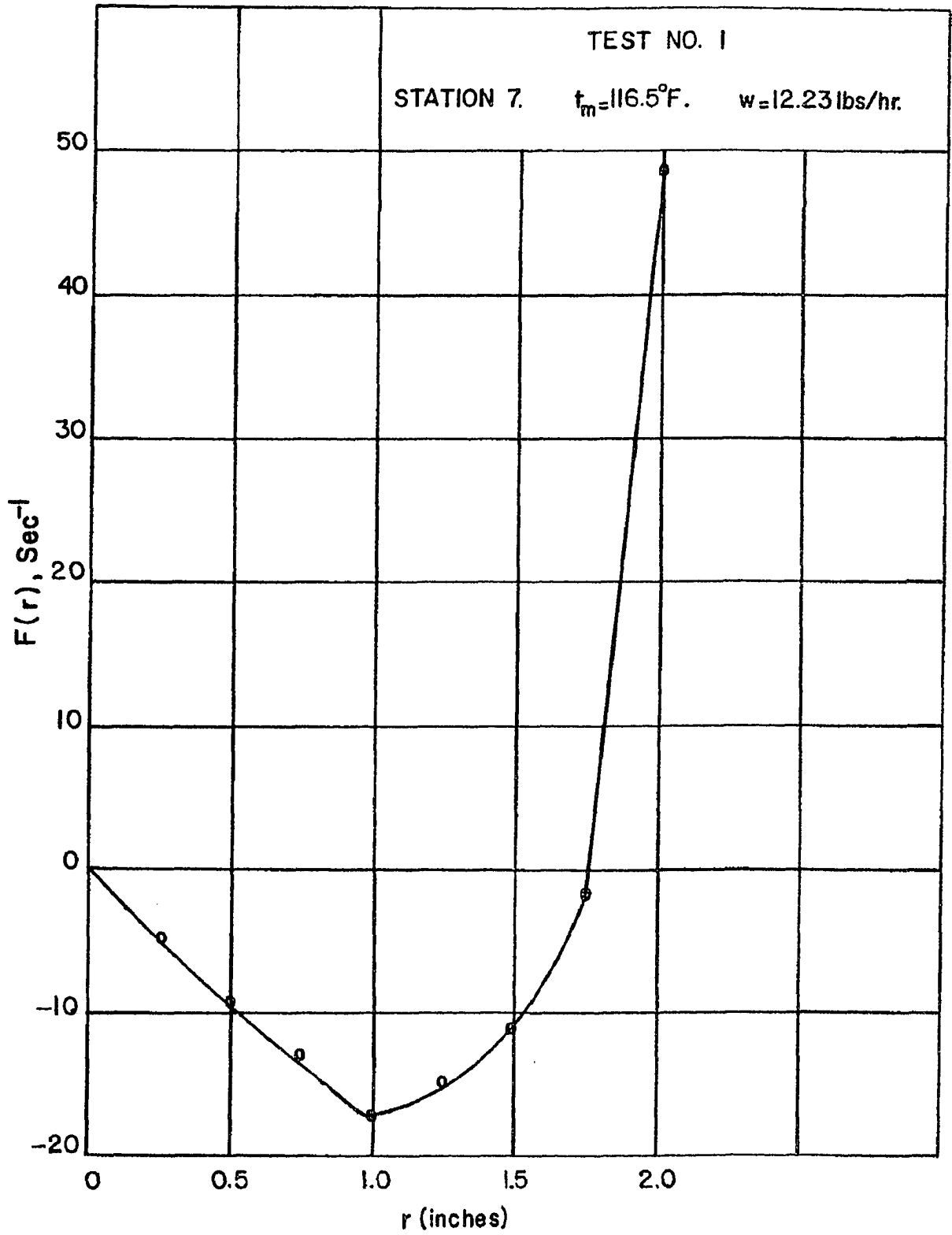
FIGURE 28   PLOT OF F(r) VERSUS r
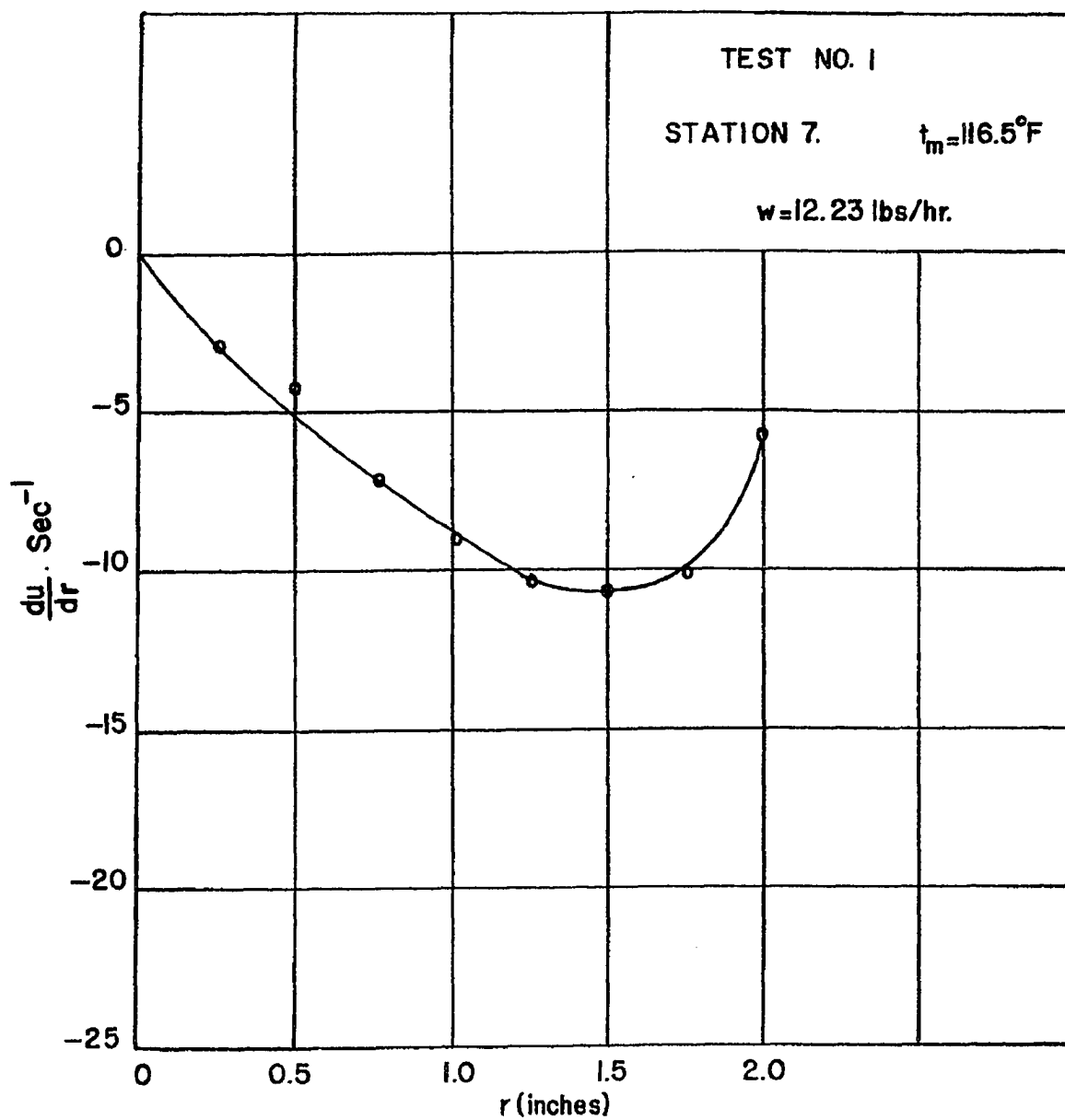
FIGURE 29 PLOT OF $\frac{du}{dr}$ VERSUS r
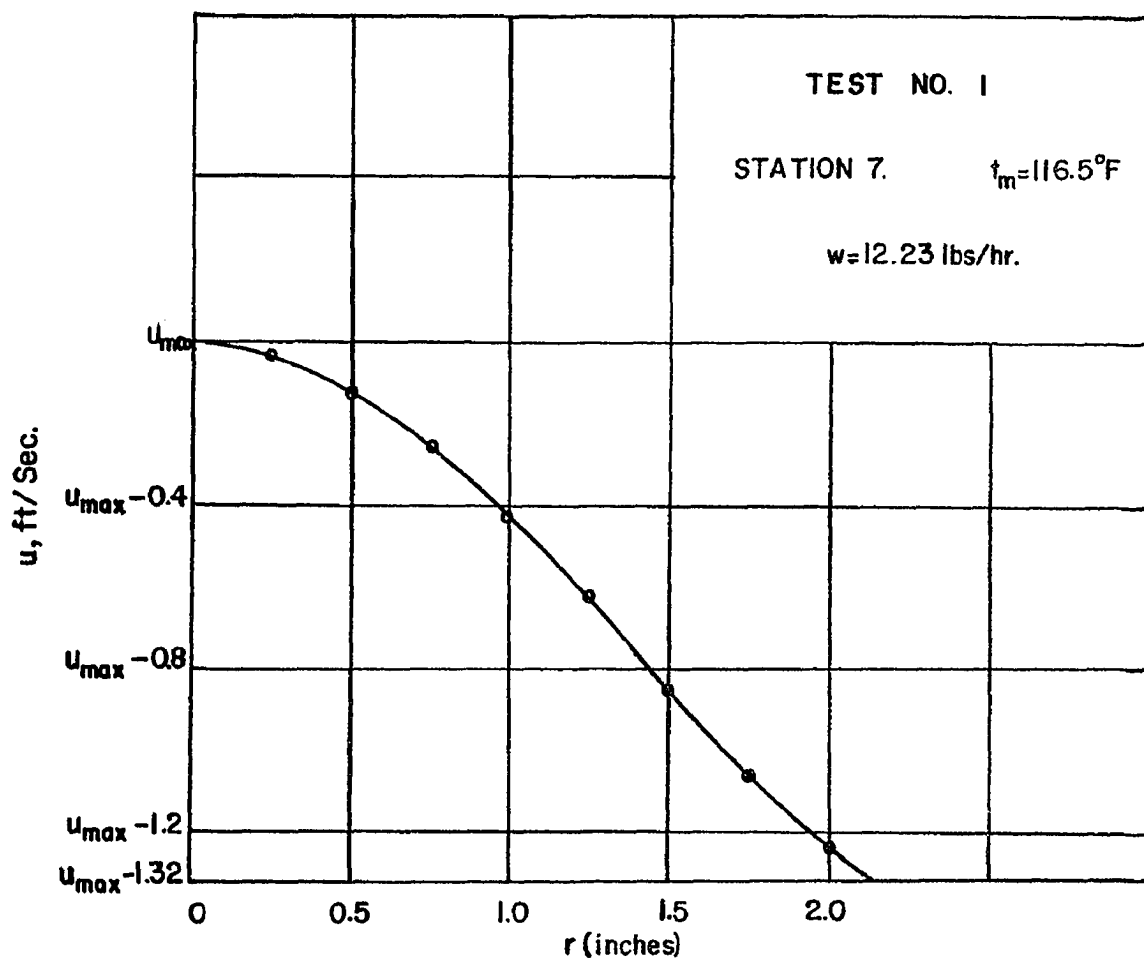
FIGURE 30 PLOT OF u VERSUS r

APPENDIX   B

TABLES AND VELOCITY PROFILES

Station No. 7, 19.5' from entrance

Actual weight flow = 12.23 lbs/hr   Inlet C.L. temperature = 355°F

Mean temperature   = 116.5°F   Ambient air temperature = 83°F

ΔP bet. Stn. 6 and Stn. 8 = 0.0052"H_2O $\dfrac{\epsilon_M}{\nu}$ = 5.5, t_w = 94.0°F

Barometric Pressure = 29.25" Hg

r (inches)	Temperature $^\circ$F	$(F_P - F_B)$ ft/sec^2	$F(r)$	$\int_0^r F(r)\,dr$	$\dfrac{du}{dr}$	u in terms of u_{max}	u/u_{max}	u/u_{mean}
0	119.1	-0.2887	0	0	0	u_{max}	1.0	2.53
0.25	119.1	-0.2887	-4.88	-0.75	-3.0	u_{max}-0.035	0.973	2.46
0.50	118.8	-02.719	-9.26	-2.10	-4.20	u_{max}-0.122	0.91	2.295
0.75	118.5	-0.2551	-12.94	-5.40	-7.20	u_{max}-0.253	0.81	2.04
1.00	118.5	-0.2551	-17.25	-9.0	-9.0	u_{max}-0.420	0.682	1.73
1.25	117.1	-0.1761	-14.88	-13.0	-10.4	u_{max}-0.622	0.529	1.34
1.50	115.9	-0.1089	-11.05	-16.05	-10.70	u_{max}-0.843	0.361	0.914
1.75	113.7	+0.0145	+1.72	-17.8	-10.17	u_{max}-1.064	0.194	0.49
2.00	110.76	+0.3513	+48.51	-11.55	- 5.78	u_{max}-1.23	0.068	0.173

u_{max} = 1.32 ft/sec;   Calculated weight flow = 12.83 lbs/hr

N_{Rem} = 944; f_n = 0.038; N_{cr} = 2.57 x 10^6; $\dfrac{f_n}{f_i}$ = 0.56

FIGURE 31   PLOT OF $^u/u_m$ VERSUS $^r/r_o$

Station No. 9, 26.5' from entrance

Actual weight flow = 12.23 lbs/hr   Inlet C. L. temperature = 355°F

Mean temperature   = 101.5°F   Ambient air temperature = 83°F

ΔP bet. Stn. 8 and Stn. 10 = 0.0025" H_2O $\frac{\epsilon_M}{\nu} = 4.0$, $t_w = 85.7^{\circ}$F

Barometric Pressure = 29.25" Hg

r (inches)	Temperature $^{\circ}$F	$(F_p - F_B)$ ft/sec^2	$F(r)$	$\int_o^r F(r)\,dr$	$\frac{du}{dr}$	u in terms of u_{max}	u/u_{max}	u/u_{mean}
0	103.0	-0.176	0	0	0	u_{max}	1.0	2.34
0.25	103.0	-0.176	-4.05	-0.504	-2.016	u_{max}-0.021	0.98	2.29
0.50	103.0	-0.176	-8.11	-2.015	-4.03	u_{max}-0.084	0.92	2.158
0.75	103.0	-0.176	-12.16	-4.53	-6.04	u_{max}-0.188	0.83	1.936
1.00	102.7	-0.1583	-14.58	-7.75	-7.75	u_{max}-0.332	0.698	1.63
1.25	102.0	-0.1183	-13.62	-11.40	-9.12	u_{max}-0.509	0.537	1.25
1.50	100.8	-0.0487	- 6.73	-13.90	-9.27	u_{max}-0.703	0.361	0.843
1.75	99.7	+0.0143	+ 2.31	-14.50	-8.28	u_{max}-0.885	0.195	0.456
2.00	98.3	+0.0831	+15.30	-12.65	-6.325	u_{max}-1.037	0.057	0.134

u_{max} = 1.1 ft/sec; Calculated weight flow = 11.88 lbs/hr

$N_{Rem} = 963$; $f_n = 0.017$; $N_{Gr} = 1.55 \times 10^6$; $\frac{f_n}{f_i} = 0.256$
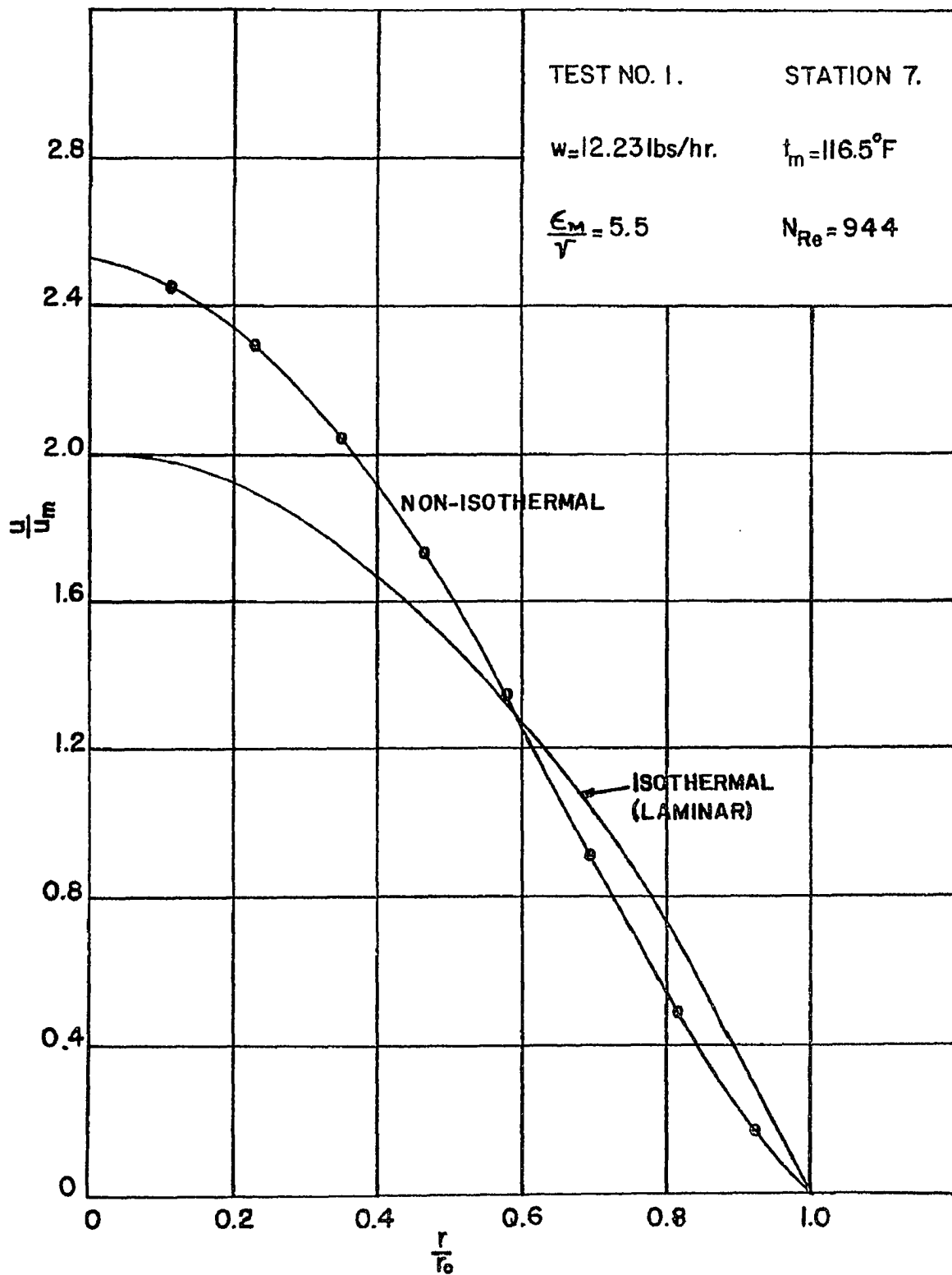
FIGURE 32   PLOT OF u/u_m VERSUS r/r_o

TEST NO. 1　　　　　　　　　　　　　　　　　　　　TABLE 4

Station No. 10, 29.5' from entrance

Actual weight flow = 12.23 lbs/hr　　　　Inlet C.L. temperature = 355°F

Mean temperature　= 96.5°F　　　　　　Ambient air temperature = 83°F

ΔP bet. Stn. 9 and Stn. 11 = 0.002" H_2O　　$\epsilon_M = 0$, $t_w = 84.0$°F

Barometric Pressure = 29.25" Hg

r (inches)	Temperature °F	$(F_P - F_B)$ ft/sec^2	$F(r)$	$\int_o^r F(r)\,dr$	$\dfrac{du}{dr}$	u in terms of u_{max}	u/u_{max}	u/u_{mean}
0	97.2	-0.042	0	0	0	u_{max}	1.0	2.597
0.25	97.2	-0.042	-4.896	-0.612	-2.45	u_{max}-0.03	0.98	2.542
0.50	97.2	-0.042	-9.79	-2.448	-4.896	u_{max}-0.109	0.922	2.395
0.75	97.2	-0.042	-14.69	-5.52	-7.36	u_{max}-0.238	0.83	2.156
1.00	97.2	-0.042	-19.60	-9.80	-9.80	u_{max}-0.417	0.702	1.824
1.25	97.2	-0.042	-29.375	-15.92	-12.74	u_{max}-0.648	0.537	1.395
1.50	96.2	-0.014	-9.82	-20.81	-13.87	u_{max}-0.925	0.340	0.88
1.75	95.7	+0.026	+21.35	-19.33	-11.05	u_{max}-1.181	0.156	0.406
2.00	95.0	+0.082	+77.51	-6.984	-3.50	u_{max}-1.333	0.048	0.124

u_{max} = 1.40 ft/sec; Calculated weight flow = 13.7 lbs/hr

N_{Rem} = 970, $f_n = 0$, N_{Gr} = 1.17 x 10^6, $\dfrac{f_n}{f_i} = 0$

71
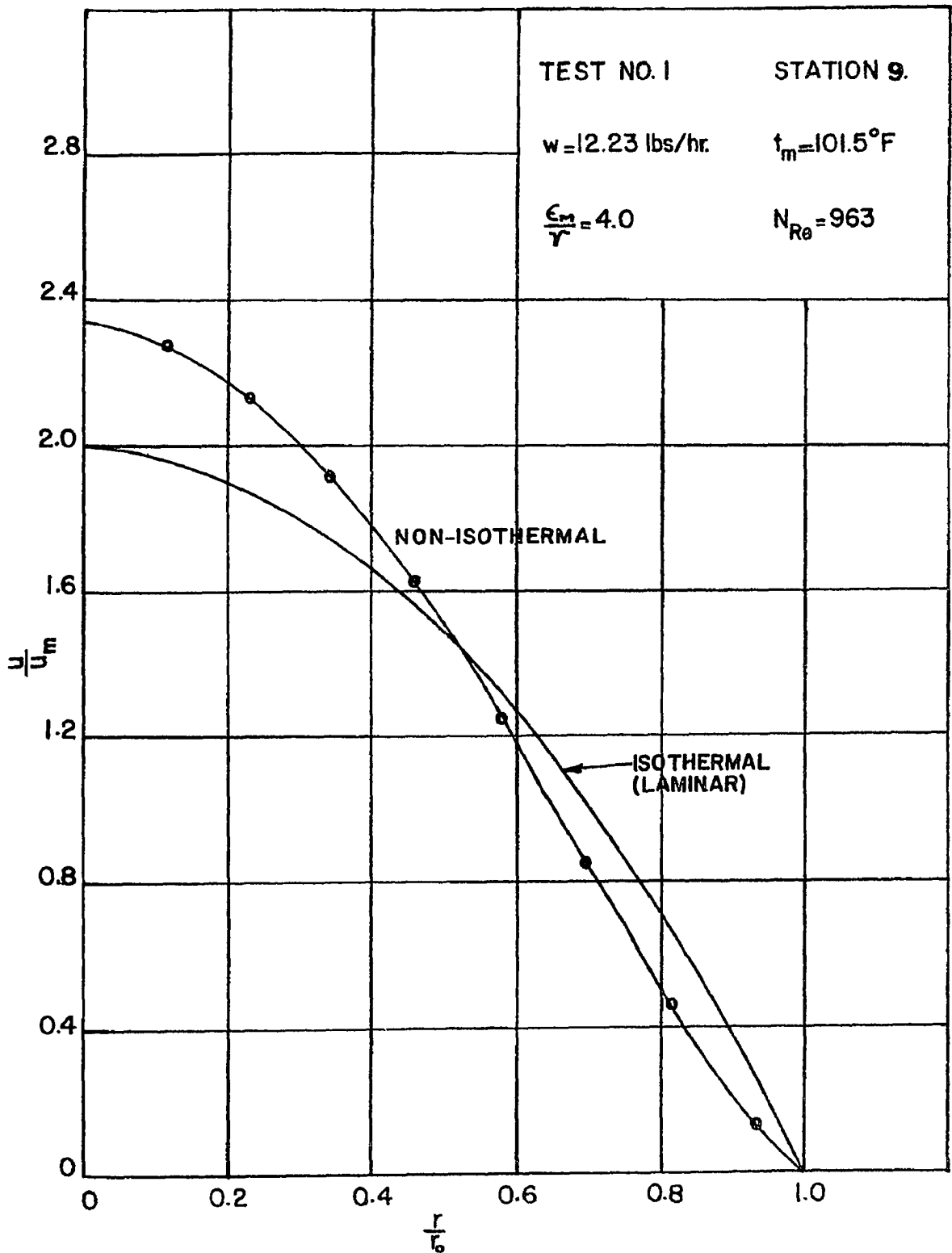
FIGURE 33   PLOT OF $^u/u_m$ VERSUS $^r/r_o$

TEST NO. 2 TABLE 5

Station No. 7, 19.5' from entrance

Actual weight flow = 17.15 lbs/hr   Inlet C.L. temperature = $460^\circ F$

Mean temperature = $139^\circ F$ Ambient air temperature = $82^\circ F$

ΔP bet. Stn. 6 and Stn. 8 = 0.0085" H_2O $\frac{\epsilon_M}{\nu}$ = 7.5, t_w = $102^\circ F$

Barometric Pressure = 29.255" Hg

r (inches)	Temperature $^\circ F$	$(F_p - F_B)$ ft/sec^2	$F(r)$	$\int_0^r F(r)\, dr$	$\frac{du}{dr}$	u in terms of u_{max}	u/u_{max}	u/u_{mean}
0	144.3	-0.542	0	0.	0	u_{max}	1.0	2.43
0.25	144.3	-0.542	-6.56	-0.75	-3.00	u_{max}-0.031	0.982	2.39
0.50	144.3	-0.542	-13.11	-3.10	-6.20	u_{max}-0.130	0.925	2.25
0.75	143.0	-0.471	-17.09	-6.60	-8.80	u_{max}-0.289	0.834	2.03
1.00	142.2	-0.427	-20.66	-11.20	-11.20	u_{max}-0.508	0.708	1.72
1.25	140.7	-0.406	-24.55	-17.20	-13.76	u_{max}-0.773	0.556	1.35
1.50	137.7	-0.184	-13.35	-21.25	-14.17	u_{max}-1.065	0.388	0.943
1.75	135.3	-0.044	-3.73	-24.5	-14.0	u_{max}-1.357	0.22	0.535
2.00	129.3	+0.27	+26.0	-24.0	-12.0	u_{max}-1.630	0.063	0.154

u_{max} = 1.74 ft/sec; Calculated weight flow = 16.91 lbs/hr

N_{Rem} = 1287, f_n = 0.0055, N_{Gr} = 4.57 x 10^6, $\frac{f_n}{f_i}$ = 0.111
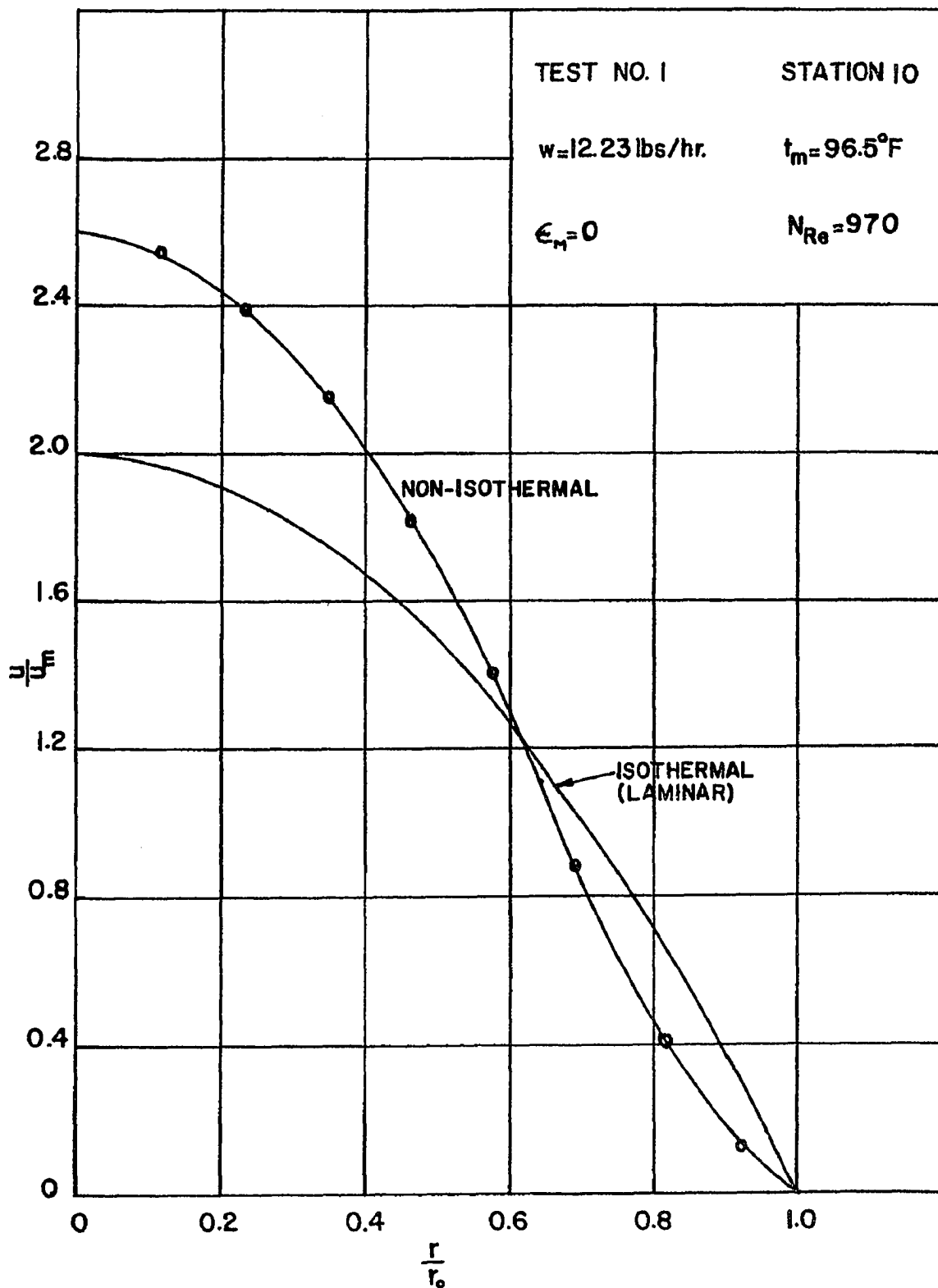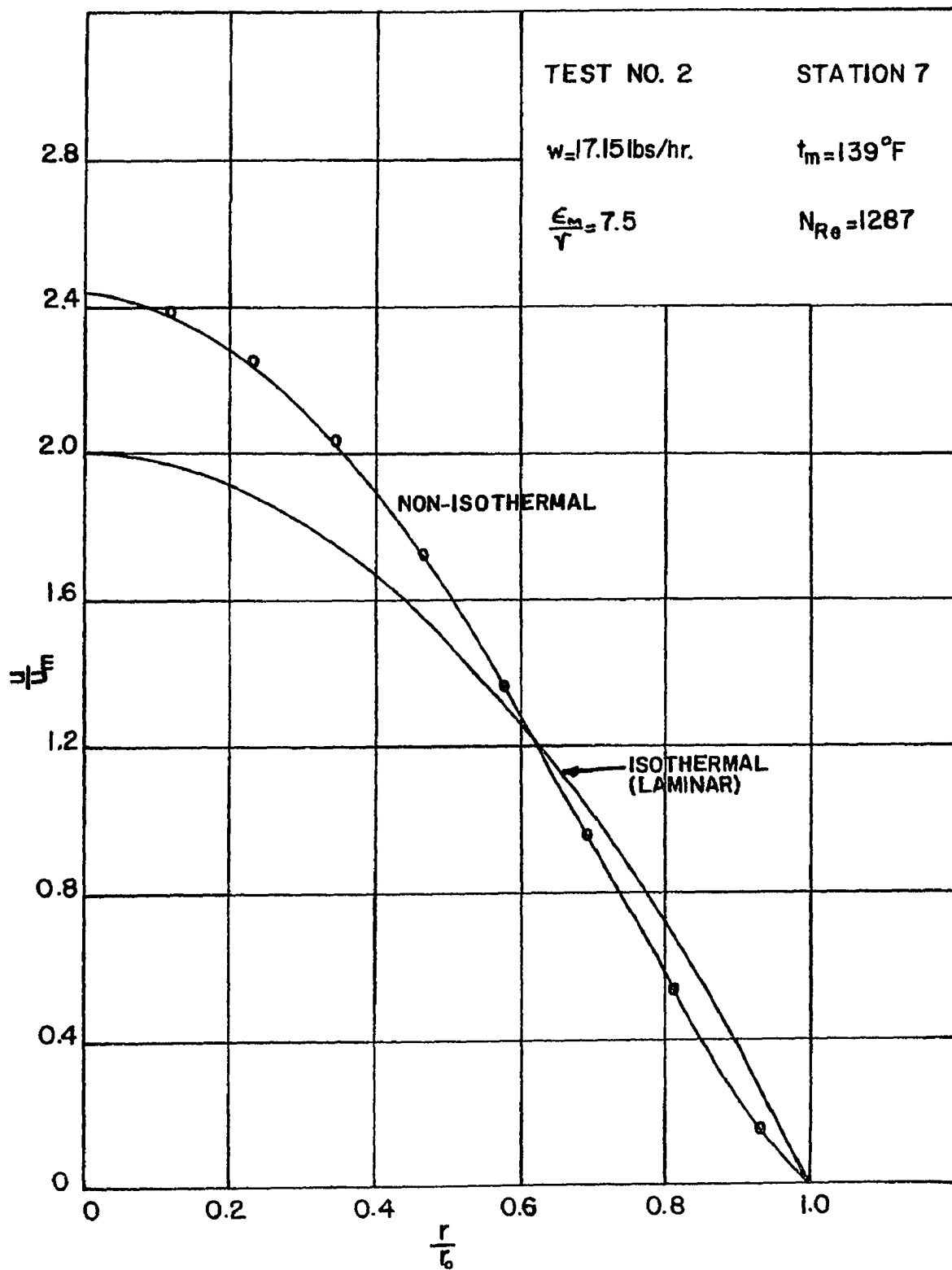
73

FIGURE 34   PLOT OF u/u_m VERSUS r/r_o

TEST NO. 2　　　　　　　　　　　　　　　　　　　　TABLE 6

Station No. 9, 26.5' from entrance

Actual weight flow = 17.15 lbs/hr　　　　　Inlet C.L. temperature = 460°F

Mean temperature = 113.3°F　　　　　　Ambient air temperature = 82.3°F

ΔP bet. Stn. 8 and Stn. 10 = 0.004" H_2O　　$\dfrac{\epsilon_M}{\nu}$ = 6.0, t_w = 89.3°F

Barometric Pressure = 29.255" Hg

r (inches)	Temperature $^{\circ}$F	$(F_P - F_B)$ ft/sec^2	$F(r)$	$\int_o^r F(r)\,dr$	$\dfrac{du}{dr}$	u in terms of u_{max}	u/u_{max}	u/u_{mean}
0	115.7	-0.331	0	0	0	u_{max}	1.0	2.315
0.25	115.7	-0.331	- 5.25	- 0.65	- 2.6	$u_{max}-0.027$	0.983	2.274
0.50	115.7	-0.331	-10.49	- 2.65	- 5.3	$u_{max}-0.11$	0.929	2.15
0.75	115.7	-0.331	-15.75	- 5.60	- 7.47	$u_{max}-0.245$	0.843	1.95
1.00	115.0	-0.291	-18.45	- 9.85	- 9.85	$u_{max}-0.427$	0.726	1.68
1.25	114.3	-0.252	-19.96	-14.85	-11.88	$u_{max}-0.653$	0.581	1.35
1.50	113.0	-0.178	-14.8	-19.25	-12.83	$u_{max}-0.912$	0.415	0.96
1.75	111.3	-0.082	-10.10	-22.55	-12.88	$u_{max}-1.178$	0.245	0.567
2.00	107.0	+0.042	+ 5.32	-23.35	-11.675	$u_{max}-1.433$	0.081	0.188

u_{max} = 1.56 ft/sec;　Calculated weight flow = 16.62 lbs/hr

N_{Rem} = 1330, f_n = 0.018, N_{Gr} = 2.47 x 10^6, $\dfrac{f_n}{f_i}$ = 0.375

75
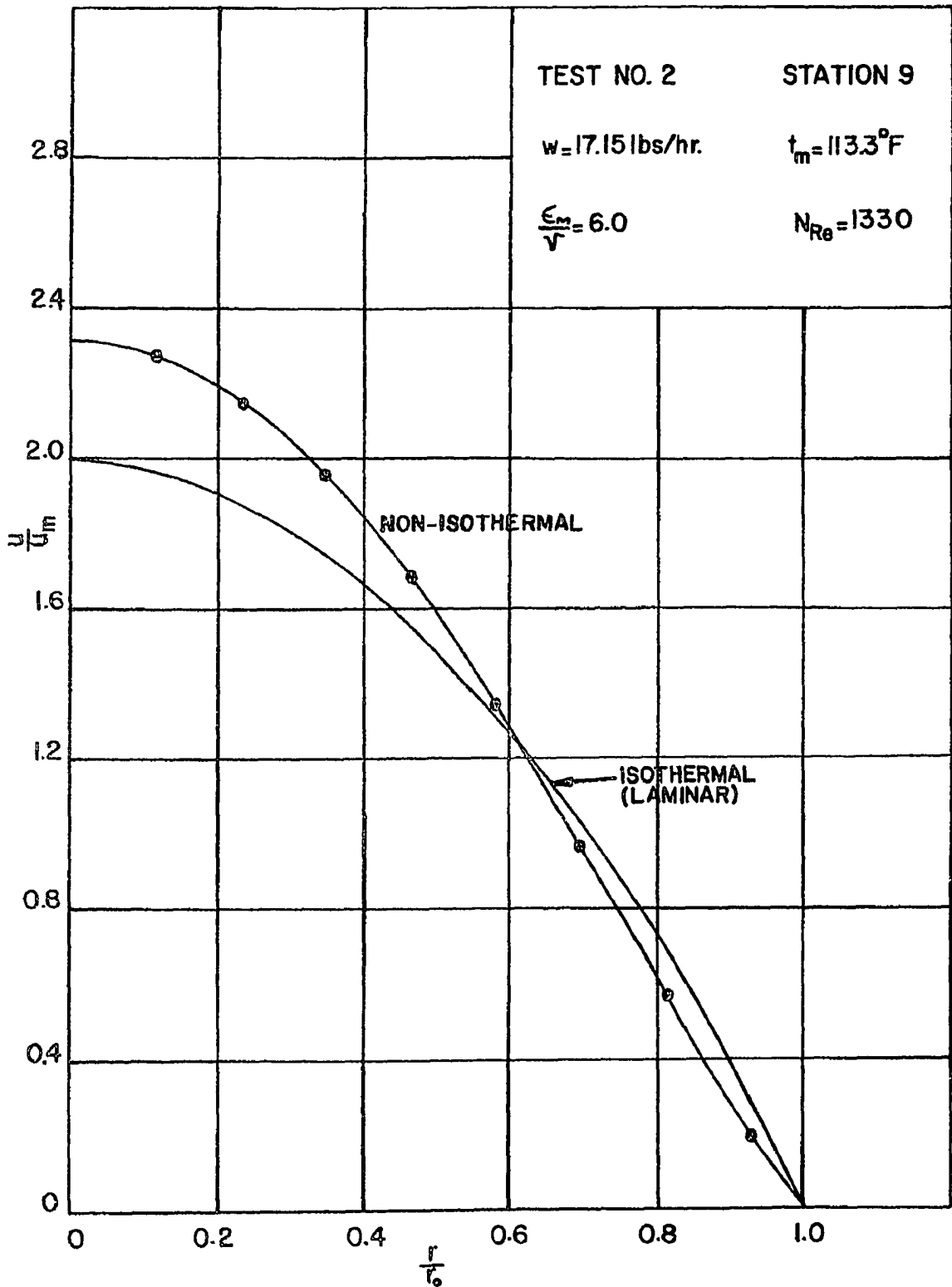
FIGURE 35   PLOT OF $^u/u_m$ VERSUS $^r/r_o$

Station No. 10, 29.5' from entrance

Actual weight flow = 17.15 lbs/hr   Inlet C.L. temperature = 460°F

Mean temperature   = 107°F   Ambient air temperature = 82.3°F

ΔP bet. Stn. 9 and Stn. 11 = 0.0033" H_2O $\frac{\epsilon_M}{\nu} = 4.5$, $t_w = 88^\circ$F

Barometric Pressure = 29.255" Hg

r (inches)	Temperature $^\circ$F	$(F_P - F_B)$ ft/sec^2	$F(r)$	$\int_0^r F(r)\,dr$	$\frac{du}{dr}$	u in terms of u_{max}	u/u_{max}	u/u_{mean}
0	109.0	-0.238	0	0	0	u_{max}	1.0	2.37
0.25	109.0	-0.238	- 4.90	- 0.61	- 2.44	u_{max}-0.026	0.982	2.33
0.50	109.0	-0.238	- 9.80	- 2.50	- 5.0	u_{max}-0.104	0.930	2.20
0.75	109.0	-0.238	-14.70	- 5.40	- 7.2	u_{max}-0.235	0.841	1.99
1.00	109.0	-0.238	-19.60	- 9.60	- 9.6	u_{max}-0.415	0.719	1.70
1.25	108.0	-0.181	-18.63	-14.65	-11.72	u_{max}-0.644	0.565	1.338
1.50	106.8	-0.113	-13.96	-18.35	-12.23	u_{max}-0.894	0.396	0.938
1.75	105.4	-0.033	- 4.75	-21.0	-12.0	u_{max}-1.149	0.224	0.529
2.00	101.0	+0.219	+36.07	-16.75	- 8.38	u_{max}-1.365	0.078	0.184

u_{max} = 1.48 ft/sec;   Calculated weight flow = 15.6 lbs/hr

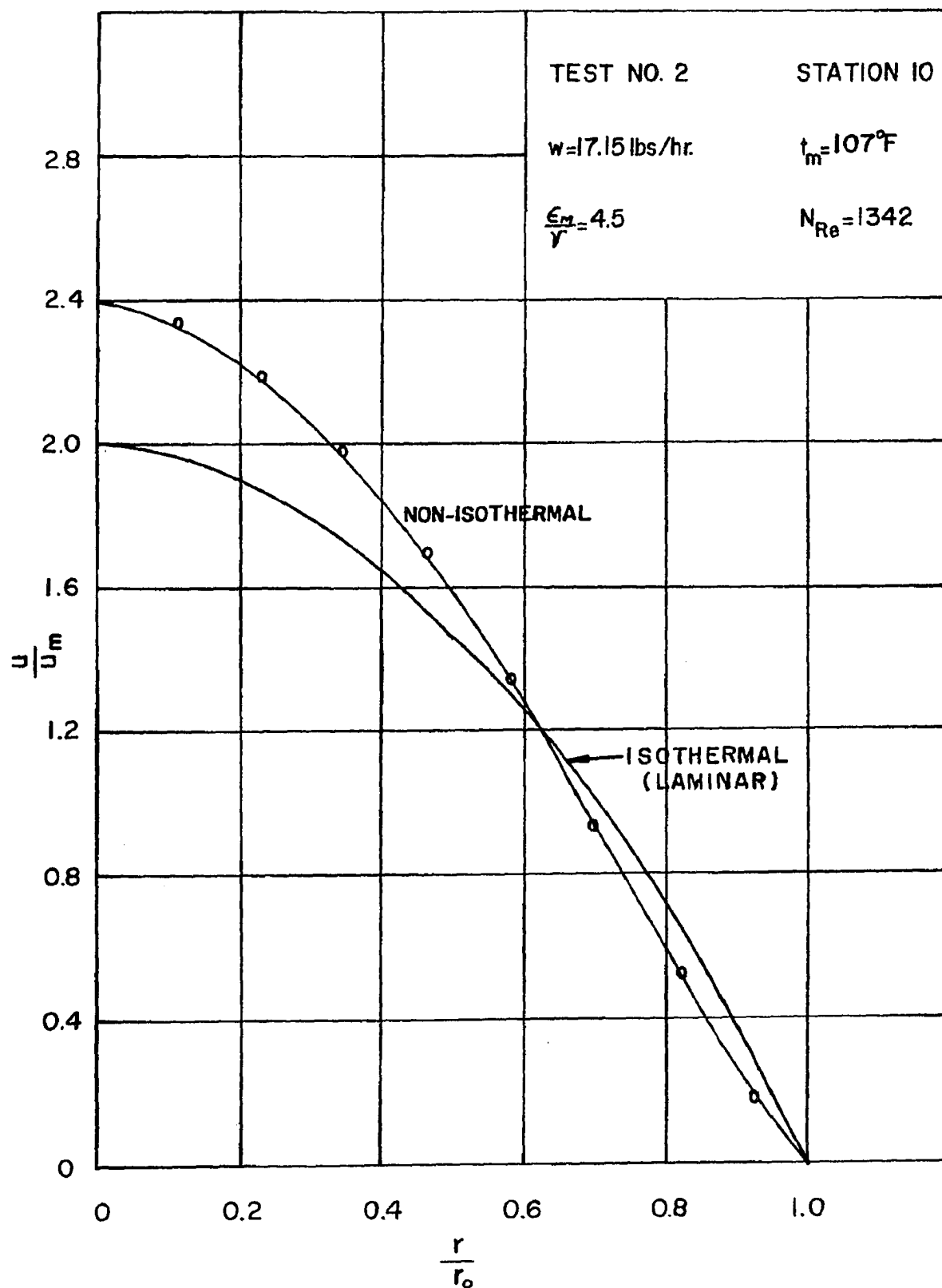$N_{Rem} = 1342$, $f_n = 0.023$, $N_{Gr} = 2.06 \times 10^6$, $\frac{f_n}{f_i} = 0.482$

FIGURE 36   PLOT OF $^u/u_m$ VERSUS $^r/r_o$

TEST NO. 3

TABLE 8

Station No. 7, 19.5' from entrance

Actual weight flow = 17.20 lbs/hr   Inlet C.L. temperature = 542°F

Mean temperature   = 155°F   Ambient air temperature = 81°F

ΔP bet. Stn. 6 and Stn. 8 = 0.0108" H_2O $\dfrac{\epsilon_M}{\nu}$ = 9.0, t_w = 106.7°F

Barometric Pressure = 29.37" Hg

r (inches)	Temperature $^\circ$F	$(F_P - F_B)$ ft/sec^2	F(r)	$\int_0^r$ F(r) dr	$\dfrac{du}{dr}$	u in terms of u_{max}	u/u_{max}	u/u_{mean}
0	161.3	-0.692	0	0	0	u_{max}	1.0	2.43
0.25	161.3	-0.692	- 6.79	- 0.83	- 3.32	u_{max}-0.037	0.98	2.38
0.50	161.3	-0.692	-13.58	- 3.6	- 7.20	u_{max}-0.150	0.92	2.23
0.75	160.3	-0.616	-18.14	- 7.45	- 9.93	u_{max}-0.329	0.823	2.00
1.00	159.3	-0.562	-22.07	-12.50	-12.50	u_{max}-0.559	0.699	1.70
1.25	157.0	-0.441	-21.65	-18.05	-14.44	u_{max}-0.835	0.55	1.34
1.50	154.3	-0.298	-17.55	-22.55	-15.03	u_{max}-1.145	0.384	0.935
1.75	150.7	-0.107	- 7.35	-26.1	-14.91	u_{max}-1.457	0.217	0.526
2.00	141.0	+0.405	+31.8	-23.25	-11.625	u_{max}-1.733	0.068	0.166

u_{max} = 1.86 ft/sec; Calculated weight flow = 17.68 lbs/hr

N_{Rem} = 1261, f_n = 0.07, N_{Gr} = 4.63 x 10^6, $\dfrac{f_n}{f_i}$ = 1.378

TEST NO. 3   STATION 7

w=17.2 lbs/hr. $t_m = 155°F$

$\frac{\epsilon_m}{\gamma} = 9.0$ $N_{Re} = 1261$

NON-ISOTHERMAL

ISOTHERMAL
(LAMINAR)

FIGURE 37   PLOT OF u/u_m VERSUS r/r_o
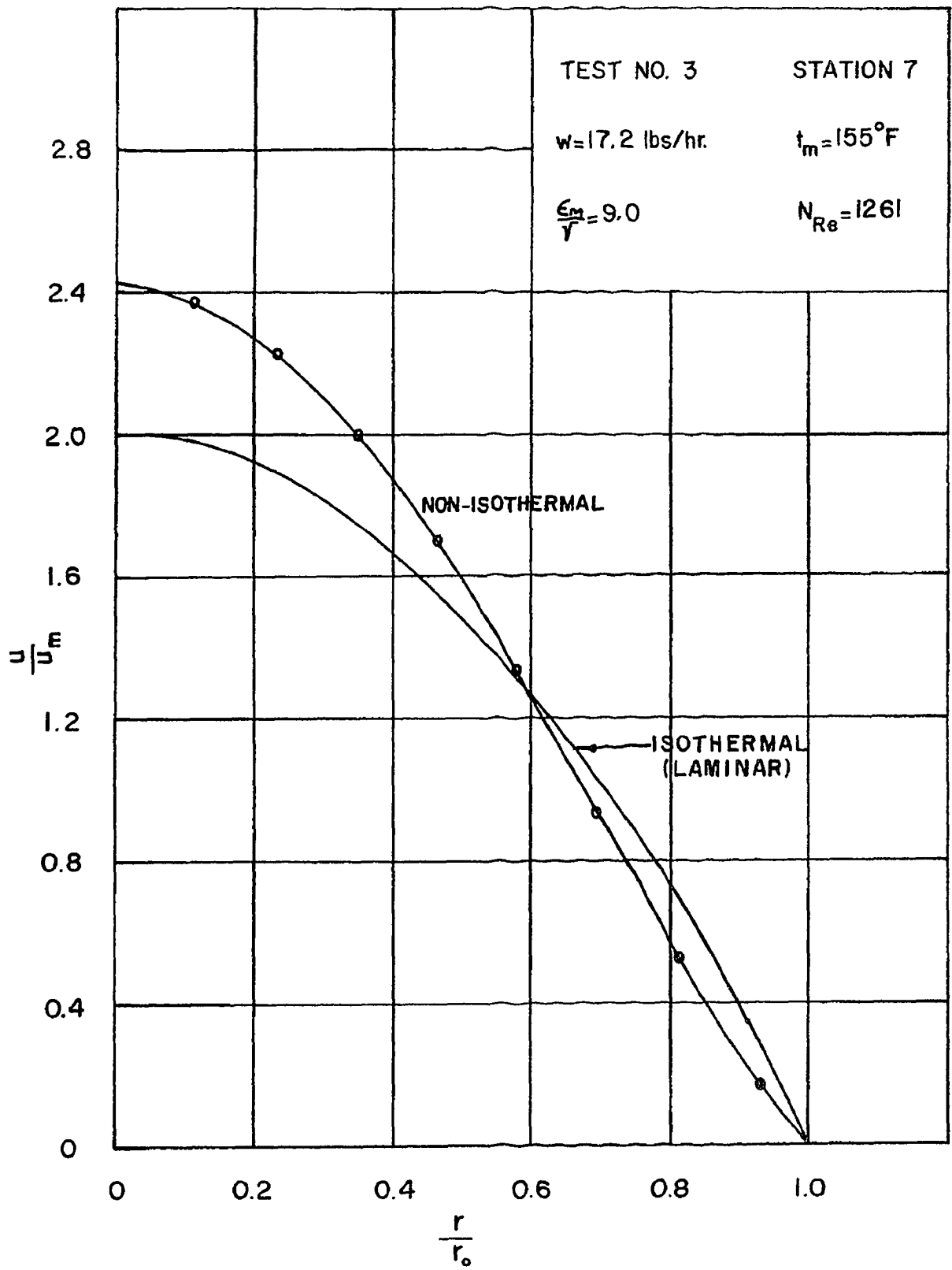
TEST NO. 9   TABLE 9

Station No. 9, 26.5' from entrance

Actual weight flow = 17.2 lbs/hr   Inlet C.L. temperature = 542°F

Mean temperature   = 123°F   Ambient air temperature = 81.3°F

ΔP bet. Stn. 8 and Stn. 10 = 0.0055" H_2O $\frac{\epsilon_M}{\nu} = 6$, $t_w = 96.1°F$

Barometric Pressure = 29.37" Hg

r (inches)	Temperature °F	$(F_P - F_B)$ ft/sec^2	F(r)	$\int_0^x F(r)\,dr$	$\frac{du}{dr}$	u in terms of u_{max}	u/u_{max}	u/u_{mean}
0	127.1	-0.416	0	0	0	u_{max}	1.0	2.57
0.25	127.0	-0.416	- 6.31	- 0.78	- 3.12	$u_{max} - 0.031$	0.981	2.52
0.50	126.7	-0.393	-12.10	- 3.00	- 6.00	$u_{max} - 0.130$	0.919	2.36
0.75	125.7	-0.339	-15.66	- 6.95	- 9.27	$u_{max} - 0.291$	0.818	2.10
1.00	125.3	-0.316	-19.46	-10.75	-10.75	$u_{max} - 0.512$	0.680	1.75
1.25	124.0	-0.244	-18.78	-15.80	-12.64	$u_{max} - 0.765$	0.522	1.34
1.50	122.3	-0.150	-13.86	-19.70	-13.10	$u_{max} - 1.036$	0.353	0.907
1.75	118.7	+0.051	+5.497	-21.75	-12.43	$u_{max} - 1.306$	0.184	0.472
2.00	113.7	+0.319	+39.3	-16.25	- 8.125	$u_{max} - 1.521$	0.0494	0.127

u_{max} = 1.6 ft/sec;   Calculated weight flow = 15.15 lbs/hr

N_{Rem} = 1313, f_n = 0.0065, N_{Gr} = 3.18 x 10^6, $\frac{f_n}{f_i}$ = 0.133

81
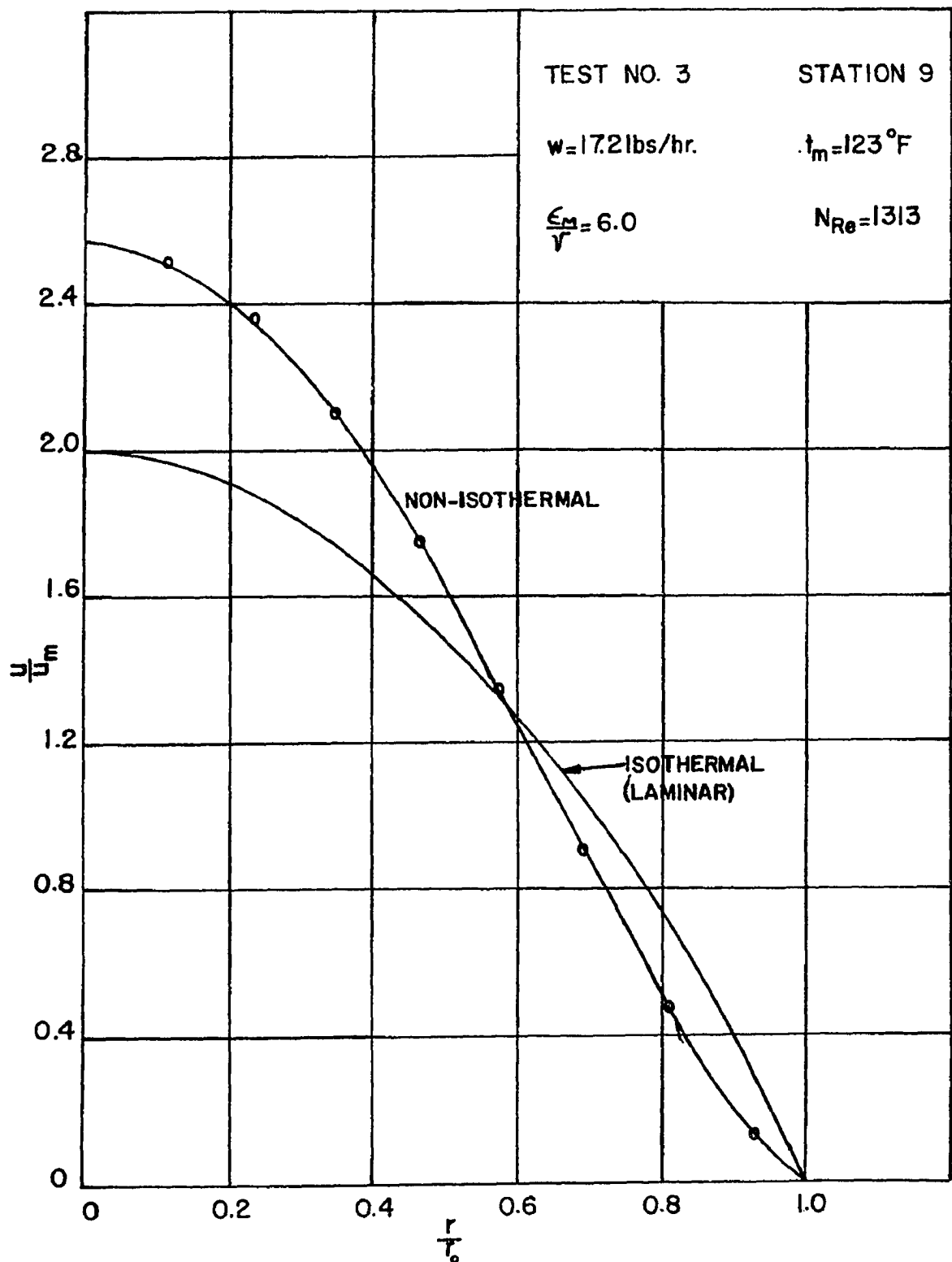
FIGURE 38   PLOT OF u/u_m VERSUS r/r_o

TEST NO. 3 TABLE 10

Station No. 10, 29.5' from entrance

Actual weight flow = 17.2 lbs/hr Inlet C.L. temperature = $542^\circ F$

Mean temperature = $114.3^\circ F$ Ambient air temperature = $81^\circ F$

ΔP bet. Stn. 9 and Stn. 11 = 0.0044" H_2O $\frac{\epsilon_M}{\nu}$ = 6.0, t_w = $93.3^\circ F$

Barometric Pressure = 29.37" Hg

r (inches)	Temperature $^\circ F$	$(F_P - F_B)$ ft/sec^2	$F(r)$	$\int_0^x F(r)\,dr$	$\frac{du}{dr}$	u in terms of u_{max}	u/u_{max}	u/u_{mean}
0	116.6	-0.306	0	0	0	u_{max}	1.0	2.29
0.25	116.6	-0.306	- 4.84	- 0.60	- 2.40	u_{max}-0.025	0.983	2.25
0.50	116.6	-0.306	- 9.67	- 2.15	- 4.30	u_{max}-0.101	0.933	2.14
0.75	116.6	-0.306	-14.51	- 5.30	- 7.07	u_{max}-0.226	0.849	1.945
1.00	116.6	-0.306	-19.35	- 9.30	- 9.30	u_{max}-0.40	0.733	1.68
1.25	115.6	-0.249	-19.68	-14.65	-11.72	u_{max}-0.622	0.585	1.34
1.50	114.0	-0.159	-15.08	-17.80	-11.87	u_{max}-0.872	0.419	0.959
1.75	111.7	-0.029	- 3.21	-21.0	-12.00	u_{max}-1.127	0.249	0.569
2.00	107.3	+0.219	+27.69	-19.1	- 9.55	u_{max}-1.352	0.099	0.226

u_{max} = 1.5 ft/sec, Calculated weight flow = 16.2 lbs/hr

N_{Rem} = 1327, f_n = 0.039, N_{Gr} = 2.7 x 10^6, $\frac{f_n}{f_i}$ = 0.81

83
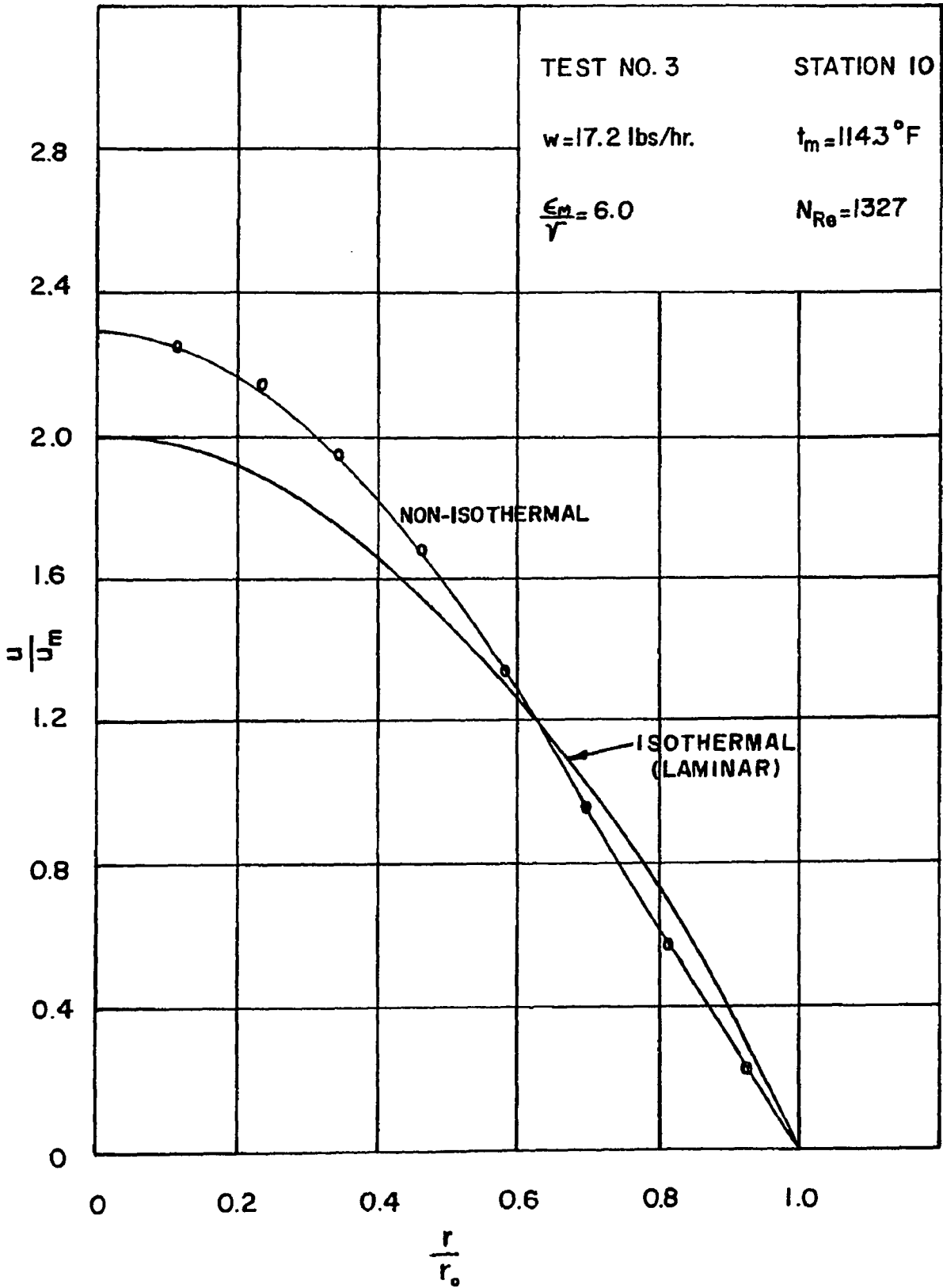
FIGURE 39   PLOT OF u/u_m VERSUS r/r_o

Station No. 7, 19.5' from entrance

Actual weight flow = 19.17 lbs/hr   Inlet C.L. temperature = $568^{\circ}F$

Mean temperature = $170.75^{\circ}F$ Ambient air temperature = $82.7^{\circ}F$

ΔP bet. Stn. 6 and Stn. 8 = 0.012" H_2O $\frac{\epsilon M}{\nu}$ = 10.0, t_w = $112.7^{\circ}F$

Barometric pressure = 29.425" Hg

r (inches)	Temperature $^{\circ}F$	$(F_p - F_B)$ ft/sec^2	$F(r)$	$\int_0^r F(r)\,dr$	$\frac{du}{dr}$	u in terms of u_{max}	u/u_{max}	u/u_{mean}
0	176.3	-0.863	0	0	0	u_{max}	1.0	2.42
0.25	176.3	-0.863	- 7.37	- 0.85	- 3.40	u_{max}-0.0375	0.982	2.37
0.50	176.3	-0.863	-14.74	- 3.45	- 6.90	u_{max}-0.15	0.928	2.243
0.75	176.0	-0.848	-21.72	- 7.95	-10.6	u_{max}-0.335	0.839	2.035
1.00	174.7	-0.780	-26.64	-13.9	-13.9	u_{max}-0.593	0.715	1.729
1.25	170.3	-0.551	-23.52	-20.5	-16.4	u_{max}-0.914	0.56	1.353
1.50	167.7	-0.424	-21.72	-26.6	-17.73	u_{max}-1.274	0.387	0.938
1.75	162.0	-0.120	- 7.17	-30.05	-17.17	u_{max}-1.638	0.212	0.514
2.00	152.3	+0.385	+26.3	-27.6	-13.8	u_{max}-1.959	0.058	0.140

u_{max} = 2.08 ft/sec; Calculated weight flow = 19.39 lbs/hr

N_{Rem} = 1376, f_n = 0.072, N_{Gr} = 4.96 x 10^6, $\frac{f_n}{f_i}$ = 1.55   85

TEST NO. 4   STATION 7

$w = 19.17$ lbs/hr. $t_m = 170.75\,°F$

$\dfrac{\epsilon_M}{\nu} = 10.0$ $N_{Re} = 1376$

NON-ISOTHERMAL

ISOTHERMAL
(LAMINAR)
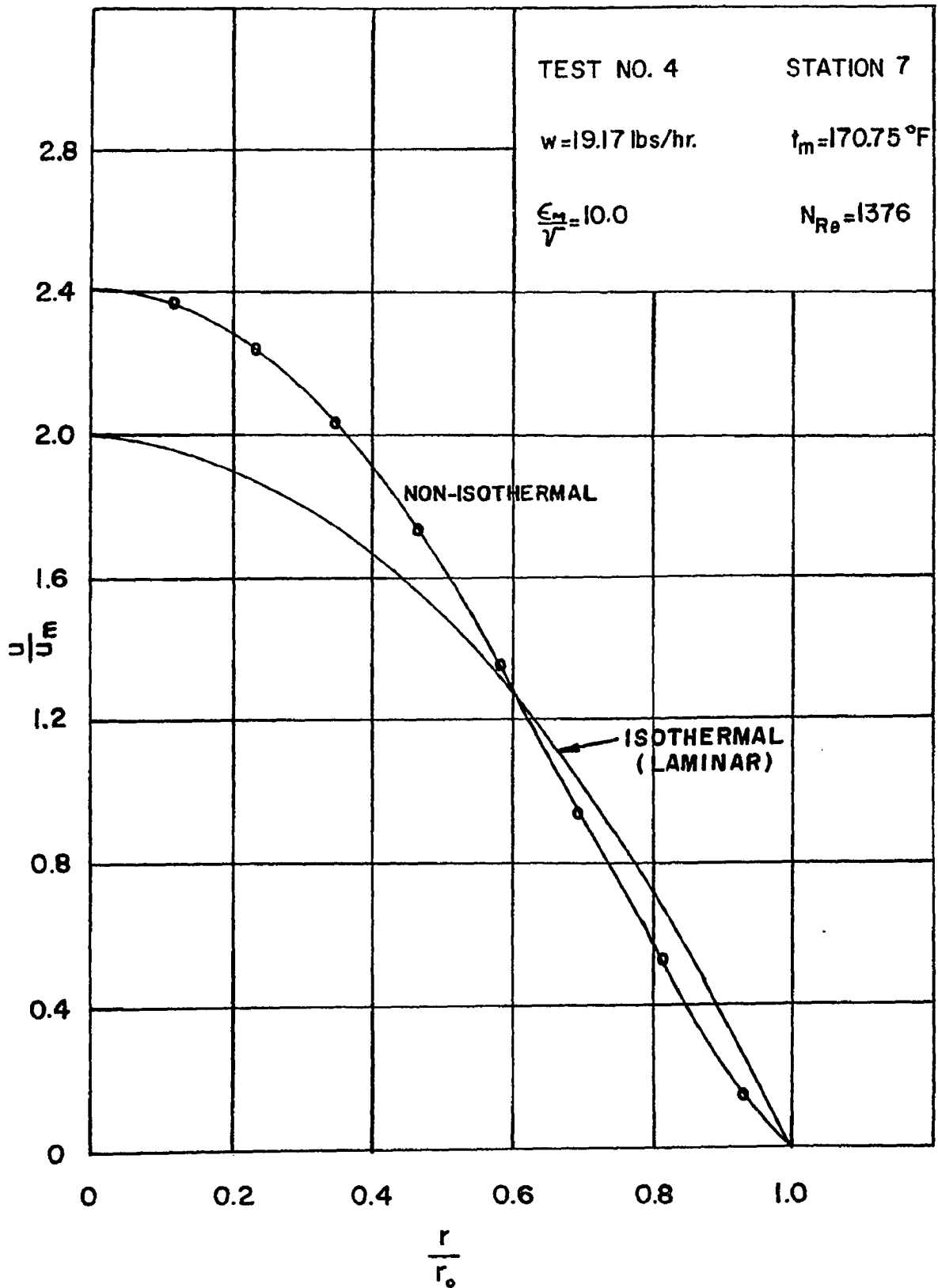
FIGURE 40   PLOT OF u/u_m VERSUS r/r_o

Station No. 9, 26.5' from entrance

Actual weight flow = 19.17 lbs/hr Inlet C.L. temperature = 568°F

Mean temperature = 133°F Ambient air temperature = 82.7°F

ΔP bet. Stn. 8 and Stn. 10 = 0.0065" H_2O $\frac{\epsilon_M}{\nu}$ = 7.0, t_w = 101.3°F

Barometric Pressure = 29.425" Hg

r (inches)	Temperature $^\circ$F	$(F_P - F_B)$ ft/sec^2	F(r)	$\int_0^r F(r)\, dr$	$\frac{du}{dr}$	u in terms of u_{max}	u/u_{max}	u/u_{mean}
0	137.5	-0.539	0	0	0	u_{max}	1.0	2.51
0.25	137.5	-0.539	- 7.05	- 0.75	- 3.0	u_{max}-0.031	0.983	2.46
0.50	137.5	-0.539	-14.1	- 3.20	- 6.40	u_{max}-0.14	0.923	2.31
0.75	137.0	-0.512	-20.1	- 7.90	-10.53	u_{max}-0.322	0.823	2.06
1.00	135.3	-0.36	-18.83	-12.90	-12.90	u_{max}-0.577	0.683	1.70
1.25	134.0	-0.289	-18.90	-17.20	-13.76	u_{max}-0.863	0.526	1.32
1.50	132.3	-0.196	-15.38	-21.70	-14.47	u_{max}-1.16	0.363	0.908
1.75	129.0	-0.016	- 1.46	-23.70	-13.54	u_{max}-1.449	0.204	0.51
2.00	122.3	+0.345	+36.1	-21.25	-10.625	u_{max}-1.701	0.065	0.164

u_{max} = 1.82 ft/sec; Calculated weight flow = 17.43 lbs/hr

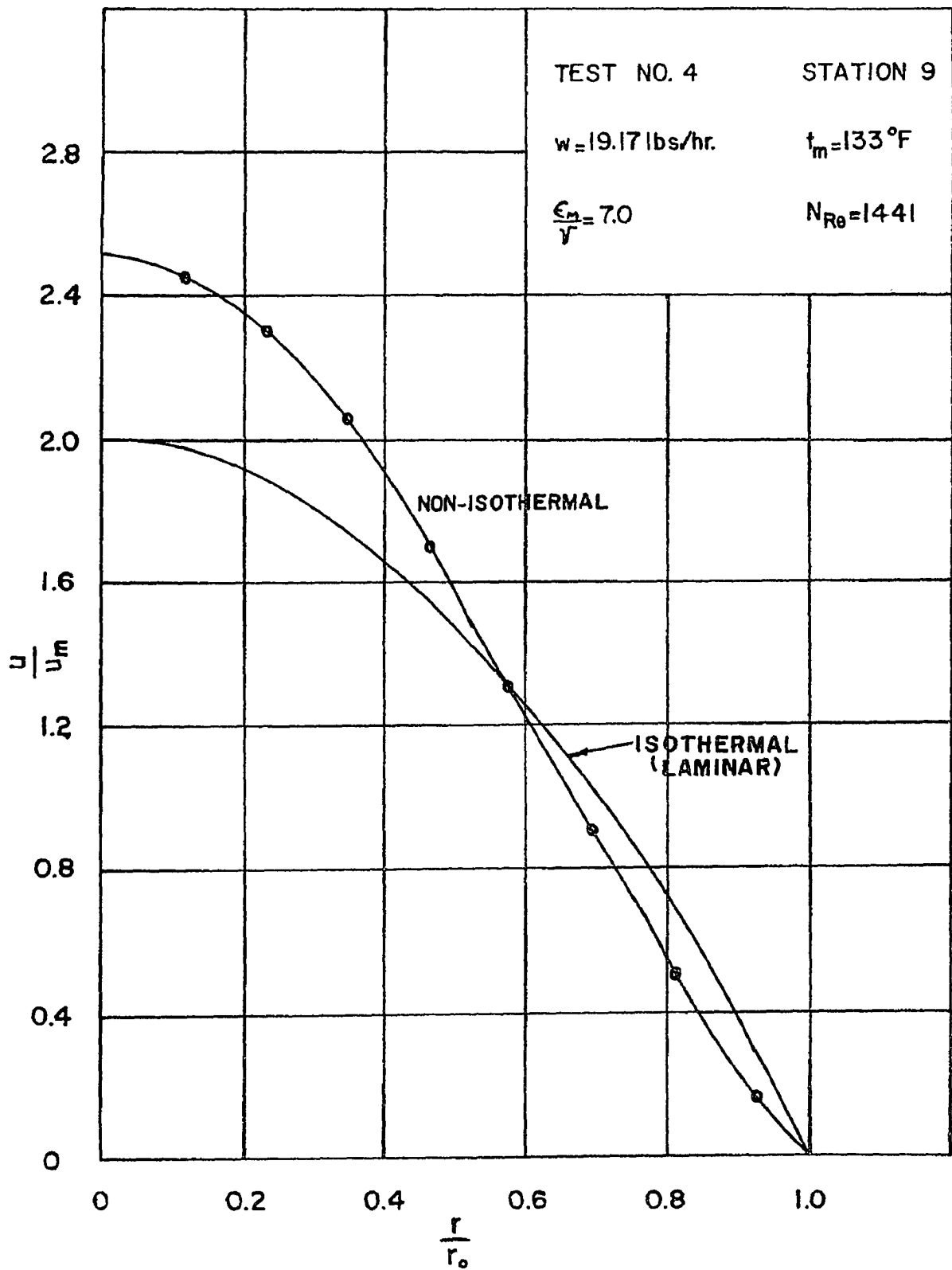N_{Rem} = 1441, f_n = 0.016, N_{Gr} = 3.51 x 10^6, $\frac{f_n}{f_i}$ = 0.36

87

FIGURE 41   PLOT OF u/u_m VERSUS r/r_o

TABLE 13

Station No. 10, 29.5' from entrance

Actual weight flow = 19.17 lbs/hr   Inlet C. L. temperature = $568^{\circ}F$

Mean temperature = $123^{\circ}F$ Ambient air temperature = $82.7^{\circ}F$

ΔP bet. Stn. 9 and Stn. 11 = 0.0052" H_2O $\dfrac{\epsilon_M}{\nu}$ = 6.0, t_w = $97.0^{\circ}F$

Barometric Pressure = 29.425" Hg

r (inches)	Temperature $^{\circ}F$	$(F_P - F_B)$ ft/sec^2	$F(r)$	$\int_o^r F(r)\,dr$	$\dfrac{du}{dr}$	u in terms of u_{max}	u/u_{max}	u/u_{mean}
0	126.7	-0.433	0	0	0	u_{max}	1.0	2.37
0.25	126.7	-0.433	- 6.67	- 0.74	- 2.96	$u_{max}-0.03$	0.984	2.33
0.50	126.7	-0.433	-13.41	- 3.20	- 6.40	$u_{max}-0.134$	0.928	2.199
0.75	126.0	-0.395	-18.24	- 7.10	- 9.47	$u_{max}-0.301$	0.838	1.986
1.00	125.3	-0.356	-21.93	-11.90	-11.90	$u_{max}-0.525$	0.718	1.70
1.25	124.3	-0.301	-23.17	-17.65	-14.12	$u_{max}-0.801$	0.569	1.35
1.50	123.3	-0.246	-22.73	-23.30	-15.53	$u_{max}-1.11$	0.403	0.954
1.75	120.3	-0.078	- 8.40	-27.35	-15.63	$u_{max}-1.437$	0.227	0.539
2.00	113.0	+0.328	+40.4	-23.35	-11.675	$u_{max}-1.729$	0.070	0.167

u_{max} = 1.86 ft/sec;   Calculated weight flow = 19.15 lbs/hr

N_{Rem} = 1460, f_n = 0.022, N_{Gr} = 2.99 x 10^6, $\dfrac{f_n}{f_i}$ = 0.502

89
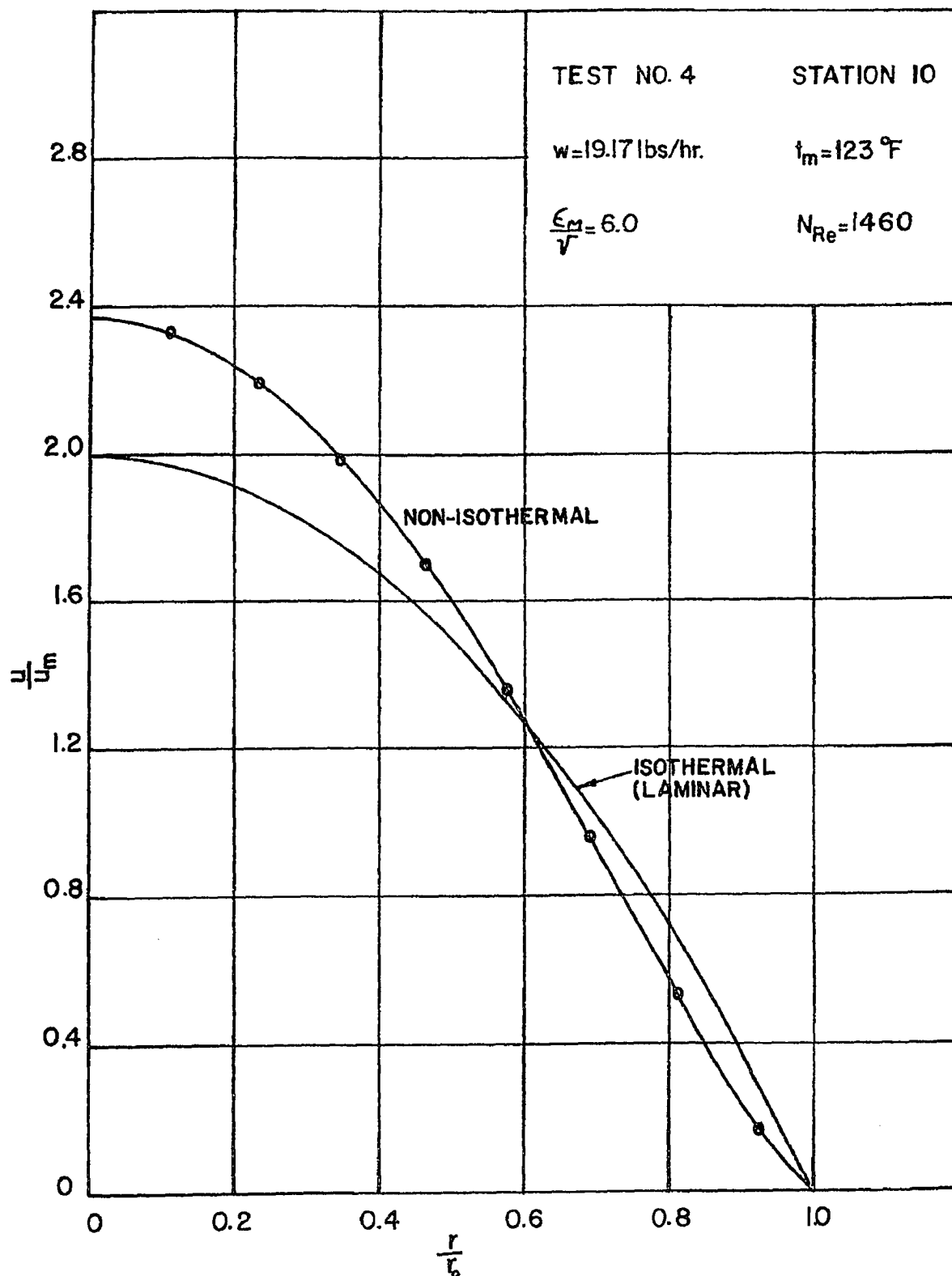
FIGURE 42   PLOT OF u/u_m VERSUS r/r_o

TABLE 14

Station No. 7, 19.5' from entrance

Actual weight flow = 22.22 lbs/hr Inlet C.L. temperature = $300^{\circ}F$

Mean temperature = $150^{\circ}F$ Ambient air temperature = $77^{\circ}F$

ΔP bet. Stn. 6 and Stn. 8 = 0.012" H_2O $\frac{\epsilon_M}{\nu} = 8.5$, $t_w = 112.3^{\circ}F$

Barometric Pressure = 29.5" Hg

r (inches)	Temperature $^{\circ}F$	$(F_p - F_B)$ ft/sec^2	$F(r)$	$\int_o^r F(r)\,dr$	$\frac{du}{dr}$	u in terms of u_{max}	u/u_{max}	u/u_{mean}
0	155.0	-0.738	0	0	0	u_{max}	1.0	2.46
0.25	155.0	-0.738	- 7.73	- 0.96	- 3.84	$u_{max}-0.047$	0.98	2.41
0.50	155.0	-0.738	-15.47	- 4.15	- 8.30	$u_{max}-0.182$	0.921	2.27
0.75	155.0	-0.738	-23.21	- 9.10	-12.13	$u_{max}-0.40$	0.826	2.03
1.00	153.3	-0.647	-27.13	-14.90	-14.90	$u_{max}-0.681$	0.704	1.73
1.25	151.3	-0.540	-28.30	-22.0	-17.60	$u_{max}-1.022$	0.555	1.37
1.50	148.7	-0.401	-25.22	-29.0	-19.33	$u_{max}-1.407$	0.388	0.956
1.75	145.0	-0.201	-14.75	-33.75	-19.28	$u_{max}-1.815$	0.211	0.519
2.00	136.0	+0.279	+23.4	-32.35	-16.175	$u_{max}-2.186$	0.049	0.122

u_{max} = 2.3 ft/sec; Calculated weight flow = 21.86 lbs/hr

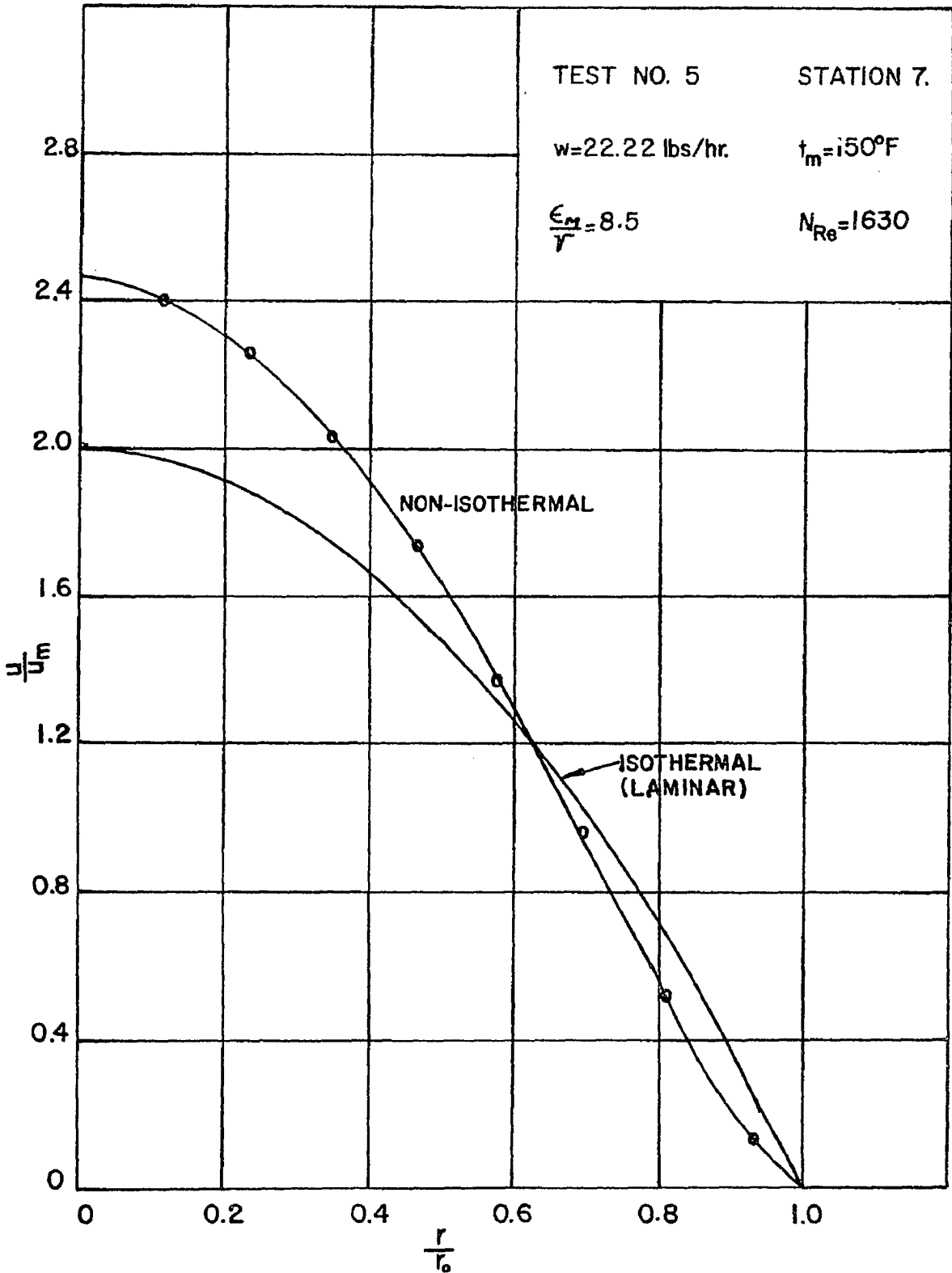N_{Rem} = 1630, f_n = 0.015, N_{Gr} = 4.64 x 10^6, $\frac{f_n}{f_i}$ = 0.382

FIGURE 43   PLOT OF $^u/u_m$ VERSUS $^r/r_o$

Station No. 10, 29.5' from entrance

Actual weight flow = 22.22 lbs/hr   Inlet C.L. temperature = 300°F

Mean temperature = 123°F   Ambient air temperature = 77°F

ΔP bet. Stn. 9 and Stn. 11 = 0.006" H_2O $\dfrac{\epsilon M}{\nu} = 6.0$, $t_w = 97.1^{\circ}$F

Barometric Pressure = 29.5" Hg

r (inches)	Temperature $^{\circ}$F	$(F_P - F_B)$ ft/sec^2	$F(r)$	$\int_o^r F(r)\,dr$	$\dfrac{du}{dr}$	u in terms of u_{max}	u/u_{max}	u/u_{mean}
0	126.0	-0.436	0	0	0	u_{max}	1.0	2.28
0.25	126.0	-0.436	- 6.71	- 0.83	- 3.32	$u_{max}-0.032$	0.985	2.25
0.50	126.0	-0.436	-13.43	- 3.35	- 6.70	$u_{max}-0.133$	0.936	2.14
0.75	126.0	-0.436	-20.14	- 7.35	- 9.80	$u_{max}-0.305$	0.854	1.95
1.00	126.0	-0.436	-26.85	-13.0	-13.0	$u_{max}-0.542$	0.742	1.69
1.25	125.0	-0.380	-29.25	-20.0	-16.0	$u_{max}-0.846$	0.597	1.36
1.50	123.0	-0.269	-24.85	-26.9	-17.93	$u_{max}-1.202$	0.427	0.976
1.75	120.7	-0.141	-15.2	-32.05	-18.3	$u_{max}-1.583$	0.246	0.562
2.00	115.7	+0.138	+16.998	-32.0	-16.0	$u_{max}-1.942$	0.075	0.172

u_{max} = 2.1 ft/sec,   Calculated weight flow = 22.53 lbs/hr

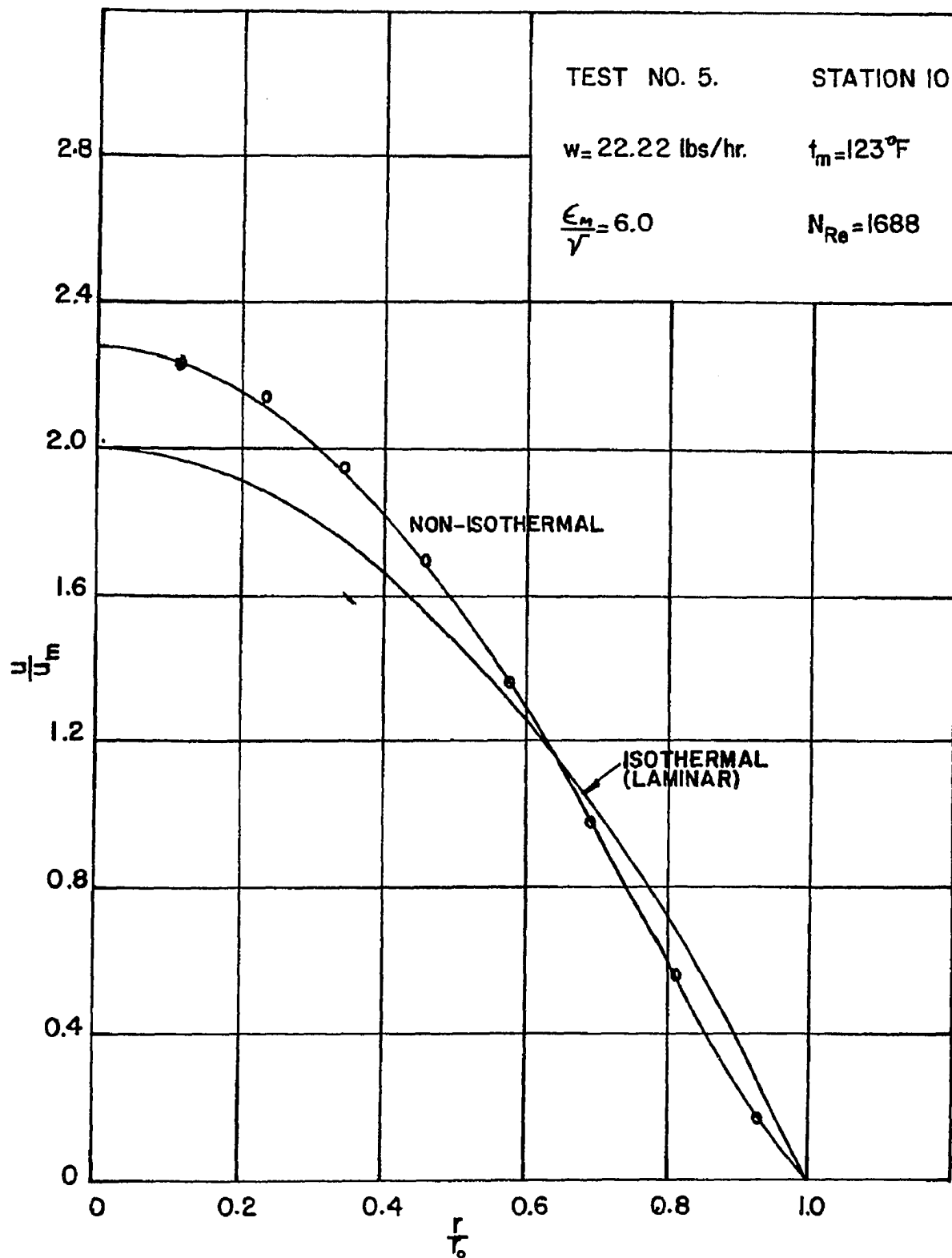$N_{Rem} = 1688$, $f_n = 0.0142$, $N_{Gr} = 3.8 \times 10^6$, $\dfrac{f_n}{f_i} = 0.375$
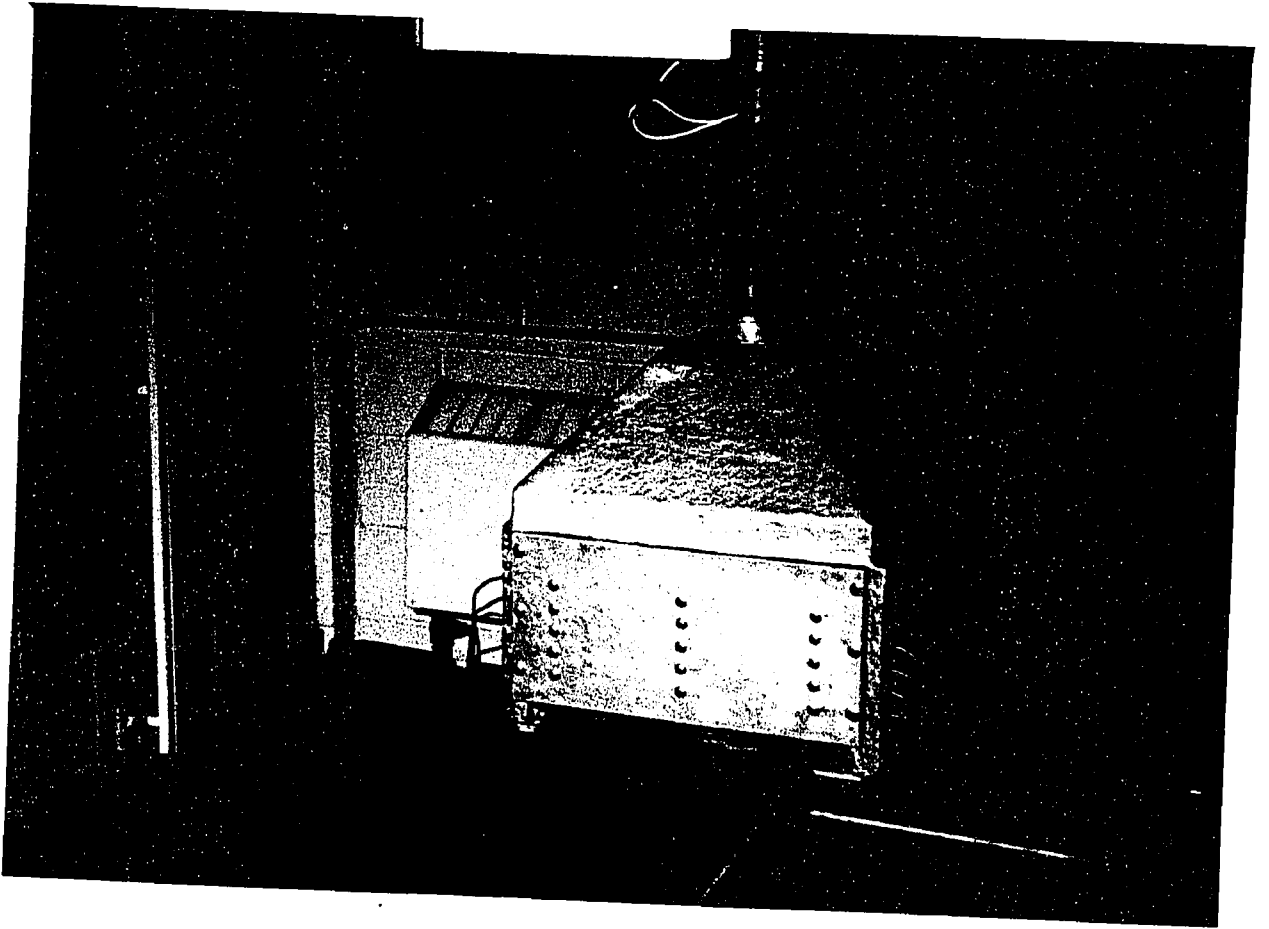
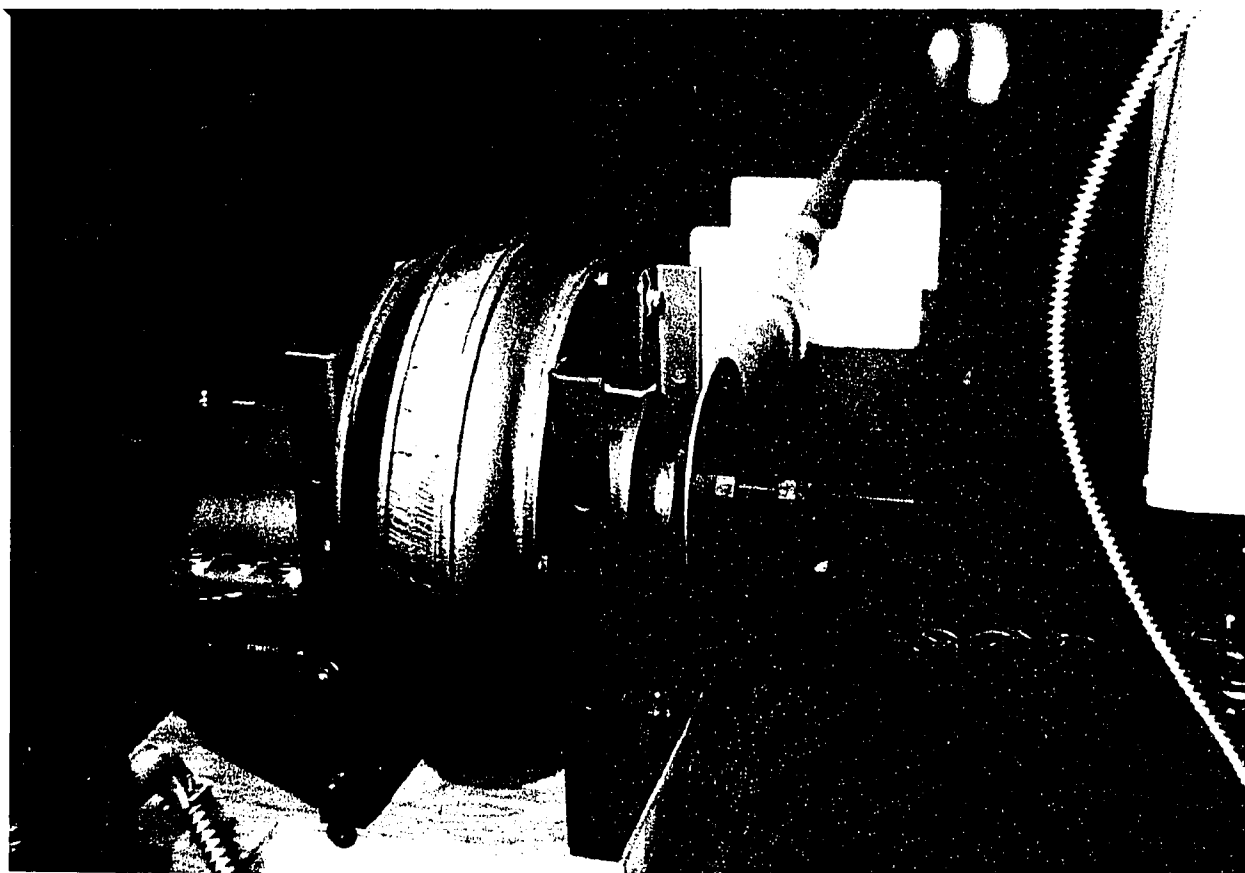FIGURE 44   PLOT OF u/u_m VERSUS r/r_o

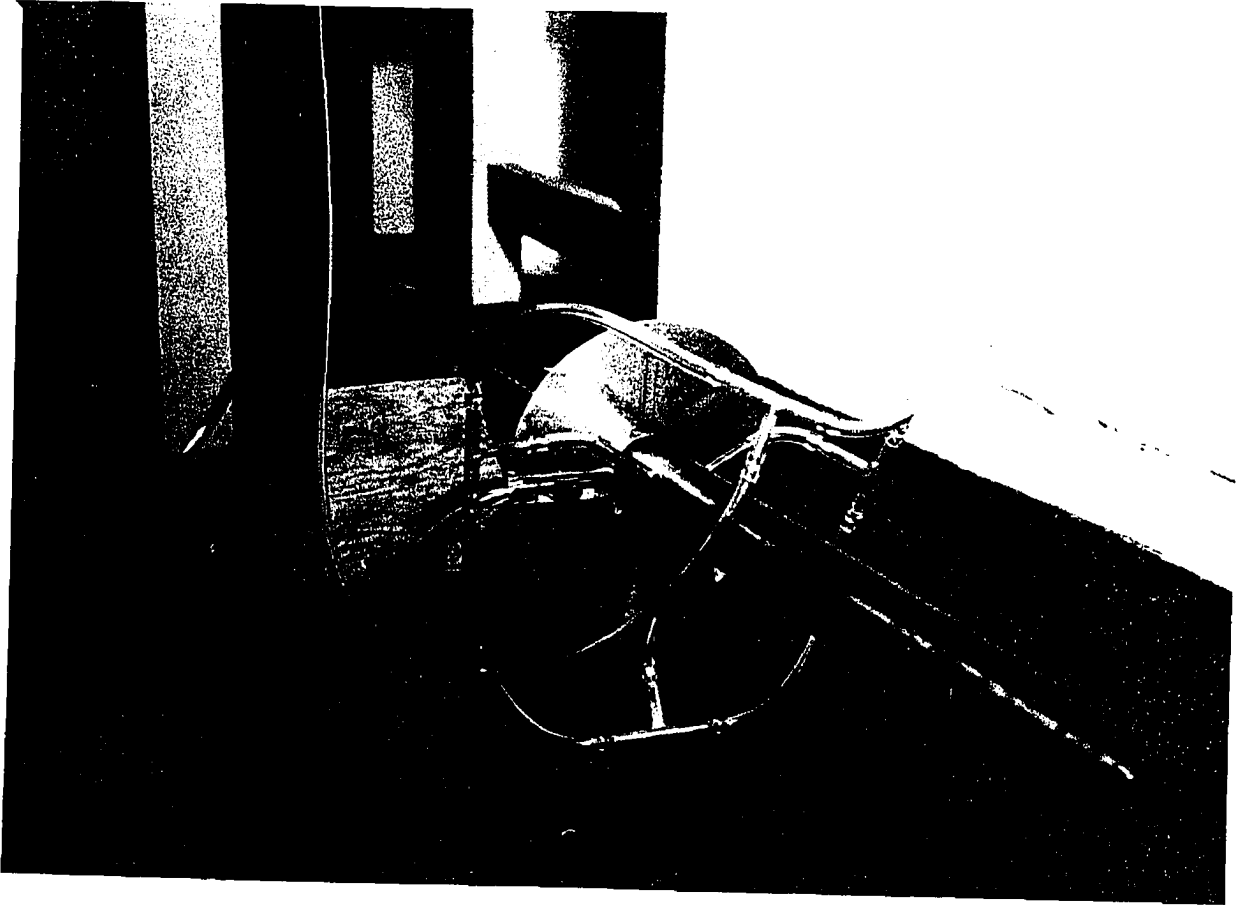FIGURE 3   FURNACE

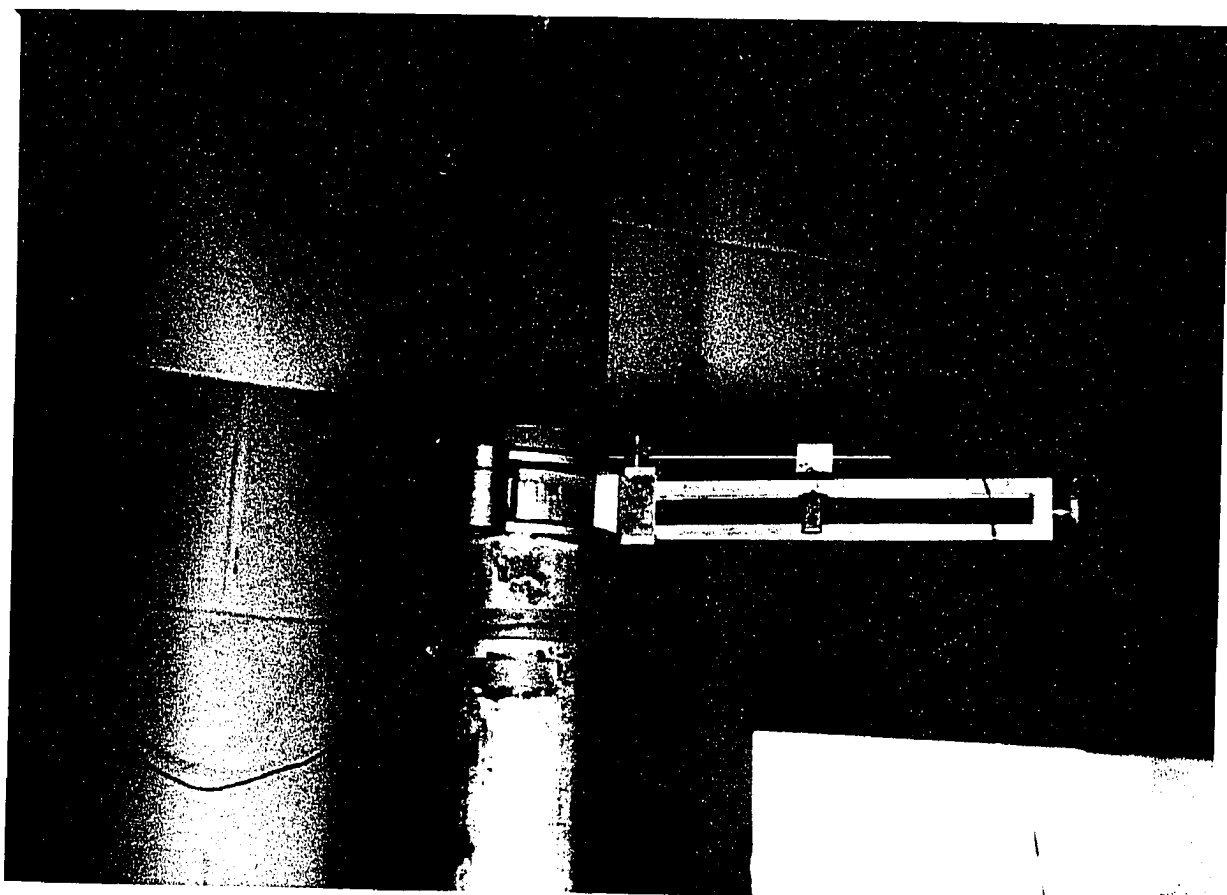FIGURE 4   FAN INLET CONTROL

FIGURE 6   MEASURING STATION

FIGURE 6a   TRAVERSING GEAR

BIBLIOGRAPHY

1. Martinelli, R. C., "Heat Transfer to Molten Metals", Trans. A.S.M.E. 69: 947 (1947).

2. Diessler, R. G., "Analytical Investigation of Fully Developed Laminar Flow in Tubes with Heat Transfer with Fluid Properties Variable Along the Radius", NACA Technical, Note 2410, July 1951, Washington.

3. Pigford, R. L., "Non-Isothermal Flow and Heat Transfer Inside Vertical Tubes", Chemical Engineering Progress Symposium, Series No. 17, Volume 51, 1955, St. Louis

4. Brown, W. G. and Wachmann, C., "Draft Performance of Chimneys", Research paper No. 108 of the Division of Building Research, Ottawa, September 1960.

5. Brown, W. G. and Colborne, W. G., "Fundamentals of Chimney Performance", Canadian Journal of Technology, 34: 354 - 365, 1956.

6. Sparrow, E. M. and Gregg, J. L., "Buoyancy Effects in Forced-Convection Flow and Heat Transfer", Trans. ASME, Series E, Vol. 81, p. 133, 1959.

7. Kiyosi Yamagata, "A Contribution to the Theory of Non-Isothermal Laminar Flow of Fluids Inside a Straight Tube of Circular Cross-Section", Memoirs of Faculty of Engineering, Kyushu Imperial University, Japan, Vol. VIII, No. 6, 1940, pp. 365 - 449.

8. Martinelli, R. C. and Boelter, L. M. K., "The Analytical Prediction of Superposed Free and Forced Viscous Convection in a Vertical Pipe", University of California Publications in Engineering, Vol. 5, No. 2, pp. 23 - 58, 1942.

9. Kays, W. M., "A Summary of Experiments and Analysis for Gas Flow Heat Transfer and Friction in Circular Tubes", Technical Report No. 22, Department of Mechanical Engineering, Stanford University.

10. Hallman, T. M., "Combined Forced and Free Laminar Heat Transfer in Vertical Tubes with Uniform Internal Heat Generation", ASME 1956, Vol. 78, p. 1831.

11. Hallman, T. M., "Experimental Study of Combined Forced and Free Laminar Convection in a Vertical Tube", NASA, TN-D-1104, 1961.

12. Hanratty, T. H., Rosen E. M. and Kabel, R. L., "Effect of Heat Transfer of Flow Field at Low Reynolds Numbers in Vertical Tubes", Ind. Eng. Chem. 50, 815, 1958.

13. Eckert, E. R. G. and Diaguila, A. J., "Convective Heat Transfer for Mixed Free and Forced Flow through Tubes", ASME 1954, pp. 497 - 504.

14. Moffatt, W. C., Fundamentals of Chimney Analysis, M.Sc. Thesis, Queen's University, Kingston, Ontario, April 1958.

15. Knudson, G. and Katz, D. L., Fluid Dynamics and Heat Transfer, McGraw-Hill Series in Chemical Engineering, New York, 1958.

16. Chapman, A. J., Heat Transfer, The MacMillan Company, New York, 1960.

17. Eckert, E. R. G. and Drake, R. M., Heat and Mass Transfer, McGraw-Hill Series in Mechanical Engineering, New York, 1959.

18. McAdams, W. H., Heat Transmission, McGraw-Hill Series in Chemical Engineering, New York, 1954.

19. Schlichting, Hermann, Boundary Layer Theory, McGraw-Hill Series in Mechanical Engineering, New York, 1960.

20. Gröber, H. and Erk, S., Fundamentals of Heat Transfer, McGraw-Hill Series in Mechanical Engineering, New York, 1961.

21. Streeter, V. L., Fluid Mechanics, McGraw-Hill, New York, 1951.

22. Giedt, W. H., Principles of Heat Transfer, Van Nostrand, Princeton, N.J., 1957.

23. Kays, W. M., "Numerical Solutions for Laminar Flow Heat Transfer in Circular Tubes", ASME 1955, pp. 1265 - 1274.

24. Brown, W. G., "Die Überlagerung von Erzwungener und Natürlicher Konvektion bei Niedrigen Durchsätzen in einem Lotrechten Rohr", VDI Verlag, G.m.b.H., Düsseldorf, 1960.

25. Kemeny, G. A. and Somers, E. V., "Combined Free and Forced Convection Flow in Vertical Circular Tubes--Experiments with Water and Oil", ASME, Paper No. 61-WA-161.

VITA AUCTORIS

1938   Born in Bannu (N.W.F.P.) India on March 23

1953   Finished high school (matriculation) from Government
                High School, Delhi Board of Higher Secondary Education,
                Delhi, India in April

1955   Finished Intermediate Science (I.Sc.) from St. Andrews
                College, Gorakhpur, India in April

1960   Received the Bachelor's Degree in Mechanical Engineering
                from M. S. University of Baroda, Baroda, India in April

1960 - 1961   Worked in Pioneer Foundry Machinery, Baroda, India

1963   Candidate for the Degree of Master of Applied Science
                in Mechanical Engineering at Assumption University of
                Windsor

101